

SCIENCO
**SOUTHERN BRAZILIAN JOURNAL
OF CHEMISTRY**

ISSN 0104-5431

**AN INTERNATIONAL FORUM FOR THE RAPID PUBLICATION
OF ORIGINAL SCIENTIFIC ARTICLES DEALING WITH CHEMISTRY AND
RELATED INTERDISCIPLINARY AREAS**

VOLUME EIGHT, NUMBER NINE

DECEMBER 2000

EDITOR

LAVINEL G. IONESCU, Departamento de Química, CCNE, Universidade Luterana do Brasil, Canoas, RS & Instituto de Química, Pontifícia Universidade Católica do Rio Grande do Sul, Porto Alegre, RS, BRASIL

EDITORIAL BOARD

- D. BALASUBRAMANIAN, Centre for Cellular and Molecular Biology, Hyderabad, INDIA
HÉCTOR E. BERTORELLO, Departamento de Química Orgánica, Facultad de Ciencias Químicas, Universidad Nacional de Córdoba, Córdoba, ARGENTINA
AÉCIO P. CHAGAS, Instituto de Química, UNICAMP, Campinas, SP, BRASIL
JUAN JOSÉ COSA, Departamento de Química y Física, Facultad de Ciencias Exactas, Universidad Nacional de Río Cuarto, Río Cuarto, ARGENTINA
GLENN A. CROSBY, Department of Chemistry, Washington State University, Pullman, WA, USA
VITTORIO DEGIORGIO, Dipartimento di Elettronica, Sezione di Fisica Applicata, Università di Pavia, Pavia, ITALIA
JOSÉ C. TEIXEIRA DIAS, Departamento de Química, Universidade de Coimbra, Coimbra, PORTUGAL
XORGE A. DOMINGUEZ, Departamento de Química, Instituto Tecnológico y de Estudios Superiores de Monterrey, Monterrey, N.L., MÉXICO
OMAR A. EL SEUD, Instituto de Química, Universidade de São Paulo, São Paulo, SP, BRASIL
ERNESTO GIESBRECHT, Instituto de Química, Universidade de São Paulo, São Paulo, SP, BRASIL
FERNANDO GALEMBECK, Instituto de Química, UNICAMP, Campinas, SP, BRASIL
NISSIM GARTI, Casali Institute of Applied Science, Hebrew University of Jerusalem, Jerusalem, ISRAEL
GASPAR GONZALEZ, Centro de Pesquisa, CENPES-PETROBRAS, Ilha do Fundão, Rio de Janeiro, RJ, BRASIL
YOSHITAKA GUSHIKEM, Instituto de Química, UNICAMP, Campinas, SP, BRASIL
WILLIAM RASE, Department of Chemistry, Wayne State University, Detroit, MI, USA
I. B. IVANOV, Laboratory of Thermodynamics and Physico-chemical Hydrodynamics, Faculty of Chemistry, University of Sofia, Sofia, BULGARIA
IVAN IZQUIERDO, Departamento de Bioquímica, Universidade Federal do Rio Grande do Sul, Porto Alegre, RS, BRASIL
V.A. KAMINSKY, Karpov Institute of Physical Chemistry, Moscow, RUSSIA
MICHAEL LAING, Department of Chemistry, University of Natal, Durban, SOUTH AFRICA
EDUARDO LISSI, Departamento de Química, Universidad de Santiago de Chile, Santiago, CHILE
WALTER LWOWSKI, Department of Chemistry, New Mexico State University, Las Cruces, N.M., USA
C. MANOHAR, Bhabha Atomic Research Centre, Chemistry Division, Bombay, INDIA
AYRTON FIGUEIREDO MARTINS, Departamento de Química, Universidade Federal de Santa Maria, Santa Maria, RS, BRASIL
FRED MENCER, Department of Chemistry, Emory University, Atlanta, GA, USA
MICHAEL J. MINCH, Department of Chemistry, University of the Pacific, Stockton, CA, USA
K. L. MITTAL, IBM Corporate Technical Institutes, Thornwood, N.Y., USA
ARNO MÜLLER, Escola de Engenharia, Universidade Federal do Rio Grande do Sul, Porto Alegre, RS, BRASIL
JOSE MIGUEL PAERERA, Instituto de Investigaciones en Catalisis y Petroquímica, Universidad Nacional del Litoral, Santa Fe, ARGENTINA
LARRY ROMSTED, Department of Chemistry, Rutgers University, Piscataway N.J., USA
GILBERTO FERNANDES DE SÁ, Departamento de Química Fundamental, Universidade Federal de Pernambuco, Recife, PE, BRASIL
DIMITRIOS SAMIOS, Instituto de Química, Universidade Federal do Rio Grande do Sul, Porto Alegre, RS, BRASIL
DIOGENES DOS SANTOS, Department of Molecular Biology, Oxford University, Oxford, ENGLAND
JOSEPH A. SCHUFLE, Department of Chemistry, New Mexico Highlands University, Las Vegas, N.M., USA
BEN K. SELINGER, Department of Chemistry, Australian National University, Canberra, AUSTRALIA
KOZO SHINODA, Department of Applied Chemistry, Faculty of Engineering, Yokohama National University, Yokohama, JAPAN
CRISTOFOR I. SIMIONESCU, Academia Română, Filiala Iasi, Iasi, ROMANIA
UMBERTO TONELLATO, Dipartimento di Chimica Organica, Università degli Studi di Padova, Padova, ITALIA
DIETER VOLLHARDT, Max Planck Institut für Kolloid und Grenzflächenforschung, Berlin, GERMANY
RAOUL ZANA, Institut Charles Sadron, CRM-EAHP, Strasbourg, FRANCE

SOUTHERN BRAZILIAN JOURNAL OF CHEMISTRY

ISSN 0104-5431

VOLUME EIGHT, NUMBER NINE DECEMBER 2000

CONTENTS / CONTEÚDO

ADSORPTION OF ETHYL ACETATE FROM ALIPHATIC ALCOHOLS ON ACTIVATED CHARCOAL S.Güktürk, M. Mahramanlioglu and M. Tunçay	1
SYNTHESIS OF S-OXIDES AND S,S-DIOXIDES OF SOME 4-NITRO- AND 4-AMINO-3-HYDROXY-10-PHENOTHIAZINES AND 3H-PHENOTHIAZIN-3-ONES Radu Gropeanu, Ioan Panea and Teodora Panea	13
OPTIMIZATION OF ETHYLENE POLYMERIZATION CONDITIONS WITH METALLOCENE CATALYST USING EXPERIMENTAL DESIGN METHODOLOGY Luciano Endres and Carlos R. Wolf	25
THE ROLE OF FIBRINOGEN IN CORONARY HEART DISEASE AND ITS POSSIBLE DEPENDENCE ON ACTIVATED POLYMORPHONUCLEAR LEUKOCYTES R. Olinescu, D.O. Crocnan and Maria Greabu	37
SPECTROPHOTOMETRIC STUDY OF THE BINARY SYSTEM Ru(III)-SOLOCHROM VIOLET RS AND THE DETERMINATION OF Ru(III) Maria Pleniceanu, Mihaela Mureseanu, Ion Ganescu and Olimpia Rusu	45
CARBON-13 NMR OF ALIPHATIC KETONES Paulo Irajara Borba Carneiro and Roberto Rittner	53
SYNTHESIS AND STRUCTURAL CHARACTERIZATION OF N-(2'-HYDROXY-1'-NAPHTHALEN METHIN)-2-AMINOANILINE COMPLEXES Dumitru Negoiu, Mirela Calinescu, Ana Emandi and Tudor Rosu	57
MAGNETIC AND SPECTRAL STUDIES ON CHROMIUM (III), NICKEL (II) AND COPPER (II) COMPLEXES OF 4-HYDROXY-5-METHOXY ISOPHTHALDEHYDE BIS DIMETHYLHYDRAZONE Mirela Calinescu, Ana Emandi, Anca Nicolae and Lidia Paruta	71
PHYSICAL CHEMICAL STUDIES OF THE AGGREGATION AND CATALYTIC PROPERTIES OF THE SURFACTANT METHYLDODECYLBENZYLTRIMETHYLAMMONIUM CHLORIDE (MBDTACl) Lavinel G. Ionescu, Silvia Dani and Elizabeth Fátima de Souza	85
CHEMILUMINESCENCE, AN OUTSTANDING PHYSICOCHEMICAL METHOD Maria Greabu, D.O. Crocnan and R. Olinescu	97
PRE-CONCENTRATION OF Cd, Cu, Ni, Pb AND Zn FROM FUEL ETHANOL AND NATURAL WATER SAMPLES BY SORPTION ON p-AMINO-BENZOIC MODIFIED CELLULOSE AND SUBSEQUENT FLAME AAS DETERMINATION Pedro de Magalhães Padilha, Ariovaldo de Oliveira Florentino, Fabrício Vieira de Moraes, Fábio Arlindo Silva, Cilene C.F. Padilha and Julio C. Rocha	113
AUTHOR INDEX	125

**ADSORPTION OF ETHYL ACETATE FROM ALIPHATIC
ALCOHOLS ON ACTIVATED CHARCOAL**

*S. Göktürk, **M. Mahramanlioğlu and *M. Tunçay

*Marmara University , Faculty of Pharmacy,
81010, Haydarpaşa, Istanbul / TURKEY

** Istanbul University, Faculty of Engineering,
Department of Chemistry, Avcılar , 34850,
Istanbul / TURKEY

ABSTRACT

The adsorption equilibria of binary mixtures of ethyl acetate and aliphatic alcohols on activated charcoal were studied at 298 K. It was found that activated charcoal adsorbed ethyl acetate preferentially from all mixtures with aliphatic alcohols. Influence of the alkyl chain length of aliphatic alcohols on the adsorption of ethyl acetate were compared by means of composite and individual isotherms. The adsorption equilibrium data were analysed on the basis of the Schay & Nagy Model.

Key Words - Activated charcoal, adsorption, aliphatic alcohols, binary mixtures.

RESUMO

A adsorção de misturas binárias de etil acetato e alcoóis alifáticos sobre carvão ativado foi estudada a 298 K. Foi constatado que o acetato de etila é adsorvido preferencialmente de todas as misturas contendo alcoóis alifáticos. O efeito do comprimento da cadeia dos alcoóis alifáticos sobre a adsorção do acetato de etila foi analisado em termos de istoermas individuais. Os dados obtidos para o equilíbrio da adsorção foram analisados usando o Modelo de Schay e Nagy.

1. INTRODUCTION

Adsorption from liquid mixtures on solids involves a number of very important processes and plays a significant role in many fields of the natural sciences.

The mechanism of the adsorption process from a binary liquid mixture onto a solid adsorbent has been studied by many investigators [1-6]. Various factors have been found to influence adsorption; such as nature of the adsorbents, chemical nature of the solute molecules, molecular size and shape [7], volatility [4], interfacial tension of components at the liquid / solid interface [6,8].

When a binary mixture is involved, the adsorbed layer has in general, a different composition from that of the bulk phase in equilibrium with it. Adsorption from a binary liquid mixture is expressed in terms of composite isotherms which is the functional relation between the surface excess of a component and its concentration in the equilibrium bulk phase [9]. The state of adsorbate may be judged directly from experimentally determined composite isotherms. The type of composite isotherm has been widely used for comparison the adsorption behavior of binary mixtures [11-13].

The purpose of the present work is to find a correlation between the hydrophobicity and adsorption tendency of the aliphatic alcohols from their mixtures with ethyl acetate on activated charcoal. Adsorption experiments were performed using binary mixtures of homologous series of alcohols ($C_3 - C_{10}$) and ethyl acetate. A simple model assuming ideal behaviour in both bulk and adsorbed phases was applied [14].

The adsorption equilibrium data were analysed on the basis of the Schay & Nagy Model. The thickness of surface layer formed in the adsorption process was determined by means of monolayer test [15,16]. Influence of chain length on adsorption was compared by means of composite and individual isotherms and the results were discussed.

2. EXPERIMENTAL

2.1 Chemicals

Ethyl acetate (99.5% pure), Propanol (99.5 % pure), Butanol (99.4 % pure), Pentanol (98 % pure), Hexanol (98% pure), Decanol (98% pure) were obtained from Sigma. The activated charcoal was microporous E. Merck (No.2184) sample and was further purified by extracting (Soxhlet) for several hours with benzene and acetone then evacuated at 423 K for 6 hours in vacuum. The specific surface area of the sample was 800 m²/g. The ratio of liquid to adsorbent was kept as low as possible to obtain maximum readings (5 milliliters per gram were chosen for all of the systems).

2.2 Procedure

A binary mixture was prepared for each experimental point ; its concentration was analyzed refractometrically using a Carl Zeiss Jena Refractometer. A weighed amount of adsorbent was then added to the binary mixture. The system consisting of the binary mixture and the adsorbent was shaken for 17-19 hr in a screw - capped Erlenmeyer flask, using a reciprocating shaker. Measurements were made over the whole range of concentrations lying between pure components. The temperature was thermostatically controlled to 298 K. The equilibrium composition of the bulk liquid , X_1 , was then analyzed refractometrically ; the calibration curves needed for the refractometric analyses were prepared by us. The refractive index composition curves of each of the binary mixtures were almost straight lines over the entire range of concentration.

3. RESULTS AND DISCUSSION

The surface excess n_1^e is related to the concentration of each component at the surface by the Eqn (1) :

$$n_1^e = n^0 \frac{\Delta X_1}{m} = n_1^s(1 - X_1) - n_2^s X_1 \quad (1)$$

where ΔX_1 is the change in the mole fraction of component 1, when n^0 moles of original solution are brought into contact with m grams of adsorbent; X_1 is the equilibrium mole fraction and n_1^s and n_2^s are the number of the moles of components 1 and 2 adsorbed from the binary mixture per gram of adsorbent respectively. The quantity $n_1^0 \Delta X_1 / m$; n_1^e is the experimentally determined specific surface excess concentration of component 1 and when plotted against X_1 gives composite isotherms.

The composite isotherms for adsorption from binary mixtures of ethyl acetate (1) + propanol (2), ethyl acetate (1) + butanol (2), ethyl acetate (1) + pentanol (2), ethyl acetate (1) + hexanol (2), ethyl acetate (1) + decanol (2) on activated charcoal surfaces at 298 (± 0.1) K were shown in Fig.1. Any isotherm point reported in Fig.1 was the mean of four or five parallel determinations.

As seen in Fig.1 the composite adsorption isotherms for all of the binary mixtures studied were U shaped with a maximum at relatively low concentrations of component 1. It is observed that the composite isotherms were almost of Type II curves as classified by Schay & Nagy's Model and reflect strong adsorption of ethyl acetate [7].

Activated charcoal is known to have dual character and in the case of alcohols and ethyl acetate mixtures the surface phase was of a mixed character, i.e., it contained the molecules of both solution components. The composition isotherms showed that there was preferential adsorption of ethyl acetate from all of the alcohol solutions throughout the whole concentration range. The composition of the adsorbed layer changed with the alkyl chain length. The amount of ethyl acetate molecules on the adsorbed layer decreased from propanol to decanol. This indicated that some ethyl acetate molecules were displaced from the surface by the longer chain alcohols.

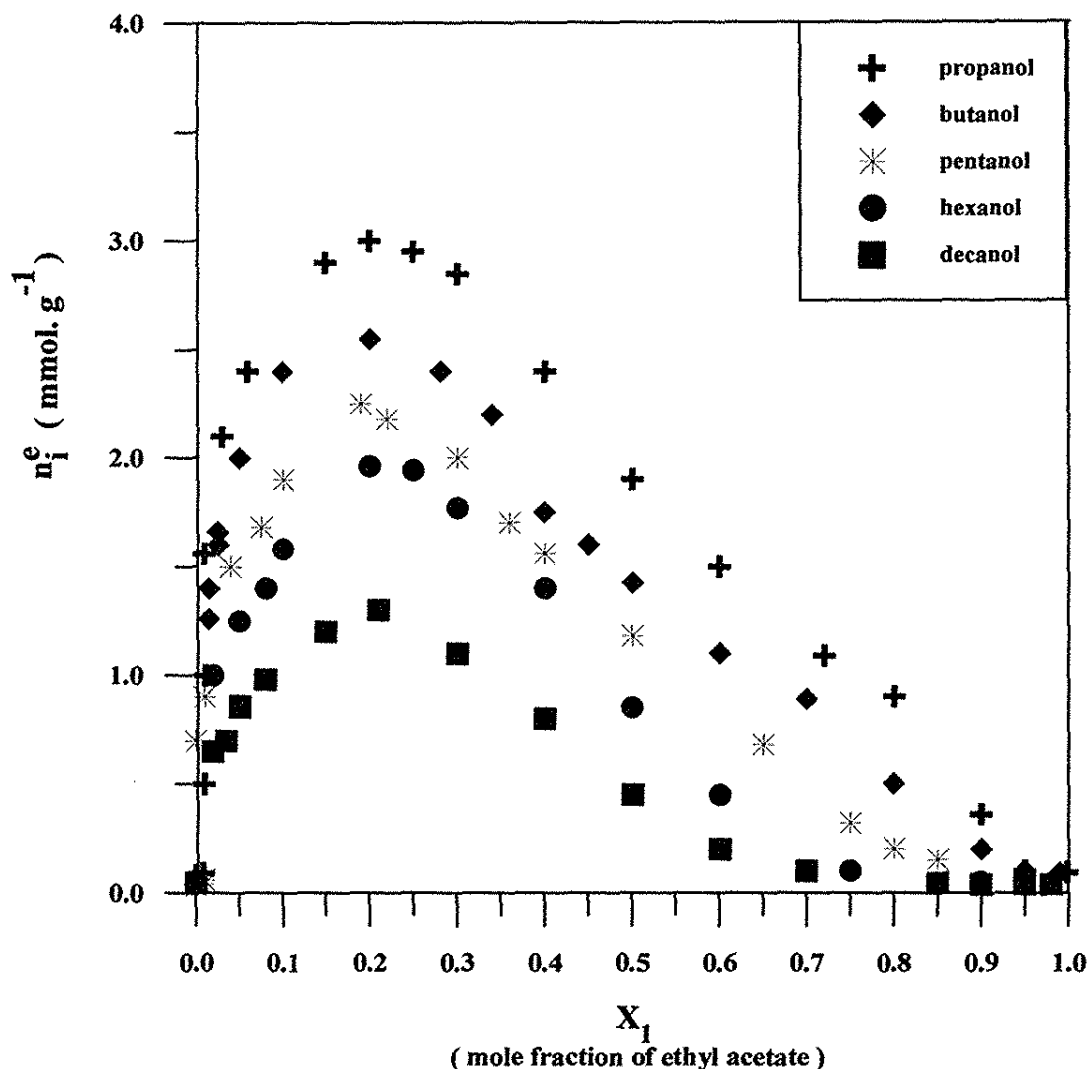


Fig.1. Specific surface excess isotherms of ethyl acetate (1) from alcohol solutions at 298 K on activated charcoal.

In order to show the relation between preference of activated charcoal for ethyl acetate and polarity of the competing solvent, the relation between surface excess amount of ethyl acetate at mole fraction of 0.4 and the number of carbons of alcohols and the relation between dielectric constants of alcohols and the number of carbons of alcohols were plotted in the same figure (Fig.2). As can be seen in Fig. 2 there is a striking similarity between the two relations. As the difference between the dielectric constants of ethyl acetate and competing alcohol decreased , the amount of ethyl acetate at the interface decreased.

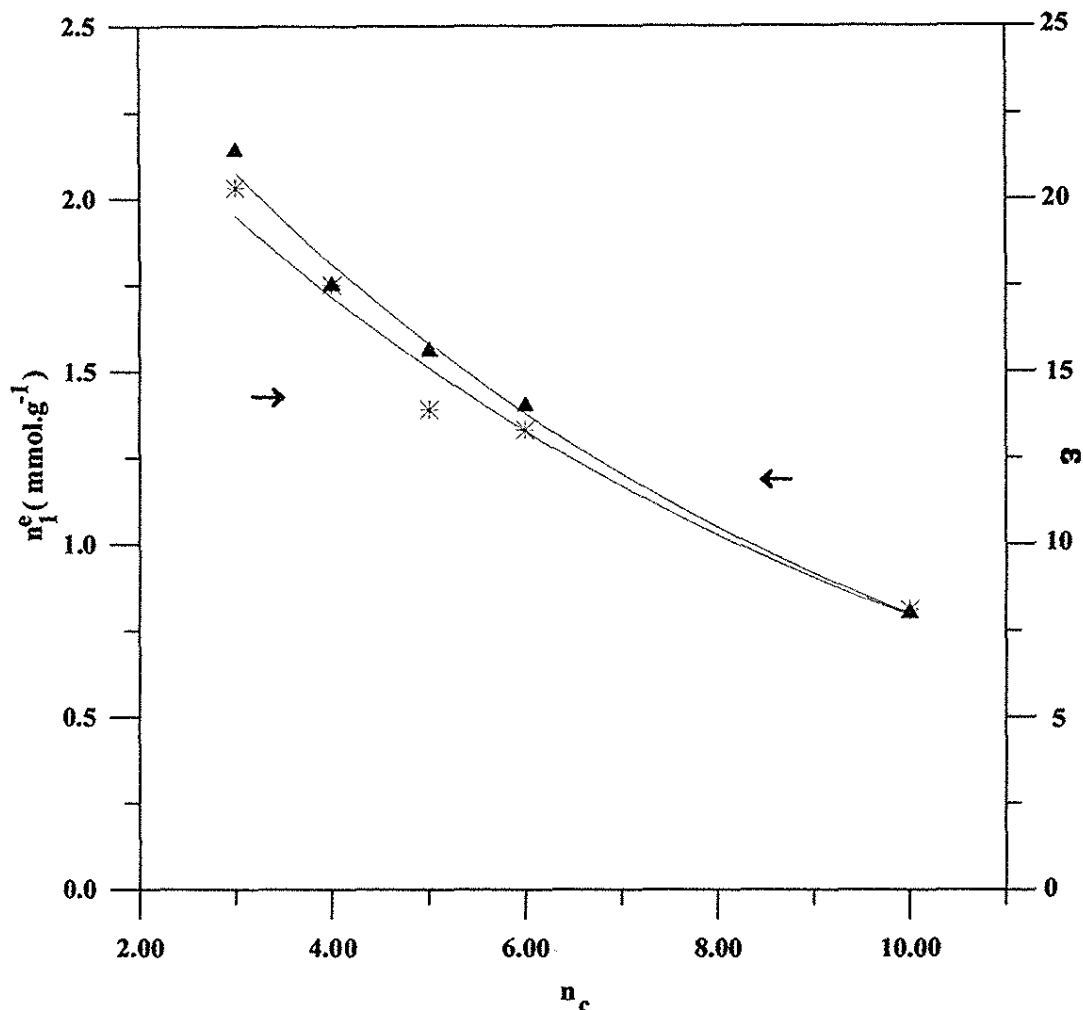


Fig.2. Dielectric constant of alcohols (ϵ) and surface excess of ethyl acetate (n_1^e) as a function of the alkyl chain length (n_c).

A simpler model assuming ideal behaviour in both phases (IBP Model) was applied to the experimental data using Eqn (2) [14] :

$$\frac{x_1 x_2}{n_1^e} = \left(\frac{1}{n^s} \right) x_1 + \frac{K}{(1-K)n^s} \quad (2)$$

where n^s is the total number of moles in the adsorbed phase that is surface layer capacity and K is the constant associated with the difference of the adsorption energies of both component of the liquid mixture. The K and n^s values derived from the linear plots according to this expression are given in Table 1. Since ethyl acetate (component 1) was preferentially adsorbed K was smaller than unity for each case.

These results are in agreement with previous studies [9,16,17]. The relation between the values of K and carbon number of alcohols were plotted in Fig.3. As seen in Fig.3 , K linearly increased with increasing chain length of alcohols.

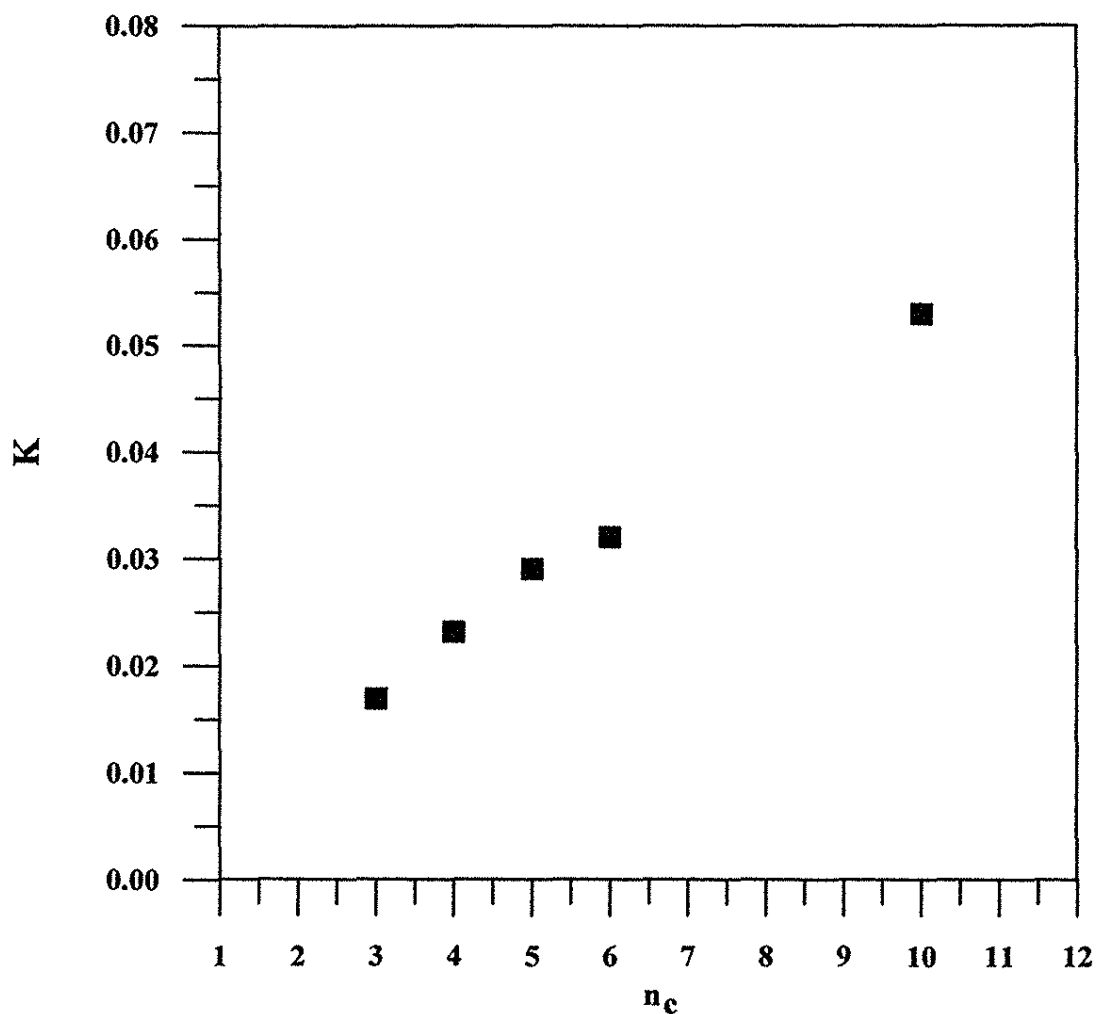


Fig.3. Adsorption equilibrium constant (K) as a function of the alkyl chain length n_c .

Taking into account the surface layer capacities n^s , the number of moles of component 1 in the surface phase is given by [18] :

$$n_1^s = n_1^e + n^s X_1 \quad (3)$$

The number of moles in the surface phase can also be calculated using the expression below [11]

$$n_1^s = \frac{Sx_1 + n_1^e A_2}{A_2 + (A_1 - A_2)x_1} \quad n_2^s = \frac{Sx_2 - n_1^e A_1}{A_2 + (A_1 - A_2)x_1} \quad (4)$$

where 'S' the specific surface area of the adsorbent ; and A_1 and A_2 the cross-sectional areas of the adsorbed molecule (1) and (2) at the interface respectively. The cross sectional areas determined from the empirical equation of Mc Lellan and Harnsberger were 31.46, 26.26, 30.05, 33.66, 36.98 and 48.80 Å^2 /molecule for ethyl acetate, propanol , butanol , pentanol , hexanol and decanol respectively . The two sets of n_1^s values calculated by Eqn (3) and Eqn (4) were compared. It was observed that the values of n_1^s calculated from Eqn (4) were almost similar to the ones calculated from Eqn (3) but a slight deviation of n_1^s values calculated by Eqn (3) occurred at higher concentrations of alcohols for all the systems. Therefore n_1^s values calculated by Eqn (4) were used preferentially for obtaining individual isotherms.

The individual adsorption isotherms $n_1^s = f(x_1)$ and $n_2^s = f(x_2)$ are shown in Figure 4 (a-e). Their shape confirmed the presence of both components on the activated charcoal phase within the whole concentration range. It was observed that n_1^s did not change significantly with X_1 at relatively high concentration. Therefore the adsorbed layer was assumed to have constant composition.

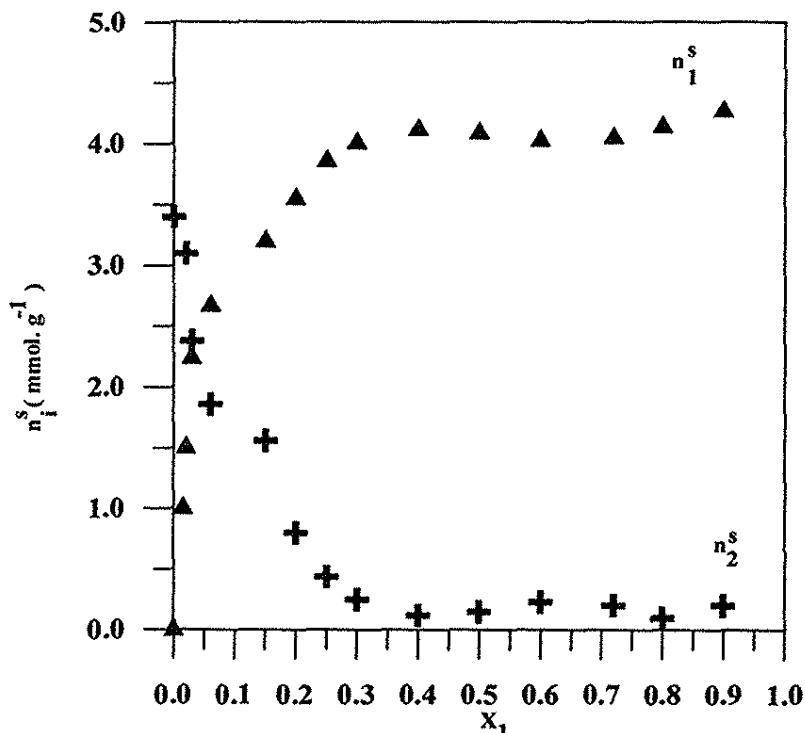


Fig.4a. Individual isotherms for adsorption on activated charcoal from ethyl acetate (1) + propanol (2) solutions at 298 K. (X_1 : mole fraction of ethyl acetate)

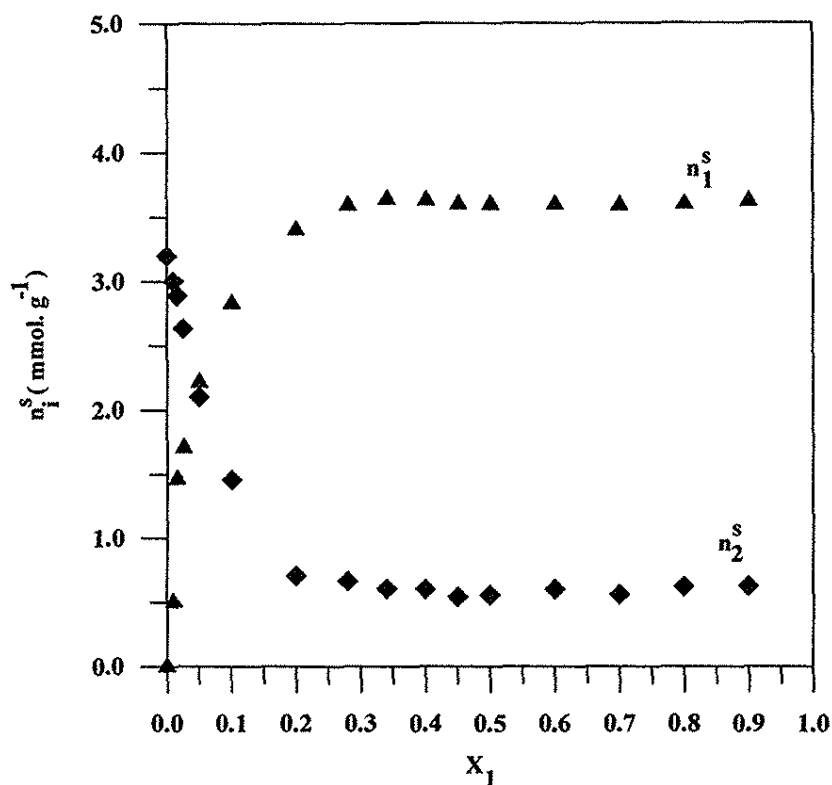


Fig.4b. Individual isotherms for adsorption on activated charcoal from ethyl acetate (1) + butanol (2) solutions at 298 K.(X_1 : mole fraction of ethyl acetate)

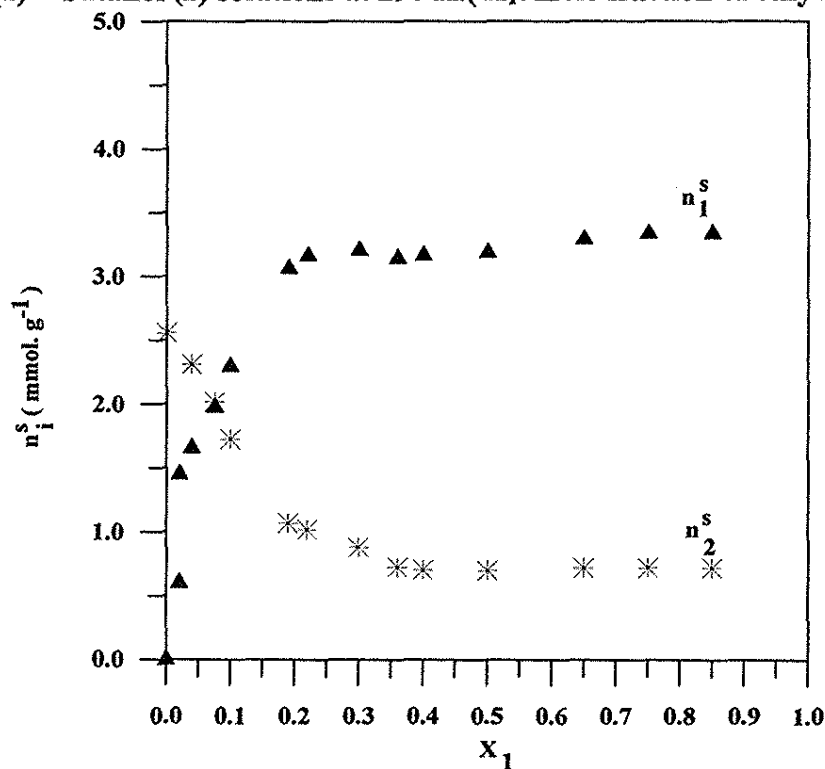


Fig.4c. Individual isotherms for adsorption on activated charcoal from ethyl acetate (1) + pentanol (2) solutions at 298 K. (X_1 : mole fraction of ethyl acetate)

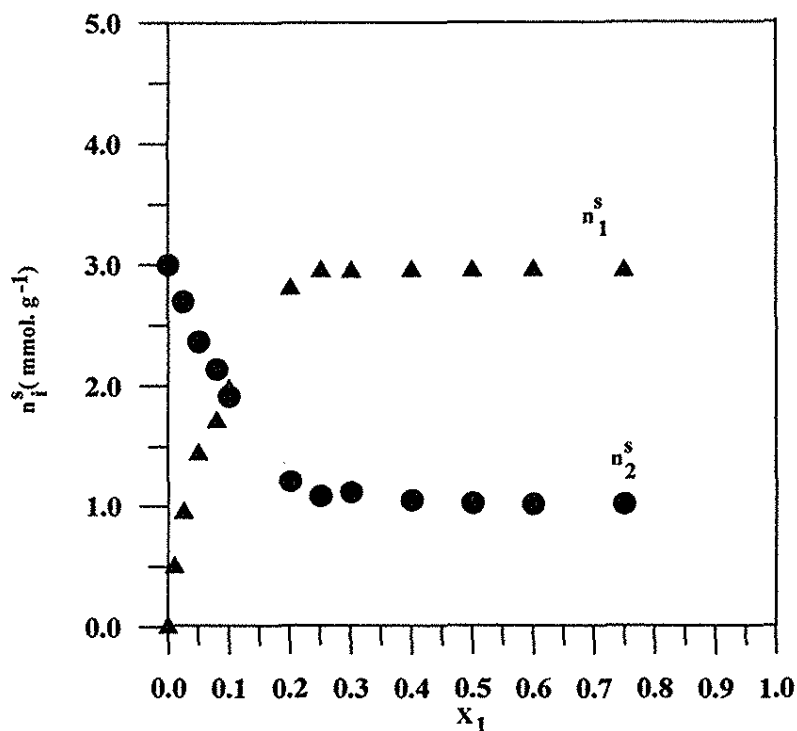


Fig.4d. Individual isotherms for adsorption on activated charcoal from ethyl acetate (1) + hexanol (2) solutions at 298 K. (X_1 : mole fraction of ethyl acetate)

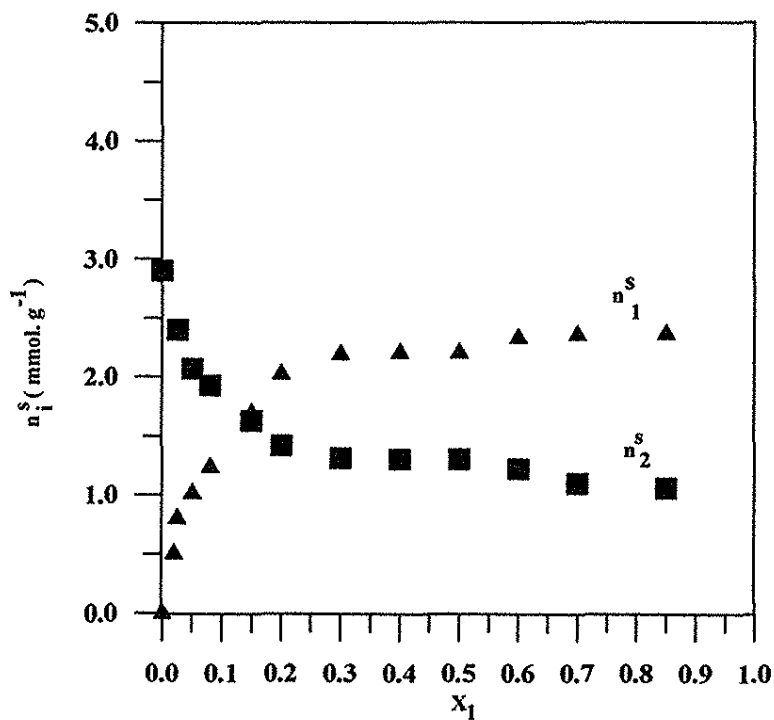


Fig.4e. Individual isotherms for adsorption on activated charcoal from ethyl acetate (1) + decanol (2) solutions at 298 K. (X_1 : mole fraction of ethyl acetate)

The composition of the adsorbed layer was determined by Schay & Nagy's Model [7] in which the composition of adsorbed layer was calculated from the expression below.

$$x_1^s = \frac{Sx_1 + n_1^e A_2}{S + (A_2 - A_1)n_1^e} \quad (5)$$

The x_1^s values were plotted as a function of x_1 in Fig.5 for all of the binary mixtures studied. As seen in Fig. 5 , x_1^s values were higher than x_1 for all systems.

The determination of the thickness of surface layers formed in the adsorption process was done by means of the monolayer test. The adsorbed layer was assumed to have a constant composition at relatively high X_1 (Fig.4a-e) which leads to a molecular thickness t of adsorbed layer defined by

$$\frac{n_1^s}{(n_1^s)m} + \frac{n_2^s}{(n_2^s)m} = t \quad (6)$$

where $(n_i^s)m$ is the number of moles of component I required to cover the surface of 1g of adsorbent completely. Values of t were found to be sufficiently close to unity for all the systems and confirmed monolayer adsorption [18]. The monolayer data was found to be compatible with experimental data.

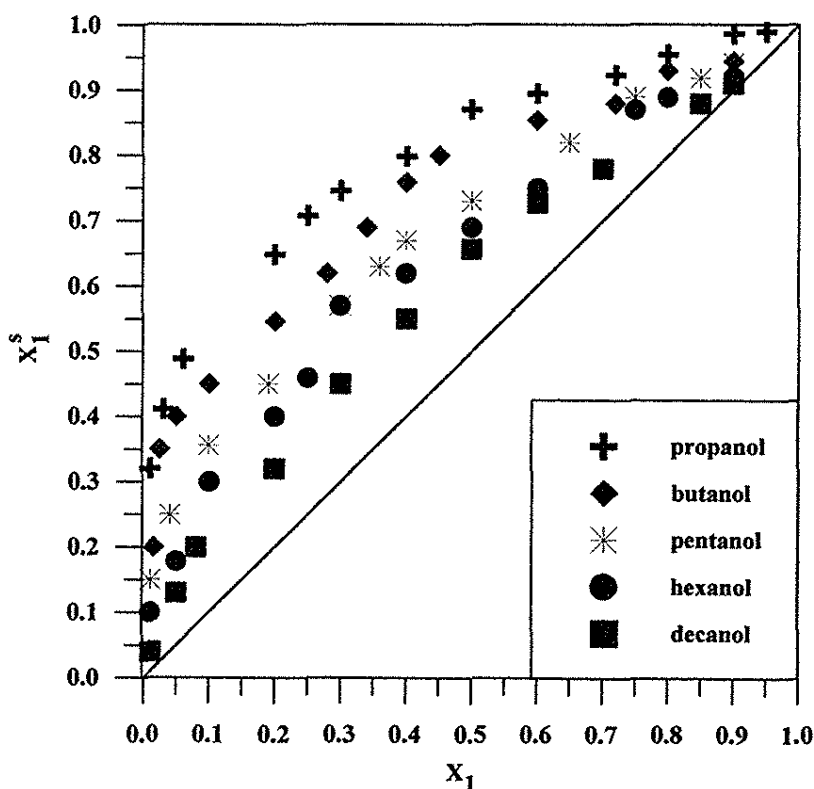


Fig.5. Composition of adsorbed layer X_1^s (composition of adsorbed layer) versus X_1 (mole fraction of ethyl acetate) at 298 K.

The surface area S of the adsorbent by assuming a monolayer model of the surface phase is given by [19]

$$S = a_1 n_1^s + a_2 n_2^s \quad (7)$$

where a_i is the area occupied by one mole of component i in the surface phase. Using molecular areas given before and the values of n_i^s calculated by Eqn 4 corresponding to $X_i=0.5$ leads to values of S . (Table 1)

Table I. Adsorption Parameters
* Determined For the Adsorption of Ethyl Acetate on Activated Charcoal.

Mixture	K	n^s (mmol.g ⁻¹)	S (m ² /g)
Ethyl acetate + Propanol	0.017	4.0	799.0
Ethyl acetate + Butanol	0.0232	3.3	801.36
Ethyl acetate + Pentanol	0.0291	3.06	786.39
Ethyl acetate + Hexanol	0.0321	2.37	786.34
Ethyl acetate + Decanol	0.053	1.901	798.57

(Specific surface area of activated charcoal obtained from nitrogen adsorption by the BET method is 800 m²/g .)

* The parameters K, n^s and S are defined in the text.

4. CONCLUSION

The adsorption of liquids from binary mixtures (alcohol - ethyl acetate) was found to be sensitive to the polarity difference of the competing liquids.

Although ethyl acetate preferentially adsorbed on activated charcoal from all of the binary mixtures of alcohols studied the composition of the adsorbed layer changed with the alkyl chain length of the alcohols.

It was found that the number of ethyl acetate molecules in the adsorption layer decreased with an increase of the alkyl chain length of alcohols indicating that some ethyl acetate molecules were displaced from the surface by the longer chain alcohols.

The results may be interpreted in terms of polarity difference between ethyl acetate and the competing alcohols for adsorption on the activated charcoal.

5. REFERENCES

1. L.C. Lloyd, and B.L.Harris, *J.Chem.Soc.* 58, 899 (1954).
2. H.R.Chipalkatti, C.H.Giles and (the late) Vallance D.G.M., *J.Chem.Soc.*, 4375 (1954).
3. J.J. Kipling and D.B. Peakall, *J.Chem.Soc.*, 4828 (1956).
4. A.Blacburn, J.J.Kipling and D.A.Tester, *J.Chem.Soc.*, 2373 (1957).
5. G.I.Berezin, A.V.Kiselev, R.T.Sagatelyan and V.A.Sinitzyn, *Colloid Interface Sci.* 38,2, (1972).
6. G.S.Ash, R.Bown, and D.H.Everett, *J.C.S. Faraday Trans.*, 1,71,123 , (1975).
7. a) L.G.Nagy, , and G.Schay, *Acta Chim. Hung.*, 39,365 (1963).
b) Schay G., in " *Surface and Colloid Science*", E.Matijevic , Ed., Interscience, New York, USA, Vol.2, (1969), p.179 .
8. T. Elton, *J.Chem.Soc.* 3813, (1954).
9. S.Sircar, and A.L.Myers, *The J.Phys.Chem.*, 74 (14),2828, (1970).
10. L.G.Nagy, and G.Schay, *J.Chim.Phys.*, 140 (1961).
11. S.K.Suri, A.S.Brar and L.D.Ahuja, *J.Colloid Interface Sci.*, 69, 347, (1979).
12. H.D.Everett, and T.R.Podoll, *J.Colloid Interface Sci.*, 82,1,14, (1981).
13. S.K.Suri, and M.Patel, *Colloid Interface Sci.*, 84,1,36, (1981).
14. T.M.Coatharp, *J.Col.Interface.Sci.*, 54(2), 311, (1976).
15. J.Oscik, J.Goworek, and R.Kusak, *J.Col.Interface.Sci.* ,79 (2), 308, (1981).
16. I.Dèkány, D.F.Szàntò, W.Armin and G.Lagaly, *Ber.Bunsenges.Phys.Chem.*, 90,422, (1986).
17. M.Tunçay, S.Göktürk, A.Mardinli and M.Mahramanlioğlu, in " *Physical Adsorption : Experiment, Theory and Applications*", J.Fraissard, Ed., Kluwer Academic Publishers, Nice, France (1997), p. 553.
18. R.E.Day, and G.D.Parfitt, *J.Phys.Chem.*, 71, 3073, (1967)
19. B.Buczek, A.Swiatkowski, and J.Goworek, *Carbon*, 33(2), 129-134, (1995).
20. A.L.Mc.Clellan, and H.F.Harnsberger, *J.Colloid Interface Sci.*, 23, 577, (1967).

**SYNTHESIS OF S-OXIDES AND S,S-DIOXIDES OF SOME
4-NITRO- AND 4-AMINO-3-HYDROXY-10H-PHENOTHIAZINES
AND -3H-PHENOTHIAZIN-3-ONES**

Radu Gropeanu,^a Ioan Panea^b and Teodora Panea^a

a) Research and Production Centre "BIOS", Academy of Agricultural and Forest Sciences, OP1 CP2, 3400, Cluj-Napoca, ROMANIA

b) "Babes-Bolyai" University, Faculty of Chemistry and Chemical Engineering, Department of Organic Chemistry, 11th Arany Janos, 3400, Cluj-Napoca, ROMANIA

ABSTRACT

The S-oxides and S,S-dioxides of some 4-nitro- and 4-amino-3-hydroxy-10H-phenothiazines and -3H-phenothiazin-3-ones were obtained starting with 4-nitro-3H-phenothiazin-3-one (**2**) through selective reductions, followed of selective oxidations, O- and N-acetylations and condensation with benzaldehydes. The chemical structure of compounds was determined using chemical and spectral (¹H-NMR-, mass-, IR and UV-VIS spectroscopy) methods.

RESUMO

Os S-óxidos e S,S-dióxidos de algumas 4-nitro- e 4-amino-3-hidroxi-10H-fenotiazinas e 3H-fenotiazin-3-onas foram obtidos a partir de 4-nitro-3H-fenotiazin-3-ona (**2**) através de reduções seletivas seguidas por oxidações seletivas, O- e N-acetilações e condensações com benzaldeídos. A estrutura dos compostos foi determinada usando métodos químicos e espectroscópicos (¹H-RMN, espectrometria de massa e espectroscopia infravermelha e ultravioleta-visível).

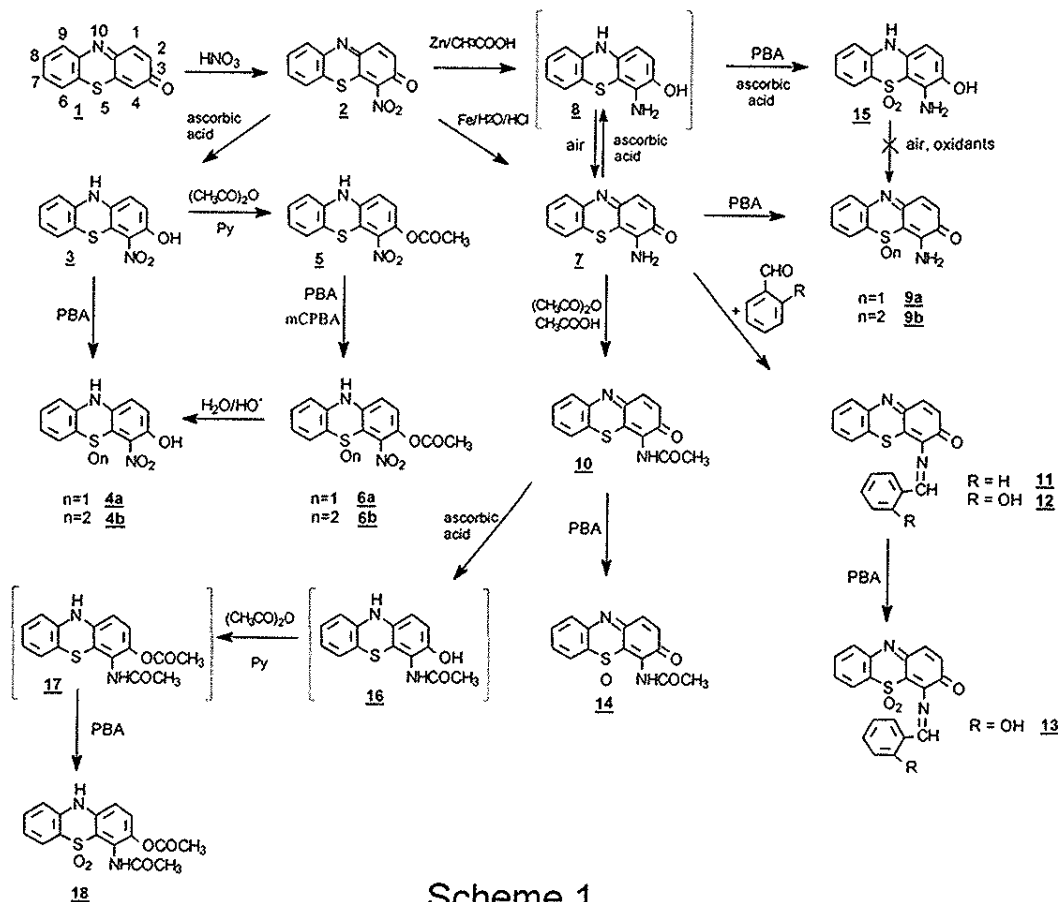
KEYWORDS: 3H-phenothiazin-3-on-S-oxides and -S,S-dioxides, 10H-phenothiazin-S-oxides and -S,S-dioxides, O- and N-acylation, selective reduction, selective oxidation, ¹H-NMR spectra.

INTRODUCTION

The interest in phenothiazine derivatives covers a wide area, but the field with the most numerous applications is the pharmaceutical one due to the biological activity of the 10H-phenothiazine and N-substituted phenothiazines.¹⁻¹² This type of compounds, substituted on the 10th position are used as antihelmintics,² antipsychotics,³⁻⁵ insecticides,⁶ antiseptics,⁷ antimicrobials,^{8,9} and anti-inflammatory agents¹⁰⁻¹² and are widely studied.

On the other hand, articles published on unsubstituted phenothiazines in the 10th position, are more scarce,¹³⁻²⁰ although these derivatives also have biological activity. Thus, some 3-hydroxy-10H-phenothiazin-S-oxides and S,S-dioxides inhibit lipoxygenase²¹ and leucotriene biosynthesis^{18,22} and were studied as metabolites of chlorpromazine with biological activity.²³ 3H-Phenothiazin-3-one (**1**) and its derivatives are cholinesterase²⁴ and leucotriene¹⁸ inhibitors, and their analgesic²⁵ and antitumor²⁶ properties have been confirmed. However, 3H-phenothiazin-3-ones S-oxides and S,S-dioxides are less studied.¹⁸

In this context this paper deals with synthesis of some new 3-hydroxy-10H-phenothiazin- and 3H-phenothiazin-3-on-S-oxides and S,S-dioxides starting with 4-nitro-3H-phenothiazin-3-one (**2**). The compounds synthesized and the transformations studied are illustrated in Scheme 1.



Scheme 1

EXPERIMENTAL SECTION

The raw material that we used was 10H-phenothiazine which was oxidized^{19,28} and then nitrated¹⁵ to obtain 4-nitro-3H phenothiazin-3-one (**2**) [IR (KBr) 1315 (NO_{2sim}) 1520 (NO_{2asim}) 1665 (C=O) cm⁻¹; UV-VIS: 376 nm, 486 nm]. Reactions and the purity of the synthesised compounds were verified using thin layer chromatography. Elemental analyses correspond to the assigned structures. Mass spectrometric measurements were performed on a Matt 3.11 mass spectrometer. Varian Gemini 300 (300 MHz) apparatus was used to record ¹H-NMR spectra; proton chemical shift are relative to deuterium signal of DMSO-d₆ as internal standard. IR spectra were recorded on a Carl Zeiss Jena UR-10 spectrophotometer (KBr) and on a Specord IR 75 (Nujol). Electronic spectra were recorded in methanol on a Specord UV-VIS spectrophotometer. Melting points were taken on an Electrothermal apparatus and are uncorrected.

3-hydroxy-4-nitro-10H-phenothiazine (3). A mixture of **2** (1g, 3.9 mmol) and ascorbic acid (3g, 16.8 mmol) in isopropyl alcohol (200 mL) was stirred at room temperature for 2 hr; water (500 mL) was added to precipitate the crude **3**. Crystallisation from methanol afforded pure **3** as violet-greyish solid (0.9g, 89.3%, m.p.=176-8°C); IR (Nujol) 1300 (NO_{2sim}) 1460 (NO_{2asim}) 3370 (N-H) cm⁻¹; UV-VIS λ(ε): 306 nm (5201), 465 nm (804).

3-hydroxy-4-nitro-10H-phenothiazin-5-oxide (4a). a). To a cooled solution (-10°C) of **3** (0.2g, 0.77 mmol) in chloroform (20 mL) was added under stirring PBA 6% (2 mL, 0.87 mmol); after 5 minutes the red insoluble solid was filtered and washed on filter (3x5 mL) with chloroform to afford **4a** (0.2g, 94%, m.p.=216-8°C); b). To a solution of **6a** (0.1g, 0.31 mmol) in acetone (50 mL) was added 20% aqueous NaOH (1 ml, 4 mmol), then the mixture was neutralised with 10% aqueous acetic acid causing precipitation of a red solid which, after filtering and washing with chloroform (3x5 mL), has the similar properties with **4a**; IR (Nujol) 985 cm⁻¹ (S=O); UV-VIS λ(ε): 364 nm (11326), 479 nm (6906).

3-acetoxy-4-nitro-10H-phenothiazine (5). A mixture of **3** (0.5g, 1.55 mmol), acetic anhydride (2 mL), pyridine (2 drops), and isopropyl alcohol (50 mL) was stirred at room temperature for 10 minutes, after which water was added (300 mL) causing precipitation of crude **5**. Crystallisation from methanol afforded pure **5** as brown fluffy crystals (0.5g, 84%, m.p.=164-6°C).

3-acetoxy-4-nitro-10H-phenothiazin-5-oxide (6a). To a solution of **5** (0.2g, 0.66 mmol) in chloroform (20 mL) was added dropwise PBA 6% (2 mL, 0.87 mmol) and stirred at room temperature for 10 minutes, when the yellow-orange suspension was filtered and the precipitate was washed with chloroform (3x10 mL) to afford **6a** as orange solid (0.2g, 95%, m.p.=226-8°C).

3-acetoxy-4-nitro-10H-phenothiazin-5,5-dioxide (6b). A mixture of **5** (0.3g, 0.99 mmol), mCPBA (2g, 11.6 mmol), methanol (30 mL) and methylene chloride (30 mL) was refluxed for 24 hr. After cooling down and evaporating to dryness, the residue was soaked with isopropyl alcohol (3x25 mL), then the resulted suspension was filtered to obtain the crude **6b**, which was soaked for 30 minutes with a mixture of benzene:acetone (4:1, 20 mL) to afford pure **6b**

(0.15g, 40.7%, m.p.=236-8°C) as beige fluffy crystals.

3-hydroxy-4-nitro-10H-phenothiazin-5,5-dioxide (4b). To a solution of **6b** (0.15g, 0.45 mmol) in acetone (20 mL) was added 20% aqueous NaOH solution (1 mL, 4 mmol), then the resulting solution was filtered and neutralised with 10% aqueous acetic acid, causing precipitation of crude **4b**, which was crystallised from methanol to afford pure **4b** (0.1g, 76,2%, m.p.=282-3°C) as light beige crystals.

4-amino-3H-phenothiazin-3-one (7). A mixture of **2** (1g, 3.9 mmol), NaCl (1g), 33% aqueous HCl (20 mL), water (200 mL) and Fe filings portionwise added was stirred vigorously at room temperature for 5 hr, then was added saturated aqueous NaHCO₃ solution to neutralise the mixture, when crude **7** precipitates; the purification of **7** was performed on a chromatographic column with Al₂O₃ III (500g) and toluene, the blue fraction was separated and vacuum distilled to afford pure **7** (0.6g, 67,89%, m.p.=185-6°C, lit.¹⁷ 186-7°C) as acicular blue crystals; IR (KBr) 1650 (C=O), 3330-3415 (NH₂), (Nujol) 1565 (C=O) 3275-3370 (NH₂), lit.¹⁷ (KBr) 1646 (C=O) 3324-3406 (NH₂) cm⁻¹; UV-VIS λ(ε): 360 nm (9210) 616 nm (3296), lit.¹⁷ (dioxane) 350 nm (12880) 587 nm (4860).

4-amino-3-oxo-3H-phenothiazin-5-oxide (9a). To a cooled solution (-10°C) of **7** (0.2g, 0.87 mmol) in chloroform (25 mL) was dropwise added PBA 6% (2.5 mL, 1.08 mmol) and stirred for 15 minutes, when the resulting suspension was filtered, and the precipitate washed with chloroform to afford **9a** (0.2g, 93.4%, m.p.=182-4 dec.) as orange solid; IR (Nujol) 965 (S=O) 1600 (C=O) 3240 (NH₂) cm⁻¹; UV-VIS λ(ε): 402 nm (4157) 486 nm (6404).

4-amino-3-oxo-3H-phenothiazin-5,5-dioxide (9b). To a solution of **7** (0.3g, 1.3 mmol) in dioxane (50 mL) was added PBA 6% (7 mL, 3 mmol) and stirred at room temperature for 30 minutes, then was added chloroform (20 mL) and 2% aqueous borax solution (100 mL). The orange organic layer was washed with water, dried over Na₂SO₄ and evaporated to dryness. The crude **9b** was crystallised in methanol to afford **9b** as dark orange solid (0.15g, 43.8%, m.p.=302-5°C dec.).

4-(acetylamino)-3H-phenothiazin-3-one (10). A mixture of **7** (0.5g, 2.2 mmol), acetic anhydride (15 mL, 147 mmol), acetic acid (10 mL), and isopropyl alcohol (100 mL) was refluxed for two days; after cooling down and evaporating to one-half of the volume, the suspension was filtered and the precipitate was washed with methylene chloride (3x5 mL) to afford **10** as acicular cherry-coloured crystals (0.4g, 67.3%, m.p.=216-8°C).

4-(acetylamino)-3-oxo-3H-phenothiazin-5-oxide (14). To a solution of **10** (0.1g, 0.37 mmol) in methylene chloride (60 mL) was added PBA 6% (0.9 mL, 0.39 mmol). After one day the resulted suspension was filtered and the precipitate was washed with methylene chloride (3x5 mL) to afford **14** as orange solid (0.1g, 94.4%, m.p.=230-2°C).

4-(benzyliden-imino)-3H-phenothiazin-3-one (11). A mixture of **7** (0.2g, 0.87 mmol), benzaldehyde (5 mL), acetic acid (10 mL), and isopropyl alcohol (30 mL) was stirred at room temperature for 2 days; after evaporation to one-third of the volume, the resulted suspension was filtered and the precipitate

was crystallised from methanol to afford **11** (0.25g, 90.9%, m.p.=160-2°C) as violet fluffy crystals.

4-[(2'-hydroxy-benzyliden)-imino]-3H-phenothiazin-3-one (12). A mixture of **7** (0.2g, 0.87 mmol), salicylic aldehyde (5 mL), acetic acid (10 mL), and isopropyl alcohol (30 mL) was stirred at room temperature for 2 days; after evaporation to one-half of the volume, the resulted suspension was filtered and the precipitate was crystallised from methanol to afford **12** (0.2g, 69.2%, m.p.=204-6°C) as violet crystals; IR (KBr) 1625 (C=O) 3585 (O-H) cm^{-1} .

4-[(2'-hydroxy-benzyliden)-imino]-3-oxo-3H-phenothiazin-5,5-dioxide (13). To a mixture of **12** (0.2g, 0.6 mmol) and dioxane (20 mL) was added PBA 6% (10 mL, 4.16 mmol). After three days was added chloroform (20 mL) and 2% aqueous borax solution (100 mL), then the yellow organic layer was washed with water, dried over Na_2SO_4 and evaporated to dryness to obtain crude **13**, which was soaked with benzene, and then the suspension is filtered to afford pure **13** (0.1g, 45,8%, m.p.=295-7°C); IR (KBr) 1130 ($\text{SO}_{2\text{sim}}$) 1330 ($\text{SO}_{2\text{asim}}$) 1653 (C=O) 3450 (O-H) cm^{-1} .

4-amino-3-hydroxy-10H-phenothiazine (8). "In situ" obtaining. To a solution of **7** (0.2g, 0.87 mmol) in isopropyl alcohol (50 mL) was added ascorbic acid (1g, 5.6 mmol) and stirred at room temperature for 15 minutes to afford the light yellow solution of **8**.

4-amino-3-hydroxy-10H-phenothiazin-5,5-dioxide (15). To the solution of **8** was added under vigorously stirring and dropwise PBA 6% (8 mL, 3.32 mmol); after 10 minutes was added chloroform (20 mL) and 2% aqueous borax solution (100 mL); then the yellow organic layer was washed with water, dried over Na_2SO_4 and evaporated to dryness. The residue was soaked with benzene, and the resulting suspension was filtered and the filtrate was evaporated to dryness to afford **15** (0.1g, 45.4%, m.p.=175-6°C dec.) as light brown solid.

4-(acetylamino)-3-hydroxy-10H-phenothiazine (16). "In situ" obtaining. To a solution of **10** (0.2g, 0.74 mmol) in dioxane (50 mL) was added ascorbic acid (1g, 5.6 mmol) and stirred at room temperature for 30 minutes to afford the light red solution of **16**.

4-(acetylamino)-3-acetoxy-10H-phenothiazine (17). "In situ" obtaining. To the solution of **16** was added acetic anhydride (5 mL, 49 mmol) and pyridine (1 mL) and the mixture was stirred at room temperature for 1 hr to afford the red solution of **17**.

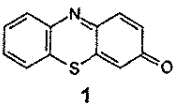
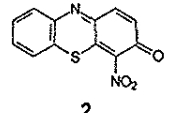
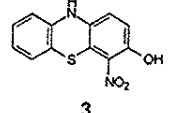
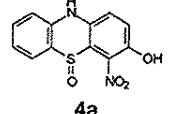
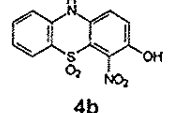
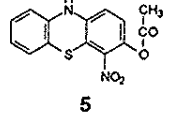
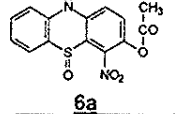
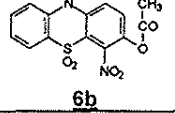
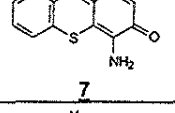
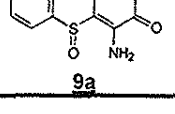
4-(acetylamino)-3-acetoxy-10H-phenothiazin-5,5-dioxide (18). To the solution of **17** was added PBA 6% (10 mL, 4.16 mmol) and stirred at room temperature for 1 hr, then was added chloroform (20 mL) and 2% aqueous borax solution (100 mL); then the organic layer was washed with water, dried over Na_2SO_4 and evaporated to dryness. The residue was soaked with benzene, the resulting suspension was filtered to afford **18** (0.1g, 35%, m.p.=252-4°C) as light red solid.

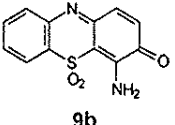
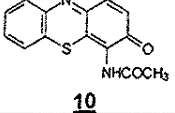
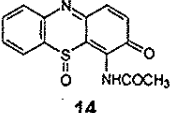
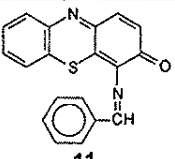
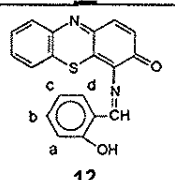
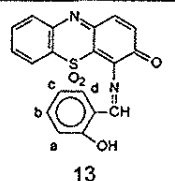
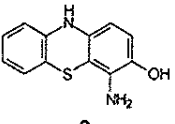
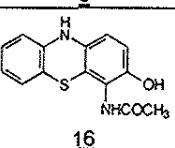
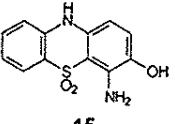
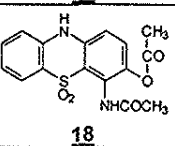
RESULTS AND DISCUSSION

The $^1\text{H-NMR}$ parameter of the synthesised compounds are presented in

Table 1. Other parameters (m.p., m/e, ν , λ_{\max}) are indicated in the Experimental section and the discussion context.

Table 1. $^1\text{H-NMR}$ Parameters of Synthesised Compounds [chemical shift (δ , ppm), coupling constant (J, Hz) and multiplicity*]

No.	COMPOUND	PHENOTHIAZINIC PROTONS							OTHER PROTONS	
		H ¹	H ²	H ⁶	H ⁷	H ⁸	H ⁹	H ¹⁰		
		3	4	5	6	7	8	9	10	
1.		7.67 10.20 d	6.90 10.20 d	7.56-7.58 - m	7.65-7.68 - m	7.56-7.58 - m	7.88 - m	-	H ⁴ : 6.86, s	
2.		7.89-7.99 - m	7.14 10.00 d	7.89-7.99 - m	8.16-8.25 - m	7.89-7.99 - m	8.17 7.22; 1.68 dd	-	-	
3.		6.75-7.10 - m							8.73 - s	O-H: 10.59, s
4.		7.55 9.12 d	7.42 9.07 d	7.92 7.63 d	7.20 7.44 t	7.61 7.31 t	7.41 8.12 d	11.23 - s		
5.		7.48 8.82 d	7.43 8.82 d	7.85 7.64 d	7.26 7.64 t	7.67 7.64 t	7.36 7.64 d	11.08 - s		
6.		7.10 8.80 d	6.96 8.80 d	7.02 7.63 d	6.86 7.45 t	7.10 7.63 t	6.77 7.63 d	9.20 - s	CH ₃ : 2.24, s	
7.		7.74 - s	7.74 - s	7.99 7.68 d	7.30 7.42 t	7.71 7.54 d	7.50 8.18 m	11.64 - s	CH ₃ : 2.31, s	
8.		7.65 9.12 d	7.80 9.33 d	7.91 8.01 d	7.35 7.54 t	7.75 7.65 t	7.44 8.37 d	11.53 - s	CH ₃ : 2.30, s	
9.		7.41 9.83 d	6.89 9.83 d	7.39-7.43 - m	7.52 5.0 t	7.65 5.0 t	7.39-7.43 - m	-	H-N: 5.70, br s	
10.		7.40 10.06 d	6.74 10.06 d	7.87 8.71 d	7.50-7.60 - m	7.71 - m	7.50-7.60 - m	-	NH ₂ : 7.71, m	

1	2	3	4	5	6	7	8	9	10
11.	 9b	7.34 10.08 d	6.76 10.08 d	8.01 7.47 d	7.62 7.17 t	7.78 6.90 t	7.70 7.47 d	-	H-N: 8.15, s
12.	 10	7.70 9.89 d	7.06 9.65 d	7.58- 7.63 - m	7.97 2.93;4.9 2 t	7.87 7.8 t	7.58- 7.63 - m	-	CH ₃ : 2.06, s N-H: 9.78, s
13.	 14	7.30 10.29 d	6.77 10.38 d	7.99 7.20 d	7.53 - m	7.76 - m	7.53 - m	-	CH ₃ : 2.13, s H-N: 5.76, s
14.	 11	7.71 9.63 d	7.07 9.81 d	7.94 7.41 d	7.86- 7.89 - m	7.49-7.52 - m	8.01 6.75 d	-	N=C-H: 9.13, s C ₆ H ₅ : 7.59, m
15.	 12	7.75 9.45 d	7.09 9.87 d	7.80 7.83 d	7.98 - m	7.41 7.41 t	7.91 4.47 d	-	N=C-H: 9.41, s O-H: 12.02, s H ^a , H ^c : 7.01- 7.04, m H ^b , H ^d : 7.62- 7.64, m
16.	 13	8.17 8.81 d	7.41 8.81 d	8.06 7.76 d	7.58 7.76 t	7.70 7.76 t	7.79 7.76 d	-	C-H: 11.22, s O-H: 11.34, s H ^a : 7.08, d, 7.34 H ^b : 7.31, t, 7.34 H ^c : 7.13, t, 7.34 H ^d : 7.38, d, 7.34
17.	 8	5.92 8.01 d	6.37 8.19 d	6.94 8.00 m	6.64- 6.72 - m	6.95 8.17 t	6.64- 6.72 - m	8.07 - s	O-H: 8.78, s
18.	 16	6.46 8.19 d	6.52 8.19 d	6.88 7.62 d	6.68 7.14 t	6.94 7.17 t	6.63 7.53 d	8.2 - s	H-O: 8.86, s 4-CO-N-H: 9.17, s
19.	 15	6.37 9.00 d	6.94 9.00 d	7.80 7.50 d	7.10 7.50 t	7.55 7.50 t	7.20 7.50 d	10.32 - s	H-O: 9.41, s H-N: 6.64, s H-N: 6.83, s
20.	 18	7.26-7.31 - m	7.48 9.08; 2.49 dd	7.87 8.16; 1.32 dt	7.26- 7.31 - m	7.64 7.8; 1.36 tt	7.22 7.95; 2.19 dd	10.98 - s	CH ₃ ³ : 2.20 CH ₃ ⁴ : 2.08 4-CO-N-H: 9.45, s

*multiplicity: s: singlet; d: doublet; t: triplet; dd: doublet of doublets; dt: doublet of triplets; tt: triplet of triplets; m: complex multiplet. CD₃SOCD₃ was used as solvent with an exception: **2** was solved in CDCl₃.

The starting compound 4-nitro-3H-phenothiazin-3-one (**2**) was synthesised from 3H-phenothiazin-3-one (**1**).¹⁵ Nitration of **1** in the 4th position is proved by the absence of the corresponding signal of the 4th position hydrogen atom in the ¹H-NMR spectrum of the 3H-phenothiazin-3-one (**1**) nitration product **2**, while the complexity of the other signals excludes the fact that the nitration occurred in the 7th position claimed before.²⁷ On the other hand, all of the ¹H-NMR spectra of the synthesised compounds from the nitration product **2** confirm the occupation of the 4th position (there does not appear any singlet signal) and the fact that the carbon atom C⁷ is linked to an hydrogen atom (the signals corresponding to H⁷ and H⁸ appear mostly as triplet and to H⁶ and H⁹ as doublet, respectively) (Figure 1).

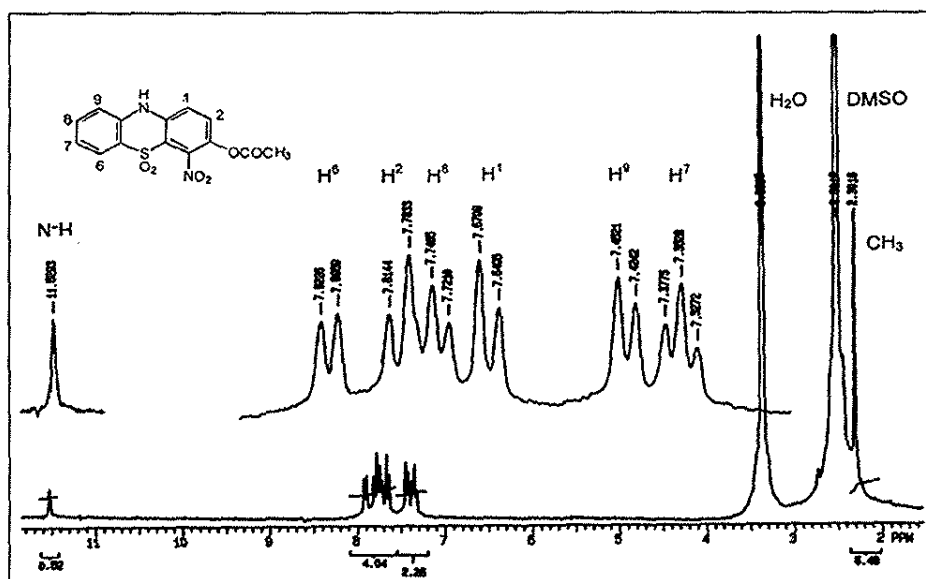


Figure 1. ¹H-NMR Spectrum of 3-Acetoxy-4-nitro-10H-phenothiazin-5,5-dioxide (**6b**) (DMSO-d₆)

Because of the presence of the p-quinon-iminic system in the 3H-phenothiazin-3-ones which is easy to reduce,^{13,14,17,18} we have tried the selective reduction its in the case of 4-nitro-3H-phenothiazin-3-one (**2**). The reduction of **2** with ascorbic acid led to 3-hydroxy-4-nitro-10H-phenothiazine (**3**); the presence of the p-hydroquinon-aminic system in **3** is proved by the ¹H-NMR spectrum where two singlet signals appears (8,37 ppm and 10,59 ppm) corresponding to the 10th position and hydroxyl group hydrogens and a general upfield shift of the hydrogens, and of the mass spectrum [*m/e*=260 (*M*⁺)], respectively.

From the literature^{13,14} is well known that perbenzoic acid (PBA) undergoes the selective oxidation of the sulphur atom, because this oxidation agent has an affinity for nonparticipating electrons of the sulphur atom.

Oxidising **3** with PBA in small excess we have obtained 3-hydroxy-4-nitro-10H-phenothiazin-5-oxide (**4a**). This selective oxidation is proved by the ¹H-NMR spectrum ($\delta_{N-H}=11,23$ ppm), mass spectrum [*m/e*=276 (*M*⁺)] and the IR one ($\nu_{S=O}=985$ cm⁻¹). The attempt to obtain directly the corresponding S,S-

dioxide **4b** through the oxidation of **3** with PBA in large excess led to a mixture of **4b** and **2**, because the excess of PBA induced the oxidation of the p-hydroquinon-aminic system, and the conversion was low due to the small solubility of the intermediate S-oxide (**4a**).

In order to avoid the oxidation of the p-hydroquinon-aminic system, the **3** was O-acetylated to obtain 3-acetoxy-4-nitro-10H-phenothiazine (**5**) [$\delta_{N-H}=9,20$ ppm, $\delta_{CH_3}=2,24$ ppm, $m/e=302$ (M^+)]. The oxidation of **5** with PBA even in great excess led only to the corresponding S-oxide [$\delta_{N-H}=11,64$ ppm, $m/e=318$ (M^+)], (Figure 2).

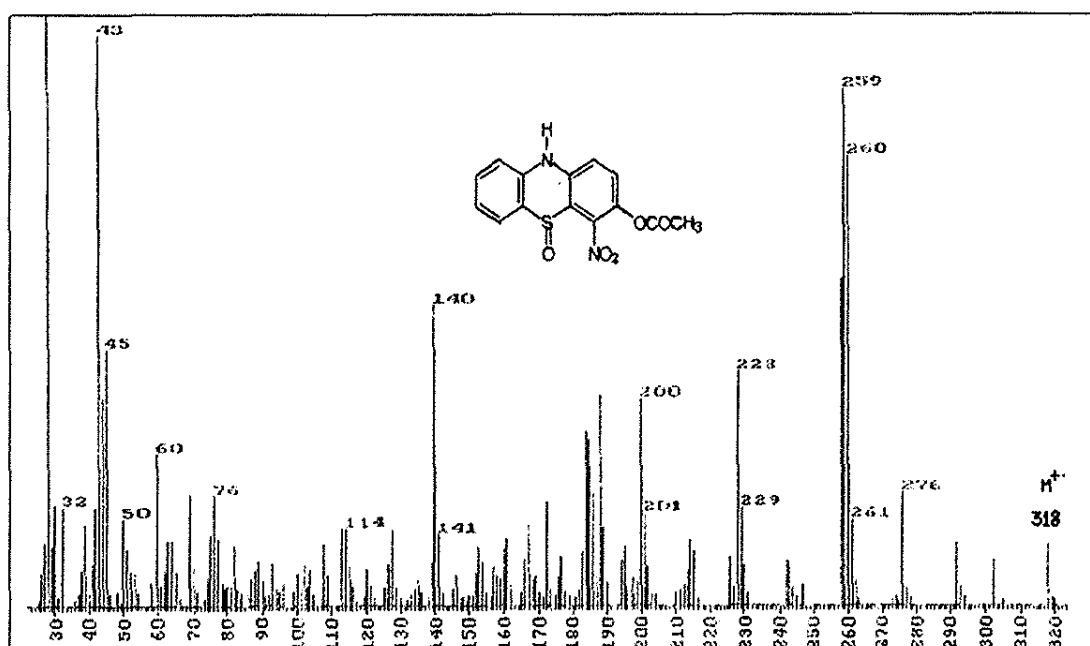


Figure 1. $^1\text{H-NMR}$ Spectrum of 3-Acetoxy-4-nitro-10H-phenothiazin-5-oxide (**6a**) (DMSO-d_6)

The corresponding S,S-dioxide **6b** was obtained using m-chloroperoxybenzoic acid (mCPBA) in harder conditions (refluxed for 24 hours). The S,S-dioxide **4b** was easily obtained through basic hydrolysis of **6b** [$\delta_{N-H}=11,08$ ppm, $m/e=292$ (M^+)]. By hydrolysing the **6a** we obtained a red coloured compound which presents the same characteristics as the S-oxide **4a**. In the $^1\text{H-NMR}$ spectra of **4a** and **4b** the signals of the hydroxy group do not appear because the signal is expanded and flattened due to the proton exchange with water from the solvent (DMSO-d_6).

The selective reduction of nitro group from 4-nitro-3H-phenothiazin-3-one (**2**) was performed with $\text{Fe}/\text{H}_2\text{O}/\text{HCl}$ to obtain 4-amino-3H phenothiazin-3-one (**7**). A small amount of 4-amino-3-hydroxy-10H-phenothiazine (**8**) was also obtained as shown by thin layer chromatography (TLC), which was rapidly oxidised to **7** by air. We have to mention that this reduction was previously done¹⁷ with $\text{Zn}/\text{CH}_3\text{COOH}$, but with lower yield. Our reduction product (**7**) has the same properties (m.p., IR, UV-VIS data) as those from literature. The $^1\text{H-NMR}$ (absence of 4th, 10th positions and O-H hydrogens corresponding signals) and mass [$m/e=228$ (M^+)] spectra confirm the assigned structure.

In order to prove in a chemical way the presence of the amino group, **7** was acetylated and condensed with carbonyls. Another reason for these reactions was to protect the amine group against oxidation.

The oxidation of **7** with a small excess of PBA led to 4-amino-3-oxo-3H phenothiazin-5-oxide (**9a**) [$\nu_{S=O}=965\text{ cm}^{-1}$, $m/e=244\text{ (M}^+)$]. Using a greater excess of PBA we obtained a mixture of oxidation products, out of which we could isolate the corresponding sulphone 4-amino-3-oxo-3H phenothiazin-5,5-dioxide (**9b**) [$m/e=260\text{ (M}^+)$].

The reactivity of amino group as nucleophile is decreased because the nonparticipating electrons of nitrogen interact with the phenothiazine Π electron system of **7**, and because of that, N-acetylation needs drastic conditions (excess of reagents, acid environment). For condensation we have chosen carbonyls with increased reactivity (benzaldehyde, salicylic aldehyde). Thus, 4-acetylamino-3H-phenothiazin-3-one (**10**), 4-benzylidenimino-3H-phenothiazin-3-one (**11**), and 4-(2'-hydroxy-benzyliden)imino-3H-phenothiazin-3-one (**12**), were obtained and were afterwards oxidised. The oxidation of these compounds occurred slowly because of sterical impediments brought by sizeable groups linked in the 4th position, which required the use a large excess of PBA (350-500%). This large excess led to complex mixtures of oxidation compounds, out of which we could isolate only 4-(2'-hydroxy-benzyliden)imino-3-oxo-3H-phenothiazin-5,5-dioxide (**13**) [$\nu_{SO_{2sim}}=1130\text{ cm}^{-1}$, $\nu_{SO_{2asim}}=1330\text{ cm}^{-1}$, $m/e=364\text{ (M}^+)$]. Surprisingly, using just a stoichiometric amount of PBA we obtained the corresponding S-oxide of **10**, 4-acetylamino-3-oxo-3H-phenothiazin-5-oxide (**14**). The hydrolysis of **13** and **14** performed in order to obtain **9b** and **9a**, respectively, was unsuccessful.

The reduction of p-quinon-iminic system from **7** with ascorbic acid occurs rapidly to obtain "in situ" 4-amino-3-hydroxy-10H-phenothiazine (**8**). All attempts to isolate **8** led to a mixture in which **7** was prevalent, because of the oxidation tendency of p-hydroquinon-aminic system, tendency that is increased by the amino group. The oxidation of **8** obtained "in situ", with PBA, led to a yellow-brown compound which has two singlet signals (9,41 ppm and 10,32 ppm) corresponding to a p-hydroquinon-aminic system (O-H and N-H, respectively) in the ¹H-NMR spectrum, proving the formation of 4-amino-3-hydroxy-10H-phenothiazin-5,5-dioxide (**15**). The existence of withdrawing sulphone group in **15** induced a relative stability of p-hydroquinon-aminic system. On the other hand, this sulphone group, which is *ortho* to the amino group, led to a destabilisation of the molecule, so **15** was unstable in solid state in the presence of air.

In order to improve the synthesis of **15** we have protected the p-hydroquinon-aminic system and the amino group by acylation. Thus, we have O-acylated "in situ" 4-acetylamino-3-hydroxy-10H-phenothiazine (**16**), which was obtained through reduction of **10** with ascorbic acid. The intermediate 4-acetylamino-3-acetoxy-10H-phenothiazine (**17**) was oxidised "in situ" to the corresponding S,S-dioxide **18**, which ¹H-NMR spectrum has the signals corresponding to the 10th position and acetylamino hydrogens (10,97 ppm and 9,45 ppm, respectively) as well as the signals of the two methyl groups of O- and N-acetyls (2,20 ppm and 2,08 ppm, respectively). The basic or the acid

hydrolysis of **18** led to complex mixtures, out of which we could not isolate the expected sulphone **15**.

CONCLUSIONS

In this paper we report the obtainment of fifteen new 10H-phenothiazine and 3H-phenothiazin-3-one compounds. Among these ten are S-oxides and S,S-dioxides, respectively. We did not succeeded to isolate the S-oxide or S,S-dioxide corresponding to 4-nitro-3H phenothiazin-3-one (**2**), unlike 4-amino-3H-phenothiazin-3-one (**7**) and its 4-amino group derivatives (**10-12**). This difference of reactivity seems to have an electronic reason (the strong positivation of the sulphur atom in **2**). However, 4-nitro-10H-phenothiazine derivatives (**3, 5**) gave S-oxides and S,S-dioxides with peracids.

We also noticed the stability of S-oxides and S,S-dioxides (**9a, 9b, 13, 14**) toward nucleophilic addition in 4th and 10th positions, addition that occurred at the unsubstituted in 4th position analogs.¹⁸ This differentiation allowed us to directly synthesise S-oxides and S,S-dioxides **9a, 9b, 13, 14**.

REFERENCES

1. A. Albert, "Selective Toxicity", 5th ed., Chapman and Hall, London, 1973, p. 18.
2. H.McL. Gordon, M.J. Lipson, *Conn. Sci. Ind. Res. (S.A.)*, **13**, 173 (1940).
3. N. Griffon, C. Pilon, F. Santel, J.C. Schwartz, P. Sokoloff, *J. Neural. Transm.*, **103(10)**, 1163-1175 (1996); Chem. Abstr. **126**, 54678v (1997).
4. G.M. Gilad, V.H.I. Gilad, **US 5,677,349**; Chem. Abstr. **127**, 341809k (1997).
5. G. Avrutskij, A.I. Altumin, **RU 2,077,322**; Chem. Abstr. **127**, 158795p (1997).
6. J. Hrivikova, V. Kello, *Chem. Zvesti*, **127**, 249-54 (1973); Chem. Abstr. **79**, 54614c (1973).
7. J.O. Thomas, *J.Pharmacol. Exp. Ther.*, **64**, 280 (1938).
8. N. Motohashi, K. Sakagami, *Anticancer Res.*, **12(4)**, 1207-10 (1992); Chem. Abstr. **121**, 78114b (1994).
9. D.M. Purshig, D.S. Mehta, V.M. Shah, *Heterocycl. Commun.*, **2(5)**, 469-74 (1996); Chem. Abstr. **126**, 74801d (1997)
10. P.C. Isakson, G.D. Anderson, A. Susan, **PCT INT Appl. WO 96 41,626**; Chem. Abstr. **126**, 166479h (1997).
11. P.C. Isakson, G.D. Anderson A. Susan, **PCT INT Appl. WO 96 41,625**; Chem. Abstr. **126**, 166481h (1997).
12. T. Ram, R. Tyagi, B. Goel, *Indian Drugs*, **35(4)**, 216-21 (1998); Chem. Abstr. **129**, 109052b (1998).
13. T. Panea, V. Farcasan, C. Bodea, *Rev. Roum. Chim.*, **18**, 1259-62 (1973).
14. a) C. Bodea, T. Panea, **Fr. Pat. 2102567** (1972); b) C. Bodea, T. Panea, **Fr. Pat. 2105307** (1972); c) C. Bodea, T. Panea, **Rom. 53,098**, 1972; d) T. Panea, C. Bodea, **Rom. 53,099** (1972).
15. C. Bodea, M. Terdic, E. Broser, *Liebigs. Ann. Chem.*, **715**, 122-7 (1968)
16. T. Panea, C. Bodea, V. Farcasan, *Rev. Roum. Chim.*, **16**, 759 (1971)
17. E. Broser, C. Bodea, *Rev. Roum. Chim.*, **17(10)**, 1747-53 (1972)

18. Y. Girard, M. Therim, J.P. Springer, J. Hirshfield, *J. Org. Chem.*, **52(18)**, 4000-6 (1987)
19. Y. Guindon, R. Fortin, C.K. Lau, **Eur. Pat. Appl. EP 115,394**; Chem. Abstr. **101**, P230555t (1984)
20. M. Terdic, *St. Cerc. Chim.*, **13(6)**, 579-94 (1965)
21. M.V. Goldenberg, **Eur. Pat. Appl. EP 155,623**; Chem. Abstr. **104**, P45759m (1986)
22. R. Fortin, Y. Guindon, C.K. Lau, J. Rokach, **Eur. Pat. Appl. EP 138,481**; Chem. Abstr. **104**, 15081s (1986)
23. B.M. Cohen, M. Herschel, A. Aoba, *Psychiatry Res.*, **1(2)**, 199-208; Chem. Abstr. 1980, **92**, 69369u (1979)
24. I. Ghizdavu, C. Bodea, L. Ghizdavu, *Bull. Inst. Agron. Cluj-Napoca*, **31**, 65-71 (1977)
25. Merck Frosst Canada Inc., **Jpn. Kokai Tokkyo Koho JP 59,144,774** [84,144,774]; Chem. Abstr. **102**, P6515t (1985)
26. H. Yoshino, N. Ueda, J. Nijima, **PCT. Int. Appl. WO 95 03,279**; Chem. Abstr. **122**, P413588 (1995)
27. M. Raileanu, I. Radulina, S. Florea, *Rev. Roum. Chim.*, **11(2)**, 1419-22 (1966)
28. M. Raileanu, *Rev. Chim.*, **34**, 113-5 (1983)

OPTIMIZATION OF ETHYLENE POLYMERIZATION CONDITIONS WITH METALLOCENE CATALYST USING EXPERIMENTAL DESIGN METHODOLOGY

Luciano Endres^a and Carlos R. Wolf^{a,b}

^a Ipiranga Petroquímica S.A., Pólo Petroquímico do Sul, Triunfo, RS, Brasil, CEP 95453-000
E-mail: endres@ipiranga.com.br Tel.00 55 51 4575600
E-mail: crwolf@ipiranga.com.br Tel. 00 55 51 4575598

^b Departamento de Química, Universidade Luterana do Brasil – ULBRA, Canoas, RS, Brasil, CEP 92420-280
E-mail: crwolf@conex.com.br Tel. 00 55 51 4779163

ABSTRACT

A study of ethylene polymerization was carried out using a 2³ full factorial design in order to obtain a better understanding of the metallocene catalyst system. Three independent variables (reaction temperature, Al/Zr ratio and ethylene pressure) were evaluated at two levels. The observed responses were catalytic yield, average molecular weight, polydispersity, melt flow rate, density, melting temperature, enthalpy of fusion and crystallinity, the yield being of primary interest. The catalyst, co-catalyst and the solvent used were, respectively, Et(Ind)₂ZrCl₂, methylaluminoxane (MAO) and n-hexane. The statistical model was efficient in describing the effect of the variables on the yield and showed that the temperature was the variable of larger influence. The results permitted conclusions about the best polymerization conditions.

RESUMO

Buscando conhecer melhor os catalisadores metalocênicos realizou-se um estudo para otimização das condições de polimerização do etileno usando metodologia de delineamento experimental via plano fatorial completo 2³. Relacionou-se as variáveis independentes temperatura de reação, razão Al/Zr e pressão de etileno com as respostas, principalmente o rendimento catalítico. Como catalisador, cocatalisador e solvente foram usados, respectivamente, Et[Ind]₂ZrCl₂, metilaluminoxana (MAO) e n-hexano. Analisando-se os dados foi possível concluir que o modelo estatístico utilizado foi eficiente e possibilitou a identificação da temperatura como variável de maior influência no rendimento das polimerizações na região testada. Demais respostas, como massa molar, polidispersidade, taxa de fluidez e densidade também foram estudadas, possibilitando conclusões a respeito das propriedades dos polímeros obtidos e das melhores condições de polimerização.

KEY WORDS: metallocene, ethylene polymerization, experimental design.

INTRODUCTION

The thermoplastic industry is undergoing an innovation phase, particularly with respect to the development and use of metallocene/methylaluminoxane catalyst systems for polymerization of α -olefins^{1,2}. They are distinctly different from Ziegler-Natta catalysts because they facilitate the production of polymers with oriented and diversified molecular structure and can be used in copolymerization with many monomers, offering great versatility in the copolymer formation. These polyolefins can substitute other materials, such as elastomers and engineering plastics, having the advantage that they facilitate recycling due to a smaller variety of materials in the reject^{3,4,5}.

There are big differences in the microstructure of the polymeric materials produced with these two types of catalysts. The metallocenes are soluble in hydrocarbon solvents and their active sites are all equivalent in reactivity. They behave in an identical way during polymerization and this results in a polymer with a narrow molecular weight distribution and high uniformity along the chain as far as ramifications and comonomer distribution are concerned. The physical properties (mechanical, thermal, electrical, optical and rheological) are better defined and can be controlled in a precise way, leading to a better performing final product. Thus, kinetic and molecular modelling of the polymer can be done for a wide variety of niches⁶.

Chemometrics Considerations

According to Hunter⁷, those involved with chemistry should be involved with statistics as well, simply because statistics tells you what your data mean. An important illustration of the influence of chemistry on statistics was the work of W. S. Gosset, under the pseudonym "Student" who empirically derived t distribution. The term chemometric was applied for the first time by chemists in order to formalize the study of the application of mathematical methods to chemical sciences. S. Wood appears to have been the first person who worked in pattern recognition methods. Although formally pattern recognition methods gave rise to the term chemometrics, the use of statistical methods for the study of chemical processes has been known for a long time⁸.

Experimental Design, Analysis of Variance (ANOVA) and Tests of Hypothesis

The statistical experimental design had its origin in work of Ronald Fisher and is best exemplified in his two classical books, "Statistical Methods for Research Workers"⁹ and "The Design of Experiments"¹⁰. He showed that, through the simultaneous combination of several factors it was possible to obtain information on separate effects from a large number of factors. Tests in which each factor is varied separately may lead to wastes and false results. The grouping of a series of experiments in blocks can show better the influence of various factors as well as reduce the number of experiments. The planning of tests in random order may guarantee additional protection against bias caused by unknown or uncontrollable factors⁷. An important

type of experimental design used in chemistry is the factorial design. In this case, m levels of k factors are worked in several combinations. Usually two levels are used (where the factors assume values of -1 and +1), giving a 2^k factorial design, that allows the estimation of the main effects of each factor (first order influence), coupled influences (2^{nd} , 3^{rd} order) can also estimate interaction effects in the obtained answers. An empirical representation of how a group of factors can influence the answer is given by the polynomial model⁷:

$$y = B_0 + \sum_i B_i x_i + \sum_i B_{ii} x_i^2 + \sum_{i \neq j} \sum B_{ij} x_i x_j$$

Where y = predicted value, x_i = controlled factors, B_0 , B_i , B_{ii} , B_{ij} are coefficients of the constant term (independent), first order, second order, and cross-product coefficient, respectively.

Analysis of Variance (ANOVA) is a technique by which it is possible to isolate and estimate the variances that contribute to the total variation of an experiment. It allows the identification of variables that are important and it establishes means to estimate their effects¹¹. When the effect of several factors on an answer variable is desired, an analysis of variance is made using more than one classification factor and a comparison of the variance of each factor in the study is done with respect to the relative variance to the residue or inherent error of the measure.

Tests of hypothesis, also called significance tests, are used a lot in analysis of variance. A test of hypothesis considers the H_0 hypothesis (null hypothesis) to be tested and the H_1 complementary hypothesis, also called alternative. These hypotheses are formulated on populational parameters, with their acceptance or rejection being based on sampling results¹². The F test in the factorial model evaluation consists of the comparison of calculated F with controlled F for the significance level chosen for the test. The calculated F consists of the ratio between the variance of the terms of the model and the relative variance to the residue. The factorial design is based on a first degree polynomial model, without quadratic terms that would give a second degree equation. For each answer a curvature test is necessary and it consists of comparison of factorial model points average with the central points average. The F test is, of course, applied also on this curvature¹³.

In order to evaluate the significance of the coefficients, the t test is applied. This consists in comparing calculated t with controlled t for the significance level chosen for the test. Calculated t is the ratio of the estimated coefficient for each factor and the standardized error. The calculated t value actually represents the number of standard deviations of the coefficient from zero¹³.

METHODOLOGY

The polymerizations were performed using a 1.5 L steel reactor. The experimental procedures were carried out under inert atmosphere, using the Schlenk technique. The ethylene, used as monomer, was provided by Companhia Petroquímica do Sul (COPESUL), Triunfo, RS, Brazil. The metallocene catalyst was supplied by Witco GmbH Polymer Chemicals Group, P.O.

Box 1620, D-59180, Bergkamen, Germany. It consist of 1,2-ethylene-bis-indenyl-zirconium dichloride, $\text{Et}[\text{Ind}]_2\text{ZrCl}_2$ (racemic mixture), with the trade name EURECEN[®]5036, code no. TA02677. The co-catalyst methylaluminoxane (MAO) was supplied by Albemarle Co., Florida Street, LA, USA. The catalyst was diluted with toluene supplied by Merck do Brasil, Rio de Janeiro. The solvent used for polymerization was n-hexane, polymeric grade, supplied by Phillips Co. The solvent was purified by drying for 12 hours with molecular sieve 10A - Grace 544, previously dried at 200°C for 4 hours, followed by fractional distillation in the presence of metallic sodium and benzophenone as indicator using a Vigreux column of 100 cm height, packed with glass.

A complete 2^3 factorial design was elaborated having three replicates in the central point, and three independent variables, temperature, Al/Zr ratio and ethylene pressure. They were evaluated at two levels (+ and -). All the design data is shown in Table 1.

Table 1. Full factorial design 2^3 for ethylene polymerization

Factors				Coded Factors		
Order*	Temp.** (°C)	Al/Zr*** Ratio	Ethylene Pressure (bar)	Temp. (°C)	Al/Zr Ratio	Ethylene Pressure (bar)
4	50.0	1000	1.00	-	-	-
9	80.0	1000	1.00	+	-	-
3	50.0	2500	1.00	-	+	-
10	80.0	2500	1.00	+	+	-
11	50.0	1000	4.00	-	-	+
8	80.0	1000	4.00	+	-	+
5	50.0	2500	4.00	-	+	+
7	80.0	2500	4.00	+	+	+
2	65.0	1750	2.50	0****	0	0
6	65.0	1750	2.50	0	0	0
1	65.0	1750	2.50	0	0	0

*Random order. **Temperature. ***Without dimension. ****Replicates in the central point.

The replicates in the central point are important because they can supply an estimate of the experimental error used in the ANOVA of the model. The central point is also useful for the evaluation of the presence of curvature. The DESIGN-EXPERT[®] software, version 5.0.9 supplied by STAT-EASE Inc., Minneapolis, MN, USA, was used to facilitate the statistical calculations, necessary for a consistent factorial model evaluation. Using the DESIGN-EXPERT[®] software each answer was analyzed according to the following sequence: selection of main effects, graphical visualization of the effects through normal probability plots^{14,15}, analysis of variance, evaluation of residues and detection of outliers. Once the existence of a valid predictive model was confirmed, a detailed interpretation of the results represented by a series of graphs was performed.

RESULTS AND DISCUSSION

The experiments for the factorial design (2^3), the yield and the activity of the polymerizations, as well as the results obtained for the characterization of the polymers are illustrated in Tables 2 and 3.

Table 2. General results obtained for the polymerization of ethylene – factorial design (2^3)

Experiments			Results					
Independent Variables			Dependent Variables					
T °C	Al/Zr Ratio	P ethylene bar	Yield g	Activity g/mmol cat	Mn* g/mol	Mw** g/mol	Mz*** g/mol	Pd****
-	-	-	3.5	7.46E+05	61500	185000	497000	3.0
+	-	-	16.2	3.45E+06	51000	155000	459000	3.0
-	+	-	7.4	1.58E+06	54400	152000	357000	2.8
+	+	-	14.9	3.18E+06	42000	126000	344000	3.0
-	-	+	5.7	1.22E+06	40900	120000	405000	2.9
+	-	+	35.6	7.59E+06	40800	127000	479000	3.1
-	+	+	12.2	2.60E+06	50200	133000	363000	2.6
+	+	+	39.8	8.49E+06	33700	98000	298000	2.9
0	0	0	17.0	3.62E+06	54400	160000	414000	2.9
0	0	0	18.2	3.88E+06	65500	198000	508000	3.0
0	0	0	18.0	3.84E+06	61200	163000	403000	2.7

*Number average molecular weight. **Weight average molecular weight. ***Z average molecular weight. ****Polydispersity = Mw/Mn.

Analysis of the Yield Results

The importance of the main effects, temperature (A), Al/Zr ratio (B) and ethylene pressure (C) is illustrated in Figure 1 in terms of half normal probability plots. This figure is useful for the selection of effects for the ANOVA.

Table 3. General results obtained for the polymerization of ethylene – factorial design (2³)

Experiments			Results				
Independent Variables			Dependent Variables				
T °C	Al/Zr Ratio	P ethylene bar	MFR (190/21,6)* g/10 min	Dens.** g/cm ³	Tm*** °C	ΔH _f **** J/g	Crys.***** %
-	-	-	0.08	0.976	125	177	59
+	-	-	1.00	0.960	125	189	64
-	+	-	0.00	1.065	122	144	47
+	+	-	1.60	0.969	124	188	63
-	-	+	2.80	0.968	126	189	63
+	-	+	2.90	0.956	125	190	65
-	+	+	0.38	0.971	126	186	61
+	+	+	2.80	0.959	125	196	66
0	0	0	0.10	0.961	124	176	59
0	0	0	0.07	0.954	122	160	52
0	0	0	0.12	0.954	122	172	58

*Melt flow rate at 190°C and 21.6 kg, according to ISO 1133/97, ASTM D1238/95. **Density according to ASTM D792/98 method B, ISO 1183/87 method A. ***Melting temperature. ****Enthalpy of fusion. *****Crystallinity. The thermal analyses were carried out according to ASTM D3417/97, ASTM 3418/97.

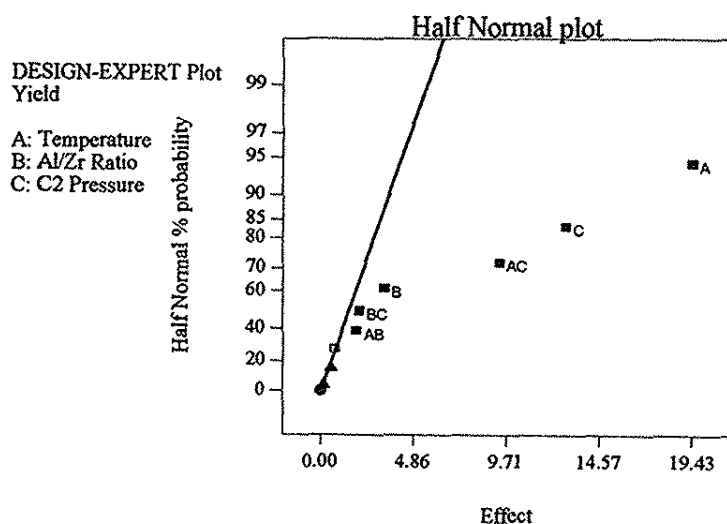


Figure 1. Half normal probability plot of effects

Values far from the straight line, which represents the error, have more significant effects, and values very close to the straight line are not considered significant. In the calculations, the effect of 3rd order (ABC) was not considered. Analysis of the ANOVA results for the polymerization yield (Table 4) shows that the terms of the model are not a consequence of population error. It is possible to reject the H_0 hypothesis (null hypothesis) considering a significance level of 0.0002 (99.98% of confiability). The F test of Snedecor was used in the evaluation.

The results of the F test for curvature, indicate that it is not possible to reject the hypothesis of the existence of curvature. The curvature presented by the model is significant and a 1st degree polynomial model is not adaptable for a significance level of 0.2226 or 77.74 % of confiability. However the predictions obtained through the equation were satisfactory, indicating a valid factorial model in spite of the existence of curvature. Analysis of the variance of the coefficients through the Student t test, considering a maximum significance level of 0.05 (95% of confiability), shows that is not possible to reject H_0 only for the central point. The results obtained for the yield are shown in Table 4.

Table 4. Analysis of variance (ANOVA) for the yield results

Model evaluation – F Test (Snedecor)		
	<i>Calculated F Value</i>	<i>Prob. > F (significance level)</i>
Model	347.6	0.0002
Curvature	2.35	0.2226
Coefficient evaluation – t Test (Student)		
	<i>t for H_0 (coef. = 0)</i>	<i>Prob. > t (significance level)</i>
A – temperature	34.86	< 0.0001
B - Al/Zr ratio	5.96	0.0095
C - C ₂ pressure	23.02	0.0002
AB	3.37	0.0433
AC	16.74	0.0005
BC	3.62	0.0361
Central point	1.53	0.2226

Once the analysis of variance was concluded, an equation for factors was obtained. This equation can be used to predict yields under various independent variables values in the analyzed area, but in this case, it is necessary to use the equation for uncoded factors. The final equation for coded factors is as follows:

$$\text{Yield} = 16.9150 + 9.7150A + 1.6600B + 6.4150C - 0.9400AB + 4.6650AC + 1.0100BC$$

The yield results representations are shown in Figures 2 and 3. The 2^3 factorial model is illustrated in Figure 2, while Figure 3 shows the surface answer of these results with respect to temperature and pressure of ethylene using a ratio of 1750 for Al/Zr. The temperature exhibits the main effect in the system studied, it showed better results in the t test and contributed the largest coefficient in the final equation of the coded factors.

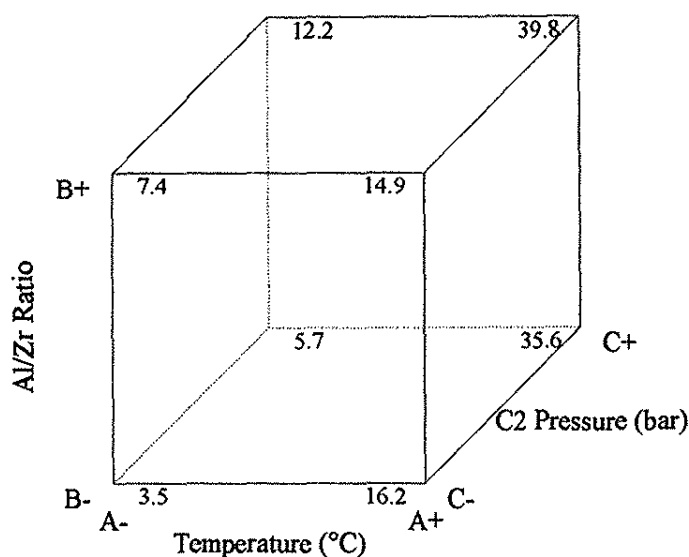


Figure 2. Yield results arranged in the vertexes of a cube

Analysis of the Characterization Tests

The ANOVA of the characterization results are shown in Table 5. As can be seen, the terms of the model are a result of the population error. This means that it is not possible to reject the null hypothesis (H_0) that affirms that the model terms are part of the population error considering a maximum significance level of 0.05 (95 % of confiability) and making use of the F test. The results of MFR (190/21.6) and density presented satisfactory results with respect to the validity of the model. However, the analysis of the coefficients estimated for the factors using the t test and considering a maximum significance level of 0.05 exhibited satisfactory results only for the density tests.

As far as the properties obtained for the polymers are concerned the results were in accordance with those reported in the literature and the best agreement was obtained for the polydispersity¹⁻⁵. A more careful analysis of the results shown in Tables 2 and 3 showed some incoherences for some structure-property relationships.

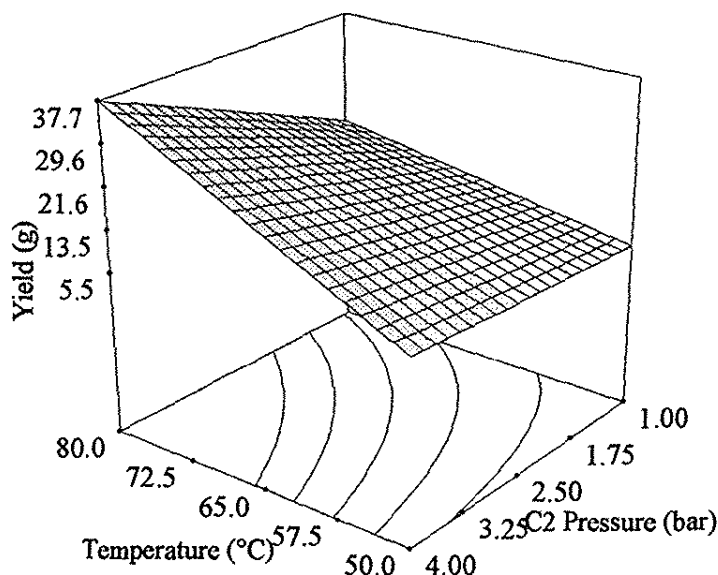


Figure 3. Surface answer of yield results with respect to temperature and pressure of ethylene using a ratio of 1750 for Al/Zr

Table 5. ANOVA for the characterization tests

Model evaluation – F Test (Snedecor)			
Characterization Tests		Calculated F Value	Prob. > F (significance level)
Mn	g/mol	2.74	0.2930
Mw	g/mol	1.57	0.4433
Mz	g/mol	1.54	0.4487
Pd	-	1.03	0.5745
MFR (190/21.6)	g/10 min	2502	0.0004
Density	g/cm ³	88.52	0.0112
Tm	°C	1.09	0.5583
ΔH_f	J/g	4.03	0.2134
Crystallinity	%	3.02	0.2715

A reduction in the melt flow rate (MFR) was not observed with the increase in the number average molecular weight (Mn) as expected. This may be due to the fact that hydrogen, that is a very important factor in molecular weight control was not used and, consequently, the polymers exhibited very high molecular weight and very low melt flow rate (MFR) and as a consequence difficulty was encountered in their material processing and characterization. The polydispersity showed very low values, confirming that polymerization occurred at a single site. The low

polydispersity values may be responsible for the low melt flow rate found. A narrow polydispersity range may be indicative of the lack of the short chain fraction that would act as lubricant during the processing, in this particular case, during the displacement of the polymer in the plastometer.

The values obtained for the density were quite high. A discrepancy was also noted between density and crystallinity. In some cases, materials with larger density (smaller free volume, closer molecules and a larger ordering of the lamellae) showed lesser crystallinity, contrary to what would be expected. These contradictory results may be explained in terms of an inadequate material morphology. Since the comonomer was absent, high density values were expected. The crystallinity had oscillations typical of values for high density polyethylene (HDPE). On the other hand, the values obtained for the melting temperature (T_m) were low and close to typical values of linear low density polyethylene (LLDPE) when compared to results of HDPE synthesized with Ziegler-Natta catalyst. This behavior was expected because lower T_m values are also usually observed for polypropylene (PP) and LLDPE synthesized with metallocenes¹⁶. A better evaluation of the structure-property relationship can be obtained using other analytical techniques such as X-ray diffraction, rheology and nuclear magnetic resonance.

CONCLUSIONS

The methodology of full factorial design (2^3) was efficient and satisfactory for the optimization of the ethylene polymerization conditions with metallocene catalyst. As expected, the temperature, the ethylene pressure and the Al/Zr ratio had important effects on the catalytic yield. The temperature was the most important variable, a small alteration in temperature resulting in an important alteration in the yield. The optimized polymerization condition was in the superior level tested ($T = 80^\circ\text{C}$; $P = 4$ bar; $\text{Al/Zr} = 2400$). The Al/Zr ratio had a small influence on the yield results and it is possible to work with temperature and ethylene pressure in the superior levels using a smaller ratio of Al/Zr than the one mentioned above.

One important factor that needs considerable additional future investigation is the presence of hydrogen and its role in molecular weight control, polydispersity and material processing. The obtained knowledge regarding the statistical techniques and physical-chemistry of the analyzed area will be useful for future works with metallocene catalyst systems.

The statistical analysis of the results obtained for M_n (number average molecular weight), M_w (weight average molecular weight), M_z (Z average molecular weight), polydispersity (M_w/M_n), melt flow rate - MFR (190/21.6), T_m (melting temperature), ΔH_f (enthalpy of fusion) and crystallinity, did not permit the establishment of a satisfactory linear correlation between them and the independent variables (temperature, ethylene pressure and Al/Zr ratio) for the conditions tested. For the density results it was possible to establish a consistent statistical model. On the other hand, some inconsistencies or incoherences were observed for the structure-property relationship. On the whole, the results were useful for the characterization for the synthesized polymers.

ACKNOWLEDGMENT

We express our gratefulness to Ipiranga Petroquímica S.A. for providing the opportunity to carry out this work and thank the laboratory technicians for the characterization tests. We also thank Witco and Albemarle for supplying, respectively, the catalyst and co-catalyst. Special thanks are also due to the research group in the Chemistry Department at ULBRA.

REFERENCES

1. J. C. Stevens, "Constrained geometry and other single site metallocene polyolefin catalysts: a revolution in olefin polymerization". Proceedings of the 11th International Congress on Catalysis, Studies in Surface Science and Catalysis. vol. 101, 1996.
2. J. H. Schutt, "The metallocene catalyst ferment continues", Plastic World, May (1995).
3. M. de F. V. Marques, P. A. C. Junior, M. J. C. Guimarães, F. M. B. Coutinho, "Catalisadores metalocênicos: aspectos gerais e heterogeneização". Polímeros: Ciência e Tecnologia, São Carlos, SP, Brazil, pp. 26-40, jul./set., 1998.
4. M. C. Porter, "Competitive strategy", The Free Press, New York, 1980.
5. F. A. Ribeiro F°, "Metalocenos: revolução tecnológica na indústria de polímeros", PETROQUISA (internal report), Rio de Janeiro, RJ, Brazil, 1994.
6. F. A. Ribeiro F°, M. J. S. F. Netto, C. A. Herais, "A introdução de catalisadores metalocênicos como estratégia competitiva da indústria de termoplásticos", Polímeros: Ciência e Tecnologia, São Carlos, SP, Brazil, pp. 53-62, jul./set, 1997.
7. J. S. Hunter, "Applying statistics to solving chemical problems", Chemtech, pp. 167-169, March, 1987.
8. P. Amaral, "Introdução à quimiometria", captured on Aug. 14th (1998), online, Internet <http://www.dq.fct.unl.pt/qof.html>.
9. R. A. Fisher, "Statistical methods for research workers", Oliver & Boyd, London, 1925.
10. R. A. Fisher, "The design of experiments", Oliver & Boyd, London, 1935.
11. F. Cunha, "Metodologia de pesquisa - planejamento de experimentos" (monograph), Gravataí, RS, Brazil, 1992.
12. M. A. C. Góes, "Métodos estatísticos para análise de processos" (monograph), Rio de Janeiro, RJ, Brazil, 1995.
13. DESIGN-EXPERT 5, Stat-Ease Corp. (reference manual), Minneapolis, MN, USA, 1998.
14. G. E. P. Box, W. G. Hunter, J. S. Hunter, "Statistics for experimenters. A introduction to design, data analysis and model building", John Wiley, New York, 1978.
15. C. Daniel, "Applications of statistics to industrial experimentation", John Wiley, New York, 1976.
16. W. Bidell, D. Fischer, R. Hingmann, P. Jones, F. Langhauser, H. Gregorius, B. Marczinke, "New metallocene-based products for future growth in the uses of polypropylene", (internal report), prepared for presentation at MetCon'96, BASF AG, Ludwigshafen, Germany, 1996.

**THE ROLE OF FIBRINOGEN IN CORONARY HEART DISEASE AND
ITS POSSIBLE DEPENDENCE ON ACTIVATED
POLYMORPHONUCLEAR LEUKOCYTES**

R. OLINESCU, D. O. CROCNAN, MARIA GREABU

Department of Biochemistry, University of Medicine and Pharmacy " C. Davila",
Eroilor Sanitari Blvd.,
Bucharest, Romania, 76241

ABSTRACT

Fibrinogen (FB), an acute phase protein, is recognized as an independent risk factor in the plasma of patients with coronary heart disease (CHD). The plasma FB level is also significantly increased in inflammation and neoplasm. We performed an in vitro study showing that the chemiluminescence (CL) emission produced by zymosan-activated polymorpho-nuclear leukocytes (PMNL) was directly related to the concentration of FB, fibrinopeptide A or FB-degradation products(FDP). Fibrin inhibited CL emission. We also found that the in vivo plasma levels of FB or FDP were significantly higher in the plasma of 100 cardiac catheterized patients with CHD than in the plasma of the age and sex matched controls. In 85% of the patients with CHD, both the plasma FB and the CL emission were significantly increased. In the other 15%, the plasma FDP level was higher than the FB level, however, the CL level was still higher than in the age and sex matched controls. Activated PMNL may increase the plasma level of FDP as a consequence of enhanced enzyme-dependent degradation of FB. Our results indicate that the role of FB and independent risk factor in CHD depends of the level of activated polymorphonuclear leukocytes in the plasma.

RESUMO

Estudos in vitro demonstraram que a emissão quimiluminescente (CL) produzida por leucócitos plimorfonucleares (PMNL) ativados por zimosano está diretamente relacionada com a concentração de fibrinogênio (FB), fibrinopeptídeo A e produtos de degradação de fibrinogênio (FDP). Foi demonstrado também que os teores de FB e FDP no plasma in vivo foram consideravelmente mais elevados em pacientes cardíacos cateterizados, comparado com controles. Os leucócitos plimorfonucleares ativados podem aumentar o nível de FDP. Os resultados indicam que o papel do FB e o fator de risco independente em pacientes cardíacos cateterizados depende do nível de PMNL no plasma.

KEYWORDS: fibrinogen, chemiluminescence, polymorphonuclear leukocytes, coronary heart disease, reactive oxygen species

INTRODUCTION

As for other acute phase proteins, such as ceruloplasmin and protein C, the plasma level of fibrinogen (FB) is significantly increased, nonspecifically in inflammations and neoplasm [1]. An increase plasma level of FB has been recognized in many studies as one of the main risk factors or biological markers in CHD [1-5]. A study of 15,000 healthy subjects [5] indicated the plasma FB level influenced the development of CHD, however the plasma FB level was also influenced by sex, race, age, smoking, physical exercise, alcohol intake and hormone use. A genetic factor that governs the plasma FB level also seems to exist [4]. Both the FB level and the plasma viscosity (significantly influenced by FB concentration) are believed to be associated positively with total cholesterol, triglycerides, and the low density lipoproteins (LDL) and negatively associated with the high density lipoprotein (HDL) concentration. Smoking is the strongest known determinant of the plasma FB level in healthy persons [6]. Congenital hypofibrinogenemia and dysfibrinogenemia are asymptomatic, but only 20% of these patients were reported to have a tendency to develop thrombosis [7]. Acquired hypofibrinogenemias include therapeutic fibrinolysis, disseminated intravascular coagulation (DIC), liver failure (decreased synthetic function) and treatment with L-asparaginase, valproic acid or antithymocyte globulin [7].

The role of inflammation in the etiology and progression of CHD has been recognized and high white cell count is considered a risk factor [8, 9]. The activation of PMNL has been recognized as a major source of reactive oxygen species (ROS) release which is considerably increased during a chronic inflammation process [2, 3]. The activation of polymorphonuclear leukocytes (PMNL) randomly influences several biological systems, that include blood coagulation and the nonspecific increase of acute phase proteins.

As FB and ceruloplasmin are acute phase proteins, their increased plasma level suggests an inflammatory response [1]. Another consequence of PMNL increased activity is plasminogen activation and release of plasmin which will trigger an additional fibrinogenolysis [10, 11]. As has been recognized [1,3], commonly used techniques for measuring fibrinogen degradation products (FDP) do not discriminate between FDP and fibrin degradation products, as both induce similar impairment of homeostatic functions [10]. Therefore, we studied the consequences of PMNL activation on the modulation of FB and FDP and subsequent chemiluminescent emission *in vitro* and *in vivo* in the plasma of patients suffering from CHD.

MATERIALS AND METHODS

Materials. Fibrinogen type I from human plasma, containing approximately 60% protein, fibrin, fibrinopeptide A, fibrinogen degrading compounds X and Y were obtained from Sigma (USA). They were dialyzed against 50mM Na-K phosphate buffer, pH 7.3. The concentrations measured at 280 nm by using a conversion factor of $E(1\%)_{280} = 15$. The purified protein solutions were adjusted to 5 mg/ml. AAPH (2,2' = azobis-2-aminodipropane) was purchased from Wako (Chicago, IL). AAPH is a water soluble azo compound that thermally decomposes, leading to formation of aqueous peroxy radical at a constant rate. The AAPH determination was performed under the conditions described by Gaziano et al [12]. This includes the procedure to isolate LDL by using removal of natural antioxidants by gel filtration and a column centrifugation.

Subject Selection. The blood used in this study was obtained from 62 men and 38 women cardiac catheterized at Fundeni Clinical Hospital. Coronary heart disease was defined as 80% stenosis of one of the major three coronary arteries as determined by angiography, according to the Budde et al procedure [13]. Of the total of 100 cardiac catheterized patients,

57.6% had 80-100% stenosis; 29.2%, 0% stenosis and the remainder had intermediate values between 30-80% of stenosis. The controls consisted of 68 age and sex matched persons apparently free of coronary heart disease.

Analytical Procedures. Fibrinogen and FDP were measured with a SIGMA Staphylococcal dumping test (proc. No. 850). For subjects with low FB levels, a second technique was added, based on calcium precipitation and subsequent protein measurement [14]. Platelet aggregation was determined by using a SIGMA kit (Proc. No. 885) based mainly on ADP reagent. For a quantitative expression, we used the proposed scale of respective kit. Ceruloplasmin was determined by its oxidase activity according to Schosinsky's method [15] and expressed in international units. The separation of cells from blood to obtain a suspension of PMNLs was accomplished by using a two step discontinuous Percol kit (SIGMA Chemical Co., St. Louis). Seventy percent of the PMNL suspension were neutrophils. The respective dilution of PMNLs to a concentration of 1×10^6 cells/ml was performed by using Hanks' balanced salt solution (Gibco, Life Technol, Grand Island, N.Y.).

Activation of leukocytes. The CL technique recommended by Trush [16] was used for the measurement of PMNL activation by using zymosan^A (Sigma) opsonized with AB serum [17]. The activation of leukocytes was expressed as the stimulatory index (SI), the ratio of CL value at 12 minutes after zymosan addition as compared to an identical sample, without opsonized zymosan [17]. The CL emission produced by the activated PMNLs was measured by using a Beckman scintillation counter LS 3801 equipped with a single photon counting program.

Statistical Analysis. The results were reported as mean \pm SD if not otherwise stated. Comparisons with the unmatched groups were made by Student's Impaired T-test. Statistical analysis was also undertaken with the use of Student's paired T-test after the groups were matched for age and sex. Individuals in the groups were arranged in a random order. Subjects with low fibrinogen level were matched to the specific control subjects. The data were transformed into logarithm to fit a Gaussian pattern. All calculations were performed by using a statistical package from BMDP Statistical Software Inc. No adjustment of the data was made for multiple comparisons, but the significance level was set at $P < 0.05$.

RESULTS

Our results indicate that PMNL modulated the biological activity of FB and FDP. *In vitro*, an interaction was found to exist between FB, FDP and activated PMNLs. Purified FB increased the concentration of zymosan-activated PMNLs. For a concentration corresponding to 200mg/dl (equivalent to a physiological level), FB did not influence the CL emission (Fig.1).

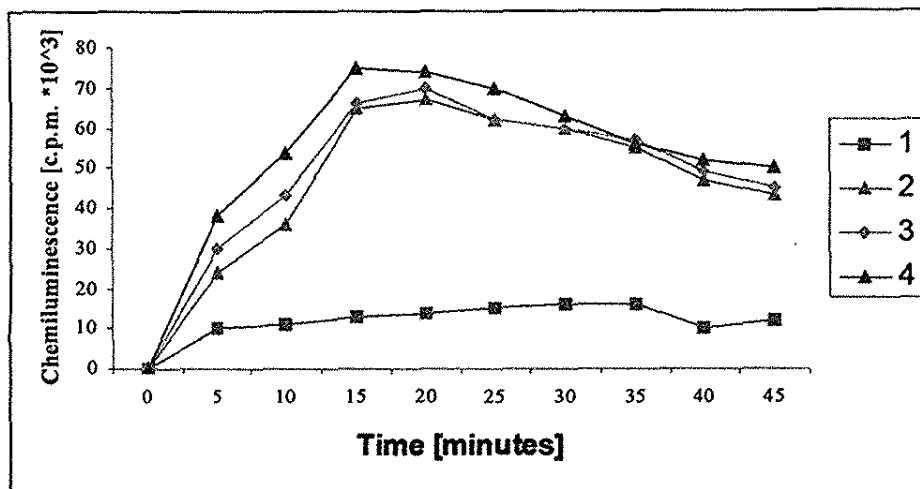


Fig. 1 The chemiluminescent response of the *in vitro* activation of polymorphonuclear leukocytes. The stimulation of LPMN was produced by opsonized zymosan (1 mg/ml). All variants have the same amount of viable PMNL (2×10^6 cell/ml) obtained from the same normal donor.

Legend: (1) nonstimulated; (2) stimulated (s); (3) S + FB (2mg/ml); (4) S + FB (4mg/ml).

The reaction mixture contained PMNL suspension ($100 \mu\text{l}$ 1×10^7 cell/ml), $100 \mu\text{l}$ luminol $100 \mu\text{M}$, the fibrinogen or related compounds in amounts already mentioned and Hanks nutritive medium (containing Mg and Ca) up to a final volume of 1.5 ml.

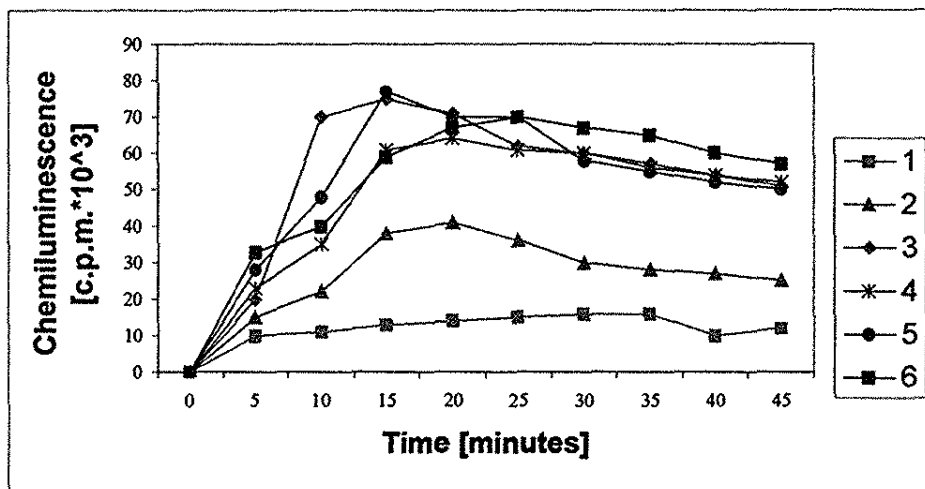


Fig. 2 The chemiluminescent response of the *in vitro* activation of polymorphonuclear leukocytes. The stimulation of PMNL was produced by opsonized zymosan (1mg/ml). All variants have the same amount of viable PMNL (2×10^6 cell/ml) obtained from the normal donor.

Legend: (1) nonstimulated; (2) stimulated (s); (3) fibrin (2mg/ml); (4) FDP-y (1mg/ml); (5) FDP-x (1mg/ml); (6) fibrinopeptide A (1mg/ml).

The reaction mixture contained PMNL suspension ($100 \mu\text{l}$ 1×10^7 cell/ml), $100 \mu\text{l}$ luminol $100 \mu\text{M}$, the fibrinogen or its related compounds in amounts already mentioned and Hanks nutritive medium (containing Mg and Ca) up to a final volume of 1.5 ml.

At a corresponding 400 mg/dl level (equivalent to the upper physiological level), a significant increase in CL was observed. Furthermore, under pathological conditions, the concentration of FDP may increase. As shown in Fig. 2, for a FDP concentration of $200 \mu\text{g/ml}$, a significant increase of CL emission was found. The increasing order is stimulated PMNLs < FDP-y < FDP-x < fibrinopeptide A. Fibrin in a similar concentration partially inhibited the CL emission of activated PMNLs. FB and FDP may interfere with LDL oxidation caused by

activated PMNLs. Ample evidence supports such an action [10, 11].

As shown in Table 1, under the condition which favors LDL oxidation (Cu^{2+} and AAPH induced), purified FB acts significantly different, as a function of its concentration. Purified FB acted as a mild pro-oxidant for a 1 mg/ml concentration and as an AO for a 4mg/ml level.

Table 1. The effects of fibrinogen and related compounds on Cu^{2+} and AAPH-induced peroxidation of LDL.

Compounds	Lag Phase (min)	
	Cu^{2+}	AAPH-induced
Control	134± 17	72 ± 8
+ Ascorbate 25 µmol/L	194± 16*	148 ± 11*
+ Albumin 20 mg/ml (300 µM)	163± 14*	134 ± 16*
+ Fibrinogen 1 mg/ml (6µ M)	102 ± 18*	61 ± 7
+Fibrinogen 4 mg/ml (12µM)	175 ± 13*	137 ± 15*
+ Fibrin 1 mg/ml	106 ± 12*	62 ± 4
+ Fibrin 3 mg/ml	113 ± 10	65 ± 6
+ Fibrinopeptide A 1 mg/ml	104 ± 8*	68 ± 5
+ Fibrinopeptide A 3 mg/ml	112 ± 13	74 ± 7
+ Fibrinogen Degradation Product Y 1 mg/ml	116 ± 15*	63 ± 7
+ Fibrinogen Degradation Product X 1 mg/ml	132 ± 11	75 ± 9
+ Cumene Hydroperoxide 10 µM	76 ± 8*	51 ± 7*

LDL (500 µg/ml protein) was incubated with 3 µM CuSO_4 or with 3mM AAPH and 0.1 mM diethylene triamine penta acetic acid in the conditions already described (PBS medium). The absorbance at 234 was measured continuously and the lag phase, before absorbance increase, was calculated by using a molar extinction coefficient for conjugated dienes of $A_{234} = 2.95 \times 10^4 \text{ cm}^{-1}$. * Significant differences as compared with the control, for $P < 0.05$.

The FDPs act mainly as pro-oxidative, depending on their concentration. As for FB, its pro-oxidative action prevails at lower concentration. As shown in Table 2, 85% of the cardiac catheterized patients had higher levels of FB, and FDP, ceruloplasmin and activation of PMNLs than age and sex matched non cardiac catheterized controls with no apparent CHD. For approximately 15% of the catheterized patients, the FB level was lower than the physiological limit of 2g/L. However, these patients still had higher levels of FDP and higher levels of PMNL activation.

Table 2. Biochemical modification in subjects with low fibrinogen level as compared with catheterized patients and matched controls.

	Non-Catheterized Patients		Catheterized Patients	
	Normal FB Matched Control	Low FB Matched Control	FB: High	FB: low
Fibrinogen g/L	2.78 ± 0.32	1.87 ± 0.34	3.85 ± 0.62*	1.52 ± 0.45
FDP (FB equiv), mg/L	217.91 ± 1.58	273.39 ± 18.3	389.47 ± 28.13**	576.48 ± 43.2**
Ceruloplasmin UI/L	108.31 ± 11.5	112.55 ± 17.3	218.46 ± 23.62*	195.06 ± 18.34*
Transaminase (GPT)(SFunits/ml)	21.42 ± 5.34	26.35 ± 5.15	25.38 ± 8.17	28.49 ± 7.35
Leuk. Phag. Stim. Index	24.62 ± 8.32	28.45 ± 9.32	58.36 ± 8.12**	64.73 ± 8.57**
Platelet aggregation (%)	88.7 ± 2.4	90.3 ± 3.4	95.6 ± 3.2*	23.4 ± 2.9

*Significant difference as compared with matched control for P < 0.05

** Significant difference as compared with matched control for P < 0.01.

DISCUSSION

This study emphasized the complex molecular modifications that occur in CHD. As acute phase proteins are constantly increased in inflammations, neoplasms and CHD, a relationship may exist with phagocytosing leukocytes and FB. Our results show that under normal physiological conditions the acute phase proteins, especially FB, did not influence significantly the activation of PMNLs. But under pathological conditions when these acute phase proteins are nonspecifically increased, especially FB may increase the biological activity of PMNLs as a function of its concentration.

Under physiological conditions, FB related compounds are found in small amounts which probably do not exert any significant action on activated PMNLs. FB was found increase in 85% of cardiac catheterized patients, including the ones with 0% stenosis [14]. But 15% of these cardiac catheterized patients exhibited low levels of FB. In these same 15% of patients as FDP is increased, the FB decreased, although the activation of PMNL was still increased. A likely explanation may be the increased concomitant activation of thrombin and plasmin which may degradate increased amounts of FB [10, 11]. Such a mechanism is compatible with the existence of a chronic, inflammatory condition in these patients and unpredictable biological consequences. Our results indicate that the role of FB and FDP as an independent risk factor in CHD depends on the level of activated polymorphonuclear leukocytes in the plasma.

ACKNOWLEDGEMENTS - We acknowledge the staff of the Cardiac Unit of Fundeni Hospital for providing the blood samples.

REFERENCES

1. L. Wilhelmsen, K. Svardsudd, B. Larson, L. Welin, G. Tibblin, *New Engl. Med.*, 311, 501-503, (1994).
2. W. B. Kannel, P.A. Wolf, W. P. Castelli, R. B. D'Agastino, *JAM*, 258, 1183-1186, (1987).

3. E. Ernst, *Atherosclerosis* 100, 1-12, (1993).
4. K. Krobot, H. W. Hense, P. Cremer, E. Eberle, U. Veil, *Arterioscler. Thromb.*, 12, 780-788, (1993).
5. E. Ernest, K. L. Rescli, *Ann. Int. Med.*, 118, 956-963, (1993).
6. S. Hulea, R. M. Olinescu, Stela Nita, D. O. Crocnan, F. A. Kummerow, *J. Environ. Pathol. Toxicol. Oncol*, 14, 3-9, (1996).
7. F. Haverkate, M. Samama, *Thromb. Haemost.*, 73, 151-161, (1995).
8. J. W. G. Yarnell, I. A. Baker, P. M. Sweetnam, D. Bainton, J. R. O'Brien, P. J. Whitehead, P. C. Elwood, *Circulation*: 83, 836-842, (1991).
9. F. Violi, M. Criqui, A. Longoni, G. Castiglioni, *Atherosclerosis.*, 120, 25-37, (1996).
10. T. E. Bithell, in *Acquired Coagulation Disorders in Wintrobe's Clinical Hematology*, 9th Edit. Lee GR, Bithell TE, Forster L. eds. L. Feibiger, Philadelphia, 1993, pp 1482-1486,
11. C. V. Dany, W. R. Bele, *Am. J. Med.*, 87, 567-576, (1989).
12. J. M. Gaziano, A. Hatta, M. Flynn, E. J. Johnson, N. I. Wrinsky, P. M. Ridker, B. Frei, *Atherosclerosis*, 112, 187-195, (1995).
13. T. Budde, C. Fechtrep, E. Rosenberg, C. Vielhauer C, *Arterioscler. Thromb.*, 14, 1730-1737, (1994).
14. A. Ratnoff, G. A. Harrison, *GA. Chemical Methods in Biochemical Analyses*, 2nd edition, Churchill, London, 1975, pp113.
15. K. H. Schosinsky, H. P. Lehman HP, *Clin Chem.*, 20, 1554-1560, (1974).
16. M. A. Trush, M. E. Wilson, K. Van Dyke, *Methods in Enzymology*, 57, 462-492, (1978).
17. R. M. Olinescu, Stela Nita, D. O. Crocnan, *Rev. Roum. Med. Int.*, 31, 109-112, (1993).
18. R. M. Olinescu, F. A. Kummerow, L. Fleischer, B. Handler, accepted for publication in *Romanian J. Biophys.*

**SPECTROPHOTOMETRIC STUDY OF THE BINARY SYSTEM
Ru(III)-SOLOCHROM VIOLET RS AND THE DETERMINATION OF
Ru(III)**

Maria Pleniceanu, Mihaela Mureseanu, Ion Ganescu and Olimpia Rusu

Department of Analytical Chemistry, Faculty of Chemistry, University of Craiova,
A.I.Cuza,13, 1100, Craiova,ROMANIA

ABSTRACT

A simple and direct spectrophotometric method using solochrom violet RS has been developed for the determination of Ru(III). The molar absorptivity and the Sandell's sensitivity are calculated to be $10^4 \text{ L mol}^{-1} \text{ cm}^{-1}$ and $0.0101 \mu\text{g cm}^{-2}$ respectively. The effect of various parameters including time, pH and added reactant volume has been studied. Beer's law is obeyed over the range 0.20- 7.07 $\mu\text{g/mL}$ of Ru(III). The method has been applied for the determination of Ru(III) in various synthetic and real samples.

RESUMO

Um método espectrofotométrico simples e directo, com solocromo violeta RS, foi usado para determinar o Ru(III). A potência de absorção molar e a sensibilidade Sandell são calculadas para ser $10^4 \text{ L mol}^{-1} \text{ cm}^{-1}$ e, respectivamente $0,0101 \mu\text{g cm}^{-2}$. O efeito dos variados parâmetros, incluindo o tempo, o pH e o volume de reactivo juntado, foi também estudado. Na série 0,20-7,07 $\mu\text{g/mL}$ de Ru(III) está respeitada a lei de Beer. O método foi aplicado para determinar o Ru(III) em exemplos reais e sintéticos variados

KEYWORDS : spectrophotometric determination, ruthenium, solochrom violet RS

INTRODUCTION

The solochrom violet RS (sodium salt of 2 hydroxynaphthyl-azo-1 phenol-4-sulphonic acid) was used for the spectrophotometric determination of the following ions: Mo(VI)¹, Zr(IV)², Th(IV)³, Cr(III)⁴, Ga(III)⁵, Al(III)⁶, In(III)⁷, U(VI)⁸, Zn(II)⁹, Cd(II)¹⁰, V(V)¹¹, Nb(V)¹², and Bi(III)¹³.

Solochrom violet RS reacts with ruthenium ions in aqueous solution, at room temperature to give a dark-red water soluble complex.

The present work reports the use of the azo compound solochrom violet RS for spectrophotometric determination of Ru(III). The method has been used for determination of Ru(III) in various samples.

EXPERIMENTAL

A Mettler Delta 320 pH-meter and UV-VIS Zeiss Jena spectrophotometer were used for measurement of pH and absorbance. All reagents used were of analytical grade. RuCl₃ acid solution (10^{-3} M) and solochrom violet RS aqueous solution (10^{-3} M) were prepared. Buffer solutions with pH ranging from 1.81 to 11.92 were prepared according to Prideaux's method¹⁴.

The real samples were decomposed using a microwave digestion under pressure Milestone MLS-1200 Mega processor in TMF vessels.

General procedure

Ru(III) chloride was dissolved in 2M HCl and the solution was standardised¹⁵. The reagent solution (6 mL) was added to a known volume of metal ion solution into 25 mL calibrated flasks. The pH was then adjusted to 3.1 with the appropriate buffer. The absorbance was measured at 550 nm against the blank 20 minutes after the mixing.

RESULTS AND DISCUSSION

The reaction between the Ru(III) and the azo compound results in formation of a complex. This complex shows an absorption maxima at 550 nm, whereas the reagent absorbed negligibly at this wavelength (Fig.1).

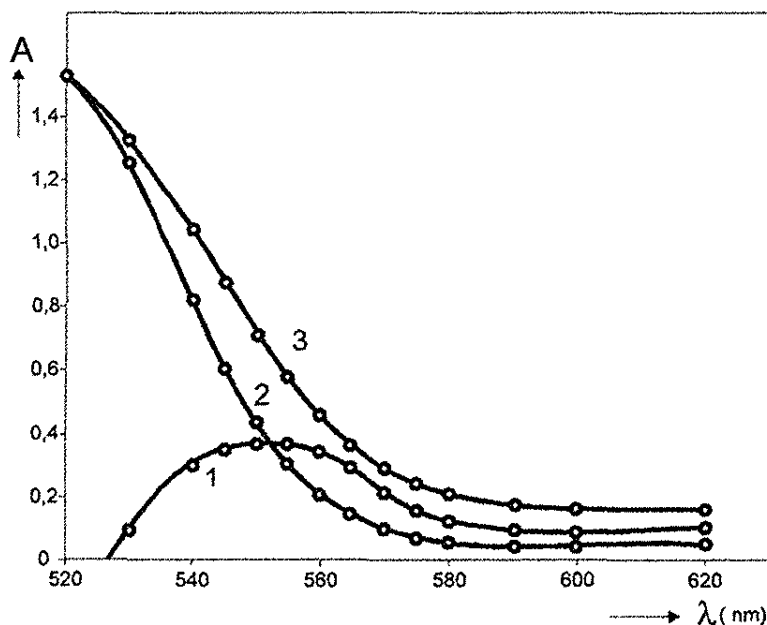


Fig. 1. Absorbance spectra of:

1. Ru(III) + solochrom versus solochrom
2. Reactive versus water;
3. Ru(III) + solochrom versus water; ($8 \cdot 10^{-5}$ M Ru(III)+ $2.4 \cdot 10^{-4}$ M solochrom; pH=3.1)

The effect of time, reactant, volume and pH on determination of Ru(III) was studied. The optimum time required for development of colour was found to be 5 minutes at room temperature. The effect of concentration of reagent was examined. For 1 mL solution of Ru(III) $10^{-3}M$, 3 mL of solochrom violet RS solution $10^{-3}M$ was sufficient. The absorbance remained practically constant above this value. The formation of the complex was studied over a wide pH range 1.81-11.92 using Prideaux buffer solutions. The results indicate that the absorbance was maximum in the acid domain at pH 3.1(Fig.2).

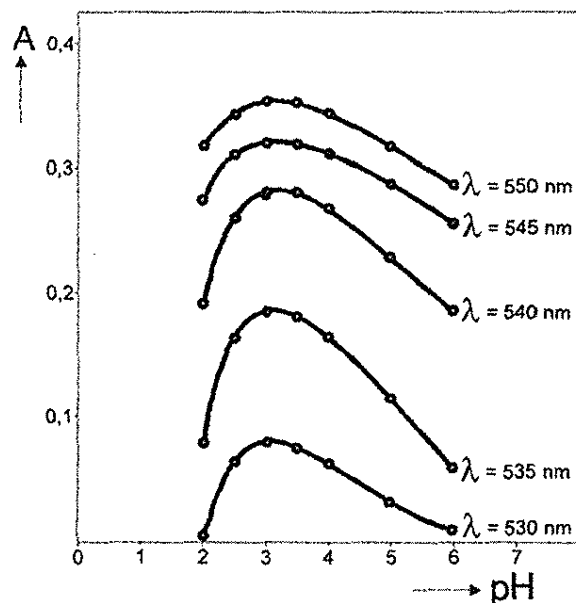
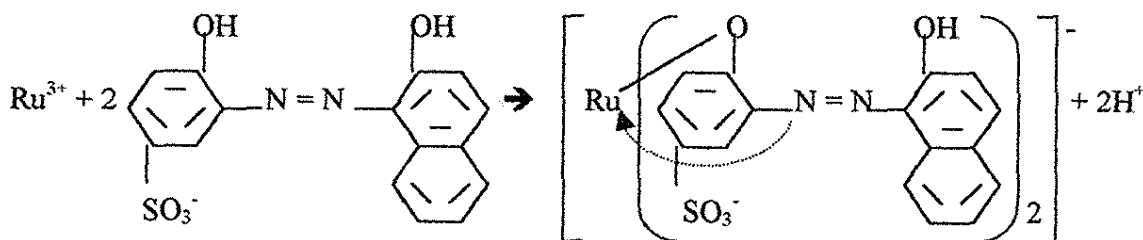


Fig.2. Variation of the absorbance versus pH ($8 \cdot 10^{-5}M$ Ru(III)+2.4 M solochrom).

The composition of the complex Ru(III)-solochrom was established using Job's method of continuous variation and mole ratio method. The mole ratio was found to be 1:1 (Fig.3 and Fig.4).

The reaction between Ru(III) and solochrom violet RS is:



The reactive molar ratio(x) for four nonisomolar series was established and the complex instability constant was calculated using the Job's relation for the 1/2 combination ratio :

$$K = \frac{c^2 p [(p+2)x - 2]^3}{(p-1)^2 (2-3x)}$$

were:

- c = the molar concentration of the Ru(III);
 p = the ratio of the molar concentration of the reactive and of the Ru(III);
 $[B]$ = the molar concentration of the ligand;
 x = the reactive molar ratio

The stability constant of the complex ($K_{st}=1/K_{inst}$) is $K_{st}=1.74 \cdot 10^{11}$ and the p_K ($p_K = -\log K_{inst}$) is $p_K = 11.38 \pm 0.01$ for a 95% probability at 25°C temperature and ionic strength $\mu=0.2$.

Table 1 presents the values of the stability constants for four nonisomolar solutions series.

Table 1
Values of the stability constant

No of the nonisomolar serie	c	p	$[B]$ ligand	x	K_{st}	P_K
1	$5 \cdot 10^{-4}$	2	10^{-3}	0.505	$0.121 \cdot 10^{12}$	11.3837
2	$4 \cdot 10^{-4}$	2.5	10^{-3}	0.450	$0.234 \cdot 10^{12}$	11.3700
3	$2.5 \cdot 10^{-4}$	4	10^{-3}	0.345	$0.101 \cdot 10^{12}$	11.3756
4	$6.66 \cdot 10^{-5}$	10	$6.66 \cdot 10^{-3}$	0.180	$0.241 \cdot 10^{12}$	11.3816

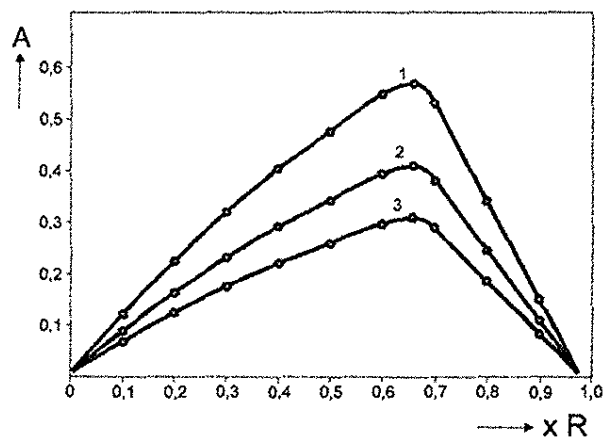


Fig.3. Variation of the absorbance in the isomolar series

1. $1 \times 10^{-3} M$
2. $6.66 \times 10^{-3} M$
3. $5 \times 10^{-4} M$.

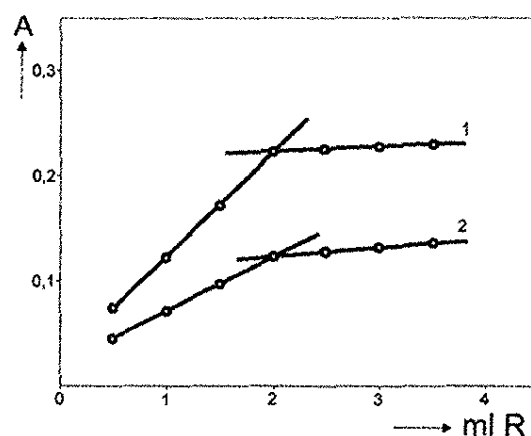


Fig.4. Complex composition determination by molar ratio method

1. $1 \times 10^{-3} M$
2. $5 \times 10^{-4} M$

The charge of the complex ion was determined by the electrophoretic migration method in the presence of a weak solution of potassium nitrate. After 10 minutes the coloured complex ion migrated towards the anode indicating the complex ion to be negatively charged.

Beer's law was obeyed over the concentration range 0.20-7.07 $\mu\text{g Ru(III)/mL}$ (Fig.5). For testing the validity of the method we have statistically interpreted the experimental data through the linear regression method.

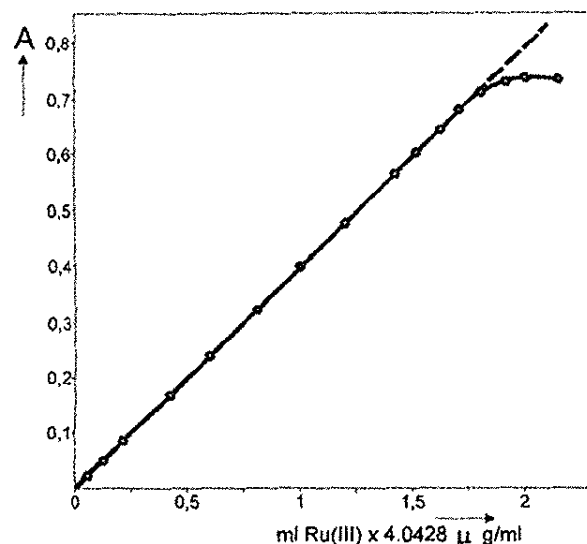


Fig.5. Variation of the absorbance versus Ru(III) concentration ($2 \cdot 10^{-6}\text{M} - 7 \cdot 10^{-5}\text{M}$ Ru(III) + $2.4 \cdot 10^{-5}\text{M}$ solochrom).

The correlation coefficient, r , having the value 0.9999 indicates a linear dependence of the absorbance on the Ru(III) concentration. The two equations are: $y=0.0989x + 1 \cdot 10^{-7}$ with the angular coefficient $m_1=0.0989$ and $x = 10.1069y + 1.9 \cdot 10^{-6}$ with the angular coefficient $m_2=0.09894$. The method proposed for determination of Ru(III) is reproducible and accurate, the relative standard deviation being $\pm 1.1\%$, not affected by systematic errors. The molar absorptivity and the Sandell's sensitivity were calculated to be $10^4 \text{ L mol}^{-1} \text{ cm}^{-1}$ and $0.0101 \mu\text{g.cm}^{-2}$ respectively.

Interference studies demonstrated that the colour reaction of Ru(III)-solochrom violet RS is specific. Various cations were added individually to a solution of Ru(III) ($4.04 \mu\text{g/mL}$) and the tolerance limits are as follows: fluoride, chloride, bromide, iodide, acetate, nitrate, sulphate, thiosulphate, carbonate, phosphate and thiourea (Ru(III): anion = 1:200), citrate, oxalate, tartrate, nitrite and EDTA (Ru(III): anion = 1: 100), W(V) and W(IV) until the $\frac{1}{4}$ ratio, Zn(II), Al(III), Ga(III), Tl(I), Tl(III), U(VI), Bi(III), Cr(III), Cd(II), Mo(IV), Zr(IV), Th(IV) at enough great ratios due to the different absorption maxim of the corresponding complexes, Pt(IV), Ir(III), Au(III), Os(VIII), Rh(III), (Ru(III)/cation =1:12), Co(II) (1:12) and Ni(II) (1:18) are tolerable in the presence of 0.5 ml EDTA solution.

Determination of Ru(III) in synthetic and real samples

The proposed method has been used for determination of Ru(III) both in synthetic mixtures and real samples and the results were statistically evaluated.

The synthetic mixtures had the following percentage composition: (1) Ru(III), 15; Ir(III),10; Au(III), 10; Pd(IV) ,5; Os(VIII),40; Fe(III), 20; (2) Ru(III),20; Pt(IV),30; Co(II),10; Ni(II),10; Mo(VI), 20; Ir(III), 10.

Each of mixtures was treated with a mixture of KOH and KNO₃(8:1.3g) and heated at 800°C for 30 minutes. The cooled melt was leached with water, acidified with concentrated hydrochloric acid(10 mL) and diluted to 100 mL. To an aliquot of the synthetic sample was added solochrom solution (3 mL) and pH was adjusted to 3.1 with the buffer solution; then were added 1% EDTA (0.5 mL) and 5% sodium thiosulphate(2 mL) solutions and ruthenium was spectrophotometrically determined . The determined concentrations (the mean of four determinations) are: 14.92±1.3%(0.53% error) and 19.96±1.1%(0.2% error).

Samples were decomposed using a microwave digestion under pressure processor in TMF vessels. Afterward the solid samples were treated depending on the sample nature either with aqua regia and H₂O₂ 30% or aqua regia, H₂O₂30%, HF and H₃BO₃. After digestion the samples were treated as in the case of synthetic mixtures . Ruthenium was determined spectrometrically and by DCP-AES technique, for comparison The results are presented in Table 2, each analytical procedure being repeated five times.

Table 2. Results obtained for the analysis of two real Ruthenium samples

Sample,mg	New method		Reference method ¹⁶	
	Ru found,%	S _r	Ru found,%	S _r
46	6.54±0.002	0.003	6.70± 0.001	0.002
86.5	6.61 ±0.003	0.002	6.74±0.002	0.001

S_r is the relative standard deviation

CONCLUSIONS

The spectrophotometric study of the binary system Ru(III)-solochrom violet RS leads to the following conclusions:

- the determinations were done in the visible region of the electronic spectrum;
- the complex stability constant is large enough and indicates a satisfactory stability of the complex,
- the present method for the determination of Ru(III) is more sensitive,selective and simple than the earlier known methods¹⁷⁻²¹ .

REFERENCES

1. J.Korkisch, M.Osman, *Z.Analyt.Chem.*,171,107 (1958).
2. J.Korkisch, M.Osman, *Z.Analyt.Chem.*,171,2371 (1959).
3. I.M.Korenman, F.R.Shenayova and Z.M.Gurieva, *Khim.Tekhnol.*, 2 , 292 (1966).
4. R.D.Bentley and J.P.Elder, *J.Soc.Dyers and Colouristes*, 72, 332 (1956).
5. V.Croitoru and G.Nicolae, "Chimie Analitica", Ed.didact. si pedagogica,Bucuresti,Romania,1971,pp155.
6. Gr.Popa, M.Pleniceanu and V.Croitoru, *Anal.Univ.Bucuresti*, 67 (1970).
7. Gr.Popa and V.Croitoru, *Proceedings of the 3rd National Conference of Analytical Chemistry* ,oct. 20,1971,Bucharest,Romania,3,65(1971).
8. Gr.Popa, L.Vladescu and V.Croitoru, *Anal.Univ.Bucuresti*, 109 (1971).
9. V.Croitoru, A.Deac and I.Parlog, *Anal.Univ.Bucuresti*, 27 (1972).
10. I.Burnea, M.Pleniceanu and L.Burnea, *Rev. Roumaine Chim*, 19, 501 (1974).
11. M.Pleniceanu and O.Rusu, *Rev. Roumaine Chim*, 20, 267 (1975).
12. M.Pleniceanu, O.Rusu, I.Ganescu and M.Mureseanu, *Indian J. Chem.* 36A, 1101-1102 (1997).
13. M.Pleniceanu and O.Rusu, *Rev. Roumaine Chim.*, 3, 58 (1975).
14. E.B.R.Prideaux, A. T. Ward, *J.Chem.Soc.*,426(1924).
15. W.W.Scott, " *Standard Methods of Chemical Analysis*", Vol I , Van Nostrand, New York, N.Y.,USA, (1969).
16. Adachi T, Takeinshi H, *Anal Chim.Acta*, 77,218 (1989).
17. A.Rao, U.Gupta, *Analyst*, 112(12), 1401-1404 (1986).
18. K.Malathi, M.Subbairjan, *Talanta*, 42(10), 1487-1491 (1995).
19. Z.L.Zhu, Z.G.Gu, *Anal.Chem Acta*, 298(1), 19-26 (1994).
20. P.G. Bhatia, A.N. Bhat, *Microchim Acta*, 72,788 (1984).
21. N.K.Beeskii, L.A. Nebalsina, *J.Anal.Chem(trans.of Zh.Anal.Khim)*, 50(9), 862 (1995).

CARBON-13 NMR OF ALIPHATIC KETONES

53

Paulo Irajara Borba Carneiro*
Instituto de Química
Universidade Estadual de Ponta Grossa – UEPG
Caixa Postal 992/993
84.031-510 Ponta Grossa – PR - BRASIL

Roberto Rittner
Instituto de Química
Universidade Estadual de Campinas – UNICAMP
Caixa Postal 6154
13.081-970 Campinas – SP - BRASIL

ABSTRACT

This work reports unpublished Carbon-13 NMR chemical shift data of three aliphatic ketones: 2-octanone, 2-nonanone and 2-undecanone; and corrected data for 2-hexanone (C-4) and 2-decanone (C-1; C-2). The empirical substituent effects of the CH₃CO group were determined more accurately and can be useful in correlation analysis.

RESUMO

Este trabalho relata dados não publicados e inéditos de deslocamentos químicos de RMN de Carbono-13 para três cetonas alifáticas: 2-octanona, 2-nonanona e 2-undecanona; e dados corrigidos da 2-hexanona (C-4) e 2-decanona (C-1; C-2). Os efeitos empíricos do substituinte do grupo CH₃CO foram determinados mais acuradamente e podem ser úteis em análise correlacional.

KEY WORDS: Carbon-13 NMR, chemical shift, aliphatic ketones.

INTRODUCTION

Recently we have studied aliphatic compounds by Carbon-13 NMR spectroscopy¹. Although aliphatic ketones are important starting material for some synthetic routes, there is a lack of NMR data in the literature². We have synthesized some aliphatic ketones like **CH₃COCH₂R** where **R** is an alkyl group containing one to eight carbon atoms (methyl, ethyl, propyl, butyl, pentyl, hexyl, heptyl and octyl). The purpose of this work was to synthesize several non-branched aliphatic ketones with sp³ hybridization, to record their Carbon-13 NMR data for their full characterization, and to determine the empirical effects to the **CH₃CO** group. The Carbon-13 NMR chemical shifts data of three aliphatic ketones: 2-octanone, 2-nonanone and 2-undecanone have not been reported in the literature. The empirical substituent effects of the CH₃CO group were determined more accurately and can be useful in correlation analysis.

*Author to whom correspondence should be addressed (email: PIBC@uepg.br)

EXPERIMENTAL PROCEDURE

Materials: All compounds were prepared by using ethyl acetoacetate synthesis: the β -keto esters alkylated by convenient alkyl halide followed by hydrolysis and decarboxylation to lead to aliphatic ketones like $\text{CH}_3\text{COCH}_2\text{R}$ where **R** is an alkyl group containing one to eight carbon atoms (methyl, ethyl, propyl, butyl, pentyl, hexyl, heptyl and octyl), according to a procedure described in the literature⁴. The physical and spectral data are shown in Tables 1-3. Solventes were of spectroscopic quality and were used without further purification.

Spectra: The C-13 NMR spectra of 1,0 M solutions in HCCl_3 with 1% TMS as an internal reference in 10 mm o.d. sample tubes, were recorded at 25,2 MHz using a Varian XL 100 spectrometer in the FT mode. The conditions were as follow: pulse width, 20 μs ; acquisition time, 0,67 s; spectral width, 6150 Hz; pulse repetition time, 0,4 s; temperature, 30 °C; internal lock, D_2O ; angle tumbling, 45°; number of transients, 6000; and number of data point, 8192. The C-13 NMR spectra were recorded in both the single-frequency off-resonance decoupling and proton noise decoupled in the FT mode.

RESULTS AND DISCUSSION

Table 1 shows the physical constants obtained for these compounds. They agree with published data. The Carbon-13 NMR data are shown in Table 2. The signals of aliphatic carbons were assigned by known chemical rules². The compound 2-hexanone was synthesized to correct the C-4 signal ($\delta = 31,9$ according the literature²; we have found $\delta = 25,2$). The compound 2-decanone was synthesized to correct the C-1 and C-2 signals ($\delta = 28,9$ and 208,0 respectively), until now unavailable in the literature. All compounds were synthesized to complete the data set to define the empirical substituent effects of the CH_3CO group. The synthesis of the aliphatic ketones: 2-hexanone, 2-decanone, 2-octanone, 2-nonanone and 2-undecanone permitted us to amplify the Carbon-13 NMR data of these ketones and to estimate the empirical substituent effect of this group. Table 3 shows the empirical substituent effect of the CH_3CO grup (substituent chemical shift). The five empirical substituent effects α , β , γ , δ and ϵ are defined by comparison of the ketone chemical shift with the corresponding alkanes.

Table 1. Physical Constantes of Aliphatic Ketones

Compounds	b.p (°C/Torr)	Yield (%)
2-butanone	80/760	82
2-pentanone	101/760	77
2-hexanone	38/30	76
2-heptanone	48/20	74
2-octanone	70/15	70
2-nonanone	95/30	78
2-decanone	98/20	72
2-undecanone	100/10	80

The difference is the substituent chemical shift whose average values are shown in the Table 3. These values can be useful in correlation analysis.

Table 2. Carbon-13 NMR Chemical Shifts of Aliphatic Ketones³

Compounds	δ (ppm)										
	C-1	C-2	C-3	C-4	C-5	C-6	C-7	C-8	C-9	C-10	C-11
2-butanone	28,4	206,7	35,3	6,5							
2-pentanone	29,0	207,6	44,9	16,7	13,0						
2-hexanone	28,8	207,2	42,5	25,2	21,6	13,0					
2-heptanone ^a	29,6	208,4	43,7	23,6	31,5	22,6	13,9				
2-octanone	29,5	208,7	43,6	23,7	28,6	31,4	22,2	13,7			
2-nonanone ^a	28,7	207,5	43,1	23,4	28,7	28,7	31,2	22,1	13,5		
2-decanone	28,9	208,0	43,7	24,1	29,5	29,5	29,5	32,0	22,8	14,1	
2-undecanone	29,2	208,3	43,5	23,7	29,1	29,1	29,1	29,1	31,7	22,5	13,9

a = in CDCl₃

Table 3. Empirical Substituent Effects of Aliphatic Ketones³

Group	δ (ppm)				
	α	β	δ	δ	ϵ
MeCO	29,6	0,8	-3,2	-0,3	-0,5

ACKNOWLEDGEMENTS

The authors thank the Fundação de Amparo e Pesquisa do Estado de São Paulo (FAPESP) for financial support of this research and the Conselho Nacional de Desenvolvimento Científico e Tecnológico (CNPq) for a fellowship to R. R. and P. I. B. C.

REFERENCES

1. P.I.B. Carneiro., *South. Braz. J. Chem.*, 4(4):93-96, 1996.
2. E. Breitmaier and W. Voelter. "Carbon-13 NMR Spectroscopy"^{3rd} edition, Weinheim, New York, N.Y., USA, 1987.
3. P. I. B. Carneiro, *Tese de Doutorado*, UNICAMP, Campinas, S. P., Brasil, 1991.
4. B. S. Furniss et al. "Vogel's Textbook of Practical Organic Chemistry", 4th edition, John Wiley, New York, N.Y., USA, 1978.

**SYNTHESIS AND STRUCTURAL CHARACTERIZATION
OF N - (2' - HYDROXY - 1' - NAPHTHALEN METHIN) - 2 -
AMINOANILINE COMPLEXES**

Dumitru Negoiu, Mirela Calinescu, Ana Emandi and Tudor Rosu

Department of Inorganic Chemistry, Faculty of Chemistry,
University of Bucharest, 23 Dumbrova Rosie, sect. 2, Bucharest ,Romania

ABSTRACT

N - (2' - hydroxy - 1 - naphthalen methin) - 2 - aminoaniline (HL) forms stable complexes with chromium(III), of the type $[CrL_2]Cl$, nickel(II) and copper(II), of the type $[ML_2]$ ($M = Cu, Ni$).

Their structures have been characterized on the basis of elemental analysis, magnetic moment determinations, IR, electronic and EPR spectral studies. Chromium(III) and copper(II) form distorted octahedral complexes, while nickel(II) forms typically a square-planar complex. Ligand field parameters have been calculated for these complexes.

KEYWORDS: Schiff bases; chromium(III), copper(II), nickel(II) complex compounds

RESUMO

N-(hidroxi-1-naftalen metin) -2 aminoanilina (HL) forma complexos estáveis com cromo (II) do tipo $(CrL_2)Cl$ e com cobre (II) do tipo (ML_2) , ($M=Cu, Ni$).

A estrutura destes complexos foi determinada usando análise elementar, determinações de momento magnético, e métodos de espectroscopia no infravermelho, ultravioleta-visível e RPE. Cromo (III) e cobre (II) formam complexos octaédricos distorcidos e o níquel (II) forma um complexo típico quadrado-planar. Parâmetros correspondentes ao campo ligante foram calculados para estes complexos.

1. INTRODUCTION

Although many investigations have been performed on transition metal complexes with Schiff's bases derived from *o*-hydroxy-naphthaldehyde with amines¹⁻⁴, no studies have been made on the ligand field parameters in such complexes.

The present paper describes the synthesis and the characterization of Cr (III), Ni (II) and Cu (II) complexes with N - (2' - hydroxy - 1' - naphthalen methin) - 2 - aminoaniline (HL). The ligand contains azomethine N and amine N, and one OH phenolic group, capable of coordination with various metal ions.

A noteworthy point here is that the amine N is not coordinated in the nickel (II) complex, but it is coordinated in the chromium (III) and copper (II) complexes.

2. EXPERIMENTAL

All the chemicals used were of analytical reagent grade. The Schiff base was synthesized by refluxing 2-hydroxy naphthaldehyde and *o*-phenylene diamine in ethylene glycol in 1:1 ratio, for 4h. The yellow product obtained was filtered and washed successively with ethylene glycol and ethanol. It was recrystallized from a mixture ethylene glycol/ethanol.

Preparation of metal complexes:

Hot ethanolic solutions of ligand (0,01 mol) and metal chlorides (0,005 mol) were mixed with continuous stirring. The resulting solutions were refluxed on a water-bath for 2h.

After concentrating and cooling, coloured solids resulted. These were filtered, washed with ethanol and air dried.

The purity of Schiff base and its complexes was determined by C, H and N analyses. Metal content was determined by standard procedures⁵.

Infrared spectra (in KBr pellets) were recorded on a Spekord M-80 Carl Zeiss Jena spectrophotometer, in the range of 4000-400 cm^{-1} . Diffuse reflectance spectra were measured on Spekord M-40 spectrophotometer in the range of 200-900 nm.

Molar conductance was measured in DMF (10^{-3}M), using a Phillips PR 9500 conductivity meter, at room temperature.

Thermogravimetric analysis was carried out in static air atmosphere, at a heating rate of 10^0 C/min, using a MOM Q-1500 derivatograph.

Magnetic susceptibility measurements were performed by the Faraday method, at room temperature, using $\text{Hg}[\text{Co}(\text{SCN})_4]$ as a calibrant.

3. RESULTS AND DISCUSSION

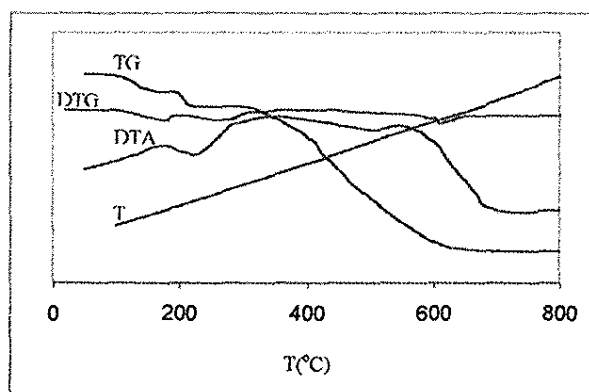
The results of elemental analysis (Table 1) reveal that the complexes have 1:2 (M:L) stoichiometry.

The thermal stability data (Figure 1) show that the decomposition of Cr(III) complex starts at 220^0C , corresponding to the removal of anionic chloride⁶. The broad exothermic peak in the range of $350-600^0\text{C}$ for all the complexes corresponds to the loss of the organic ligand^{6,7}.

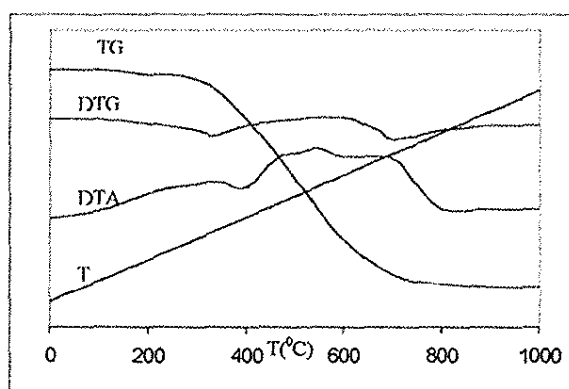
The significant bands (cm^{-1}) observed in the infrared spectra of the Schiff base and its metal complexes are listed in Table 2.

Table 1. Analytical Data for the Complexes Studied

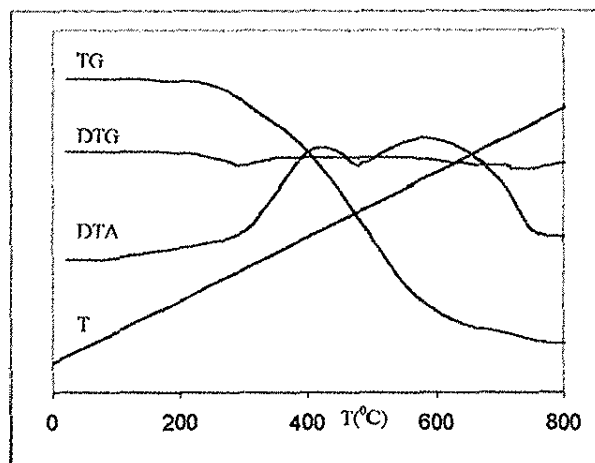
Complex	Colour	C% Calc/exp	N% Calc/exp	Metal% Calc/exp	$\lambda(\text{DMF})$ $\Omega^{-1}\text{cm}^2\text{mol}^{-1}$
[CrL ₂]Cl	Brown	66,90	9,18	8,53	66
		66,07	8,34	7,96	
[NiL ₂]	Red	69,98	9,60	10,36	34
		69,60	9,34	10,22	
[CuL ₂]	Orange	69,62	9,55	10,92	27
		68,92	8,92	10,34	



(a)



(b)



(c)

Figure 1. Thermogravimetric curves of Cr(III) (a), Ni(II) (b) and Cu(II) (c) complexes

Table 2. Characteristic Bands in the IR Spectra of the Ligand and its Complexes (ν_{\max} , cm^{-1})

HL	[CrL ₂]Cl	[NiL ₂]	[CuL ₂]	Assignments
3410 ms	3380 ms	3408 ms	3382 ms	$\nu_{\text{as}}(\text{NH}) \text{NH}_2$
3320 m	3305 m	3320 m	3302 m	$\nu_{\text{sim}}(\text{NH}) \text{NH}_2$
2970 ms	-	-	-	ν_{OH} chelatic
1620 s	1595 s	1600 s	1585 s	$\nu_{\text{C=N}}$
1620 s	1610 s	1620 s	1600 s	$\delta(\text{NH}_2)$
1490 ms	1460 ms	1480 m	1480 m	ν_{sim} C-N
1320 s	1350 s	1365 s	1365 s	$\nu_{\text{C-O}}$ phenolic
-	570 w	560 w	630 w	$\nu_{\text{M-O}}$
-	505 w	500 w	520 w	$\nu_{\text{M-N}}$ azomethinic
-	450 w	-	500 w	$\nu_{\text{M-N}}$ aminic

The strong absorption band in the infrared spectrum of the ligand, appearing at 1620 cm^{-1} , was assigned to the stretching vibration of >C=N group ($\nu_{\text{C=N}}$) and to the deformation in the plane vibration of the amine group (δ_{NH})⁸⁻¹¹. In the IR spectra of all the complexes this band splits into two components.

In the spectra of Cr(III) and Cu(II) complexes, these two bands appear at lower wave numbers, indicating the coordination of the nitrogen atom of the azomethine group and the nitrogen atom of amine group to the metal ion.

The bands assigned to asymmetric and symmetric N-H stretching mode of NH_2 group are also lowered, which confirms the coordination of the ligand through the amine group to the metal ion¹².

In the IR spectrum of Ni(II) complex, only one component of the band at 1620 cm^{-1} appears at lower wave number. No shift is observed for the bands due to asymmetric and symmetric N-H stretching modes of NH_2 . It is therefore concluded that in the Ni(II) complex the coordination takes place through the nitrogen atom of the azomethine group, but NH_2 group is not involved in the complexation^{12,13}.

The band due to the intramolecularly bonded phenolic group is not observed in the case of the metal complexes, indicating that the deprotonation of the phenolic group has taken place during the complexation. The positive shift in $\nu_{\text{C-O}}(\text{phenolic})$ is also in agreement with the coordination of the ligand through the phenolic oxygen¹³⁻¹⁵.

At lower frequencies, the complexes exhibit new bands with low intensity, at $570\text{-}630\text{ cm}^{-1}$ and $460\text{-}500\text{ cm}^{-1}$, which are assigned to $\nu_{\text{M-O}}$ and $\nu_{\text{M-N}}$, respectively^{9,10,16,17}.

The IR spectral data indicate clearly that the coordination of the ligand takes place through the azomethine and the amine nitrogen and the phenolic oxygen in Cr(III) and Cu(II) complexes and through the azomethine and the phenolic oxygen in Ni(II) complex.

Magnetic and electronic spectral data .

The nickel(II) complex was found to be diamagnetic, suggesting square planar geometry. This conclusion is further supported by the electronic spectrum of the complex (Figure 2), which exhibits three strong bands: at 19758 cm^{-1} (${}^1\text{A}_{1g} \rightarrow {}^1\text{A}_{2g}$), 22321 cm^{-1} (${}^1\text{A}_{1g} \rightarrow {}^1\text{B}_{1g}$) and 25201 cm^{-1} (${}^1\text{A}_{1g} \rightarrow {}^1\text{E}_g$).

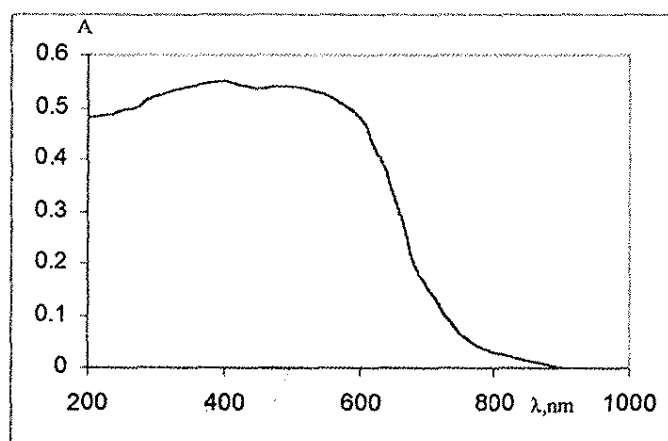


Figure 2. Diffuse-reflection electronic spectrum of the Ni(II) complex

The observation of a spin-forbidden $d-d$ transition at 15220 cm^{-1} (${}^1A_{1g} \rightarrow {}^3A_{2g}$) permitted the calculation of the strong field parameters Δ_1 , Δ_2 and Δ_3 (we assumed the $C/B=4$)¹⁸. The following values of the spectral parameters were determined:

$$\Delta_1 = 22027\text{ cm}^{-1}$$

$$\Delta_2 = 4831\text{ cm}^{-1}$$

$$\Delta_3 = 2313\text{ cm}^{-1}$$

$$B = 567\text{ cm}^{-1}$$

Therefore, the sequence of the d antibonding molecular orbitals is:

$$a_{1g}(d_{z^2}) < e_g(d_{xz}, d_{yz}) < b_{2g}(d_{xy}) < b_{1g}(d_{x^2-y^2})$$

These results are in agreement with those obtained by Goyal and Lal⁸.

The magnetic moment of the chromium(III) complex, 3,84 M.B., is very close to spin-only value in octahedral stereochemistry.

The electronic spectrum (Figure 3.) shows six spin allowed transitions, in agreement with an octahedral symmetry, with tetragonal distortion¹⁹. The transition with low intensity, appearing at 14925 cm^{-1} , is a spin-forbidden transition, due to ${}^4A_{2g} \rightarrow {}^2A_{1g}, {}^2B_{1g}, {}^2A_{2g}, {}^2E_g$.

Due to low energy of first spin-allowed transition, its assignment is difficult and the correlation of the electronic spectral data with the results of Electronic Paramagnetic Resonance (EPR) Spectroscopy is absolutely necessary.

The chromium(III) complex shows an axial Electronic Paramagnetic Resonance spectrum, with $g_{||} > g_{\perp}$ (Figure 4.)

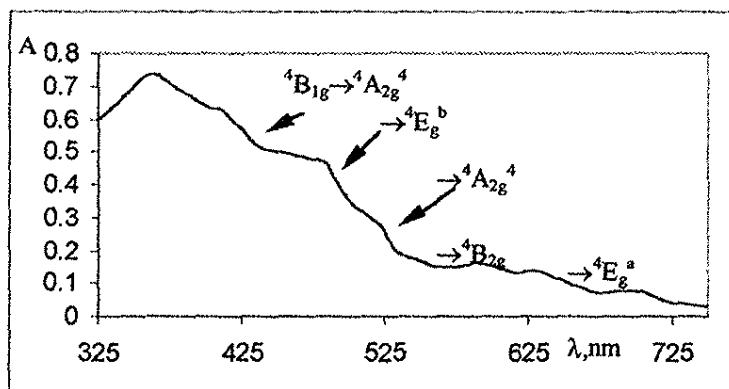


Figure 3. Diffuse-reflection electronic spectrum of the Cr(III) complex

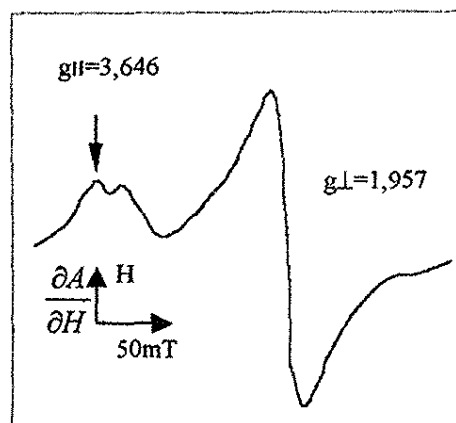


Figure 4. Electronic Paramagnetic Resonance powdered spectrum (X band) of the Cr(III) complex

This is in accordance with a higher energy of ${}^4B_{2g}$ level than that of ${}^4E_g^a$ level, suggesting an octahedral symmetry distorted by elongation along z axis.

On the basis of these observations, the UV-VIS absorption bands may be assigned to the following transitions (Table 3):

Table 3. Electronic Transitions for the Cr(III) complex

Observed bands (ν_{max} , cm^{-1})	Assignments
14925	${}^4B_{1g} \rightarrow {}^2A_{1g}, {}^2B_{1g}, {}^2A_{2g}, {}^2E_g$
15151	${}^4B_{1g} \rightarrow {}^4E_g^a$
16890	${}^4B_{1g} \rightarrow {}^4B_{2g}$
19607	${}^4B_{1g} \rightarrow {}^4A_{2g}^a$
20920	${}^4B_{1g} \rightarrow {}^4E_g^b$
25640	${}^4B_{1g} \rightarrow {}^4A_{2g}^b$
28571	${}^4B_{1g} \rightarrow {}^4E_g^c$

The observation of all the six spin-allowed transitions permitted the calculation of the ligand field parameters, in terms of the Crystal Field Theory and the Angular Overlap Model.

Two approaches were utilised for the analysis of the electronic spectrum:

1. the weak field approach and
2. the strong field approach¹⁹.

In the weak field approach, the splitting of the lowest energy quadruplet term gives the value of the D_t parameter¹⁹⁻²¹:

$$D_t = 4/7 (Dq_{xy} - Dq_z) \text{ (for } D_{4h} \text{ symmetry)};$$

$$Dq_{xy} = Dq_L = \text{in-plane (xy) ligand field strength};$$

$$Dq_z = \text{out-of plane (z) ligand field strength.}$$

The value of D_s was determined using the splitting of the second "octahedral" band :

$$-6D_s + 5/4 D_t = E(^4A_{2g}^a) - E(^4E_g^b)$$

The values of the ligand field parameters calculated with this approach are given in Table 4.

Table 4. Ligand Field Parameters of the Cr(III) complex (cm^{-1})

Parameter	Weak field method	Strong field method
Dq_L	1689	1689
Dq_z	1340	935
D_t	199	431
D_s	-177	-257
$d\sigma$	-107	-423
$d\pi$	763	1465
Δ_1	-1526	-2931
Δ_3	287	1128
$e'_\sigma(L)$	6591	5075
$e'_\sigma(Z)$	6447	4511
$e'_\pi(L)$	721	19
$e'_\pi(Z)$	1484	1484
B_{55}	710	710
B_{35}	335	773
B_{33}	156	833

The positive value of D_t corresponds to an octahedron elongated along the z-axis.

The signs of $d\sigma$ and $d\pi$ parameters suggest that the phenolic oxygen is a poorer σ donor, but a better π donor toward chromium(III) than nitrogen. As a consequence of the sign of $d\pi$, Δ_1 is negative, indicating that the d_{xy} level is lower than d_{xz} and d_{yz} levels.

In order to use the relations proposed by Lever for the determination of AOM parameters¹⁹, we assigned $e'_\pi(z) = 1484\text{cm}^{-1}$, value determined for the phenolic oxygen²².

Because in xy plane we have azomethinic nitrogen and amine nitrogen and $e'_\sigma(N)$ azomethinic = 7682cm^{-1} ²², we have determined $e'_\sigma(N)_{\text{amitic}} = 5500\text{cm}^{-1}$.

Thus, the primary aromatic amine nitrogen is a poorer σ -donor towards Cr(III) than the aliphatic amine nitrogen (for which e'_σ varies between $6700\text{-}7300\text{cm}^{-1}$)²³.

The value of $e'_\sigma(L)$ comprises only the contribution of the azomethinic nitrogen, since the amines do not possess any orbitals capable of a π -interaction with the metal ion.

In the strong field approach, the energy of the states is expressed in terms of the $\Delta_1, \Delta_2, \Delta_3$ and B parameters¹⁹. The results of this method are also given in Table 4 (column 3).

The agreement between the two sets of data may be considered good.

In both approaches, Δ_1 is negative and Δ_3 is positive, which implies the following sequence of energy levels :

$$d_{xy} < d_{xz}, d_{yz} < d_{z^2} < d_{x^2-y^2}$$

If we express the distortion of the octahedral symmetry by DS, DT and DQ parameters²⁴, we obtain:

Weak field approach

$$DS = 1239\text{cm}^{-1}$$

$$DT = 2698\text{cm}^{-1}$$

$$DQ = 43248\text{cm}^{-1}$$

$$DT/DQ = 0,06$$

Strong field approach

$$DS = 1799\text{cm}^{-1}$$

$$DT = 5842\text{cm}^{-1}$$

$$DQ = 39527\text{cm}^{-1}$$

$$DT/DQ = 0,14$$

The magnitude of DT/DQ ratio is a measure of the degree of tetragonal distortion and one observes that the strong field approach indicates a stronger distortion from octahedral symmetry than the weak field approach.

The X-band EPR spectrum of the powdered complex (Figure 4.) has been used to complete the informations on the metal-ligand bond.

The spin Hamiltonian parameters have the following values:

$$g_{\parallel} = 3,646 \quad g_{\perp} = 1,957$$

$$D = 785\text{G} (0,072\text{cm}^{-1})$$

$$E = 200\text{G} (0,018\text{cm}^{-1})$$

The anisotropy of the g factor is consistent with an axial distortion, but its values give little information on distortions in the crystal field. McGarvey showed that the g factor is not very sensitive to the distortions in the crystal field, but it is very sensitive to the nature of the molecular orbitals²⁵. The g factor can be greater than 2,0023 for the complexes in which the ligand atoms have large values for the spin-orbit interaction parameter and possess considerable σ and π bonding capability.

Because the parallel g shift depends on interactions involving the bonding in xy plane, a great value of g_{\parallel} may be correlated with a high degree of overlap between the nitrogen atomic orbitals and the $d_{x^2-y^2}$ and d_{xy} orbitals.

The axial zero-field parameter, D , is related both to the square of spin-orbit coupling constant and the splitting of the first excited state. Thus, the small value of D for our complex indicates a small axial distortion, in agreement with the results of electronic spectroscopy. The small rhombic distortion ($E = 0,018\text{cm}^{-1}$) is due to the existence of two types of nitrogen atoms in the equatorial plane.

Using the equation²⁶ :

$$2D = 8/9 \xi^2 \frac{E(^4B_{2g}) - E(^4E_g^a)}{\Delta^2}$$

which neglects the contribution of the doublet states of the spin-orbit coupling constant value, we obtained $\xi = 163\text{cm}^{-1}$ ($\lambda = 54\text{cm}^{-1}$). This small value is due to the radial expansion of d orbitals through the ligand orbitals, a direct result of this process being the reduction of interelectronic repulsion parameter.

Garrett and DeArmond²⁶ found a direct relation between the spin-orbit coupling constant and the F_2 parameter (or B parameter). Thus, the small value of ξ is in agreement with the small value determined for B.

The electronic spectrum of the copper(II) complex shows a broad band at 16129 cm^{-1} and another at 19700 cm^{-1} , which are in agreement with a distorted octahedral symmetry (Figure 5.).

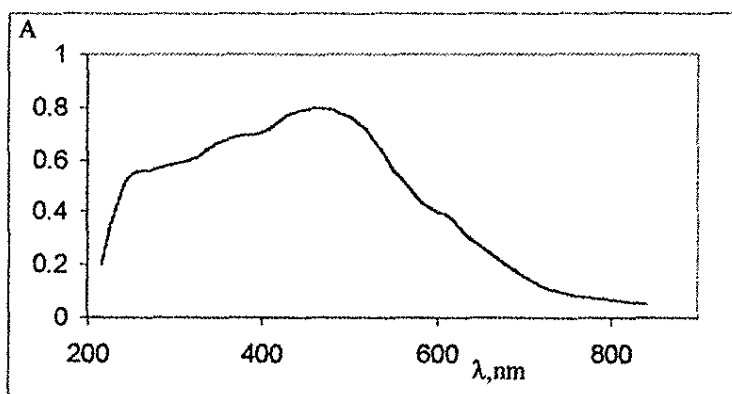


Figure 5. Diffuse-reflection electronic spectrum of the Cu(II) complex

The magnetic moment (1,89 MB) is normal for the d^9 system with one unpaired electron. The EPR spectrum (Figure 6.) gives the following values for the g factor :

$$g_{\parallel} = 2,193 \text{ and } g_{\perp} = 2,060.$$

Since $g_{\parallel} > g_{\perp} > g_e$, the unpaired electron will be in the $d_{x^2-y^2}$ orbital and the octahedron will be along the z axis²⁷⁻²⁹.

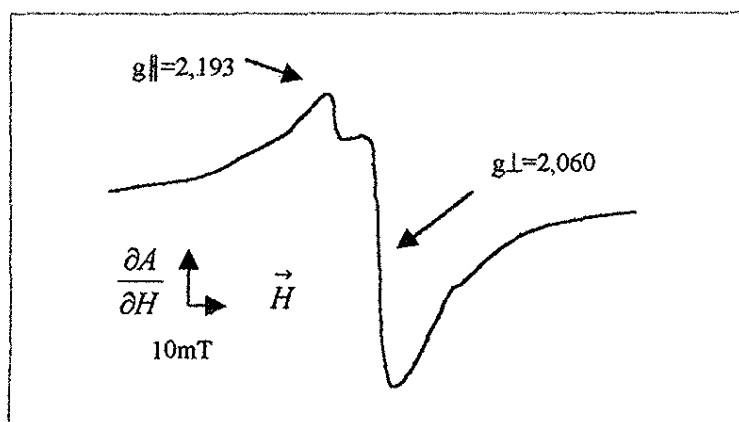
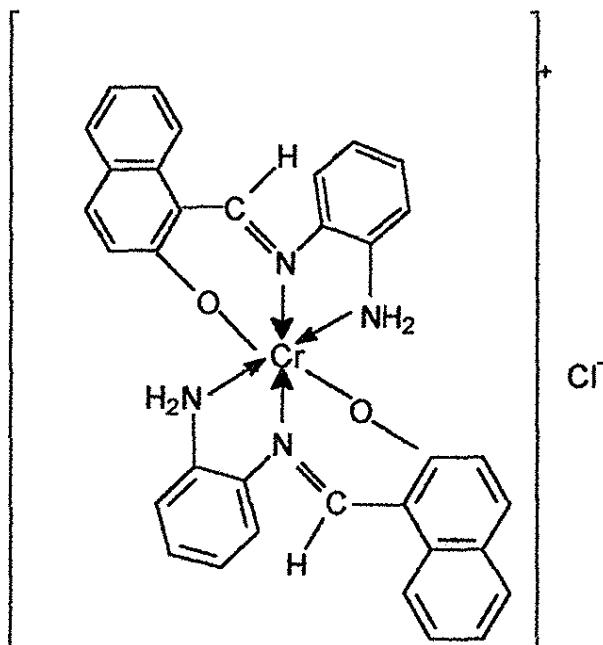


Figure 6. Electronic Paramagnetic Resonance powdered spectrum (X band) of the Cu(II) complex

Thus, the two bands observed in UV-VIS may be assigned to ${}^2B_{1g} \rightarrow {}^2A_{1g}$ and ${}^2B_{1g} \rightarrow {}^2E_g$ transitions, respectively. Using the energy of the transition ${}^2B_{1g} \rightarrow {}^2A_{1g}$ (Δ_0) and g_{\parallel} value²⁷, we obtained for the spin-orbit coupling constant the value: $\lambda = -348\text{cm}^{-1}$. The magnitude of $\lambda/\lambda_0 = 0,46$ ratio indicates an important covalent character of the metal-ligand bond.

On the basis of the results of physico-chemical analyses, the following structures may be assigned for the complexes obtained (Figure 7.):



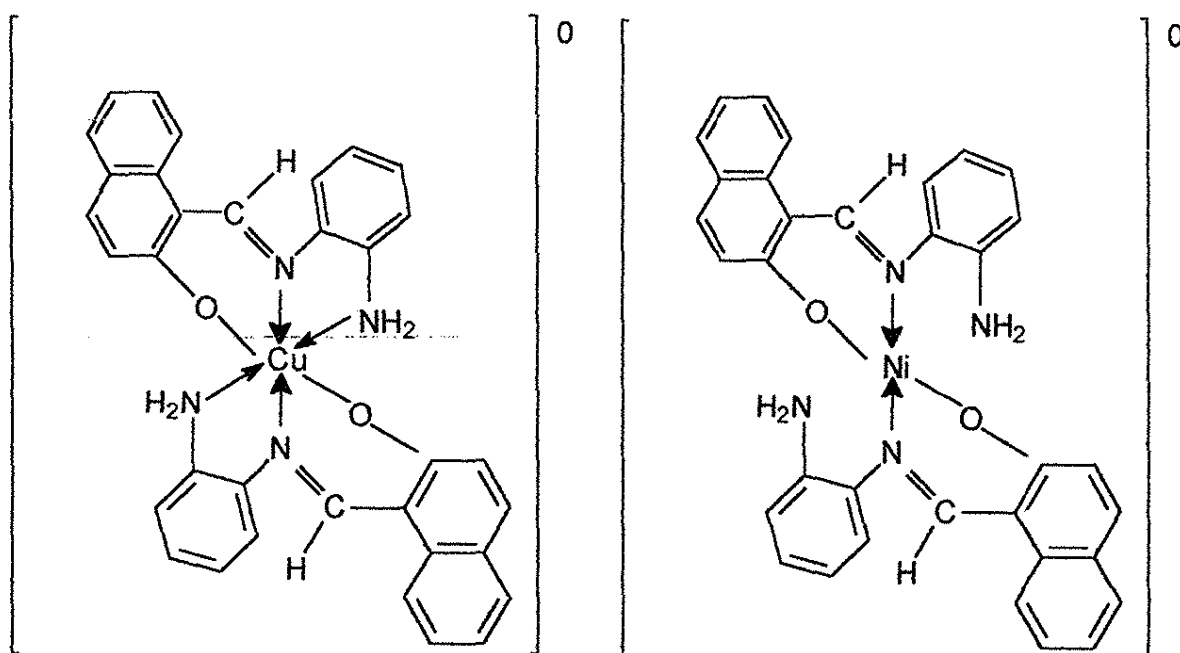


Figure 7. Structures of the Complexes Studied

REFERENCES

1. M.S. Mayadeo, R.L. Ganti, A.P. Rao, *J. Indian Chem. Soc.*, 58, 79-80(1981)
2. C.K. Bhaskare, P.G. More, *Indian J. Chem.*, 25A, 166-169(1986)
3. D.K.Dwivedi, B.V. Agarwala, A.K. Dey, *J. Indian Chem. Soc.*, 65, 461-463(1988)
4. S.Dagaonkar, B.H. Mehto, *Asian J. Chem.*, 7(3), 611-614(1995)
5. C.G. Macarovici, Ed. "Quantitative Inorganic Chemical Analysis", Academia Republicii Socialiste România, Bucharest, 1979, pp. 222, 350, 352
6. D.Z.Obadovic, D.M.Petrovic, V.M.Leovac, S.Caric, *J.Therm.Anal.*, 36, 99-108 (1990)
7. M.M. Abou Sekkina, M.G. Abou El-Azm, *Thermochim. Acta*, 79, 47-53(1984)
8. S. Goyal, K.Lal, *Acta Chim. Hung.*, 127(3), 353-358(1990)
9. M. Mohan, A. Kumar, M. Kumar, *Inorg. Chim. Acta*, 136, 65-74(1987)
10. M. Mohan, N.K. Gupta, M. Kumar, *Inorg. Chim. Acta*, 197, 39-46(1992)
11. R.C. Sharma, J. Ambwani, V.K. Varshney, *J. Indian Chem. Soc.*, 69, 770-772(1992)
12. M.J.M. Campbell, *Coordin. Chem. Rev.*, 15, 279-319(1975)
13. K.Lal, S.R. Malhotra, *Rev. Roum. Chim.*, 30(5), 395-400(1985)
14. S. Bhardway, M.N. Ansari, M.C. Jain, *Indian J. Chem.*, 28A, 81-82(1989)
15. S.A. Patil, V.H. Kulkarni, *Acta Chim. Hung.*, 118(1), 3-10(1985)

16. R.C. Sharma, V.K. Varshney, J. Ambwani, *J. Indian Chem. Soc.*, **69**, 772-774(1992)
17. K. Ueno, A.E. Martel, *J. Phys. Chem.*, **60**, 1270-1275(1956)
18. R.F. Fenske, D. Martin, K. Ruedenberg, *Inorg. Chem.*, **1**(3), 441-452(1962)
19. A.B.P. Lever, *Coordin. Chem.Rev.*, **3**, 119-140(1968)
20. J. Perumareddi, *J. Phys. Chem.*, **71**(10), 3155-3165(1967)
21. W.A. Baker Jr., M. Phillips, *Inorg. Chem.*, **5**(6), 1042-1046(1966)
22. D. Negoiu, M. Calinescu, in press.
23. M.A. Hitchman, *Inorg. Chem.*, **11**(10), 2387-2392(1972)
24. J.C. Donini, B.R. Hollebhone, G. London, A.B.P. Lever, J.C. Hempel, *Inorg. Chem.*, **14**(3), 455-461(1975)
25. B.R. McGarvey, *J. Chem. Phys.*, **14**(2), 3743-3758(1964)
26. B.B. Garrett, K. DeArmond, H.S. Gutowsky, *J. Chem. Phys.*, **44**(9), 3393-3399(1966)
27. A. Abragam, B. Bleaney, Ed. Ed. "Electron Paramagnetic Resonance of Transition Ions", Oxford University Press, London, 1970, pp. 449
28. H. Yokoi, T. Isobe, *Bull. Chem. Soc. Japan*, **42**(8), 2187-2193(1969)
29. H. Yokoi, M. Sai, T. Isobe, *Bull. Chem. Soc. Japan*, **42**(8), 2232-2238(1969)

**MAGNETIC AND SPECTRAL STUDIES ON CHROMIUM(III),
NICKEL(II) AND COPPER(II) COMPLEXES OF 4-HYDROXI-5-
METHOXY ISOPHTHALDEHYDE BIS DIMETHYLHYDRAZONE**

Mirela Călinescu^{*}, Ana Emandi^{*}, Anca Nicolae^{*} and Lidia Paruta^{**}

^{*}Faculty of Chemistry, University of Bucharest, 23 Dumbrova Rosie, Bucharest, Romania

^{**}Institute of Physical Chemistry of Romanian Academy, Spl. Independentei 202, Bucharest, Romania

ABSTRACT

A new hydrazone Schiff base, 4-hydroxy-5-methoxy isophthaldehyde bis dimethylhydrazone and its chromium(III), nickel(II) and copper(II) complexes have been synthesized and characterized by elemental analysis, molar conductance and magnetic moment determinations, infrared(IR), electronic and Electronic Paramagnetic Resonance(EPR) spectral studies. The complexes have distorted octahedral symmetry. Ligand field parameters have been calculated for Cr(III) and Ni(II) complexes on the basis of their electronic transitions, using the weak field approach and the strong field approach.

KEYWORDS: hydrazones; chromium(III), nickel(II), copper(II) complexes

RESUMO

Foi preparada a nova base hidrazona, 4-hidroxi-5-metoxi isoftaldeído bis dimetilhidrazona e seus complexos com cromo (III), níquel(II) e cobre (II). Os novos compostos foram caracterizados através de análise elemental, medidas de condutância molar e momento magnético e técnicas de espectroscopia no infravermelho, ultravioleta-visível e ressonância paramagnética eletrônica (RPE). Os complexos possuem simetria octaédrica distorcida. Parâmetros para o campo ligante foram calculados na base das transições eletrônicas usando os métodos de campo fraco e campo forte.

INTRODUCTION

Due to their activity, especially as potent tuberculostatic agents, the hydrazone Schiff bases and their metal complexes have been intensively investigated during the last few years¹⁻⁸.

In continuation of our studies of the metal complexes of Schiff bases derived from 5-formylvaniline⁹⁻¹², we have synthesized a new hydrazone Schiff base, 4-hydroxy-5-methoxy isophthalaldehyde bis dimethylhydrazone, and its Cr(III), Ni(II) and Cu(II) complexes.

The hydrazone Schiff base shows a bidentate ON monobasic character in all the complexes.

The splitting of "octahedral" bands of the electronic spectra of chromium(III) and nickel(II) complex compounds permitted the determination of ligand field parameters for these complexes.

EXPERIMENTAL

Synthesis of the hydrazone:

To a solution of 5-formylvaniline in ethanol (3,6g/25 ml ethanol) was added 4 ml dimethylhydrazine dissolved in 30 ml ethanol. The resulting mixture was heated under reflux for 1 hr and concentrated under vacuum. To the residue was added 3-4 ml petroleum ether. The solid product that resulted was recrystallised from diethyl ether and precipitated with petroleum ether, m.p.=87°C. Its formula was confirmed by elemental analysis (exp. C: 58,97, H: 7,62, N: 21,03; calc. C:59,09, H:7,57, N: 21,21%) and IR spectrum (Table 2).

Preparation and analysis of metal complexes

All the metal chelates were prepared by the following general method: a solution of the ligand (0,001 mol) in ethanol was added to a solution of metal salt (0,0005 mol)-CrCl₃·6H₂O, NiCl₂·6H₂O and Cu(CH₃COO)₂·2H₂O, respectively, in water. The resulting solution was heated under reflux for 2hr. After cooling at room temperature, the resulting precipitate was filtered, washed successively with ethanol and ether and dried in air.

Carbon, hydrogen and nitrogen were determined by micro-analysis. Metals were analysed employing standard procedures¹³, after destroying the organic part with sulfuric acid and 30% H₂O₂. The analytical data are given in Table 1.

Physical measurements.

Molar conductance of the complexes in dimethylformamide was measured with a Phillips PR 9500 conductivity meter. Magnetic susceptibility measurements were carried out at room temperature, by the Faraday method, using Hg[Co(SCN)₄] as calibrant.

IR spectra (in KBr pellets) were recorded on a Spekord M-80 Carl Zeiss Jena spectrophotometer, in the range 4000-400 cm⁻¹. Diffuse reflectance spectra were recorded on Spekord M-40 spectrophotometer, in the range 200-900 nm. The near infrared spectra were registered on Nirs Sisten Pharma-5100 (USA) spectrophotometer, with monofascicle, in reflection.

Thermogravimetric analysis was carried out with a MOM Q-1500 derivatograph, in static air atmosphere, at a heating rate of 10°C/min, from room temperature to 1000°C.

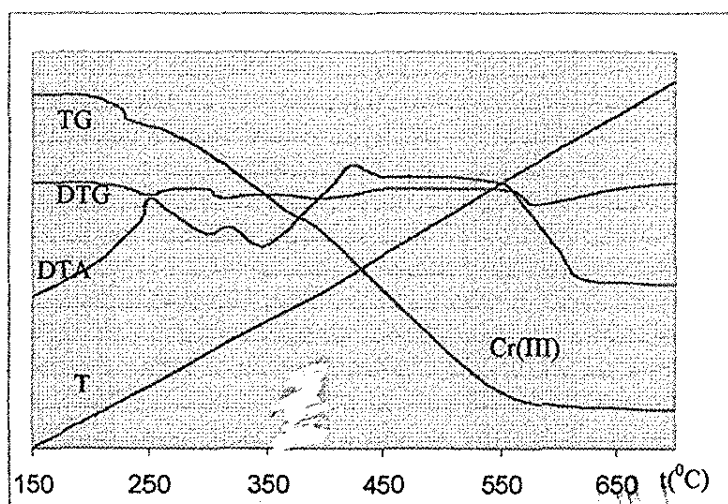
RESULTS AND DISCUSSION

The analytical data (Table 1) show 1:2 metal:ligand composition for the complexes. Molar conductance values of the complexes in DMF show that the Ni(II) and Cu(II) complexes are non-electrolytes, while the Cr(III) complex is 1:1: electrolyte (Table 1).

Table 1. Analytical Data and Molar Conductibility for the Complexes Studied

Complex	C% Calc/exp	N% Calc/exp	Metal% Calc/exp	λ_M (in DMF) $\Omega^{-1}\text{cm}^2\text{mol}^{-1}$
[CrL ₂ (H ₂ O) ₂]Cl (I)	48,07 47,90	17,20 16,87	8,47 8,02	70
[NiL ₂ (H ₂ O) ₂].3H ₂ O (II)	46,22 45,86	16,59 16,30	8,74 8,04	27
[CuL ₂ (H ₂ O) ₂] (III)	49,84 49,31	17,89 17,13	10,22 9,93	30

The presence of coordinated water is supported by TG and IR spectral data. Thus, the thermogravimetric curves for all the three complexes show an exothermic peak in the range of 180-240°C, which corresponds to the loss of coordinated water¹⁴. For the Ni(II) complex, the first exothermic process, with a maximum at 120°C, corresponds to the loss of crystalline water. The exothermic process, with a maximum at 290°C, observed on the thermal diagram of the Cr(III) complex, is due to the loss of anionic chlorine. All the complexes lose the organic ligand in a large exothermic process, in the range of 300-800°C. Figure 1. gives the characteristic thermal diagrams of the complex compounds.



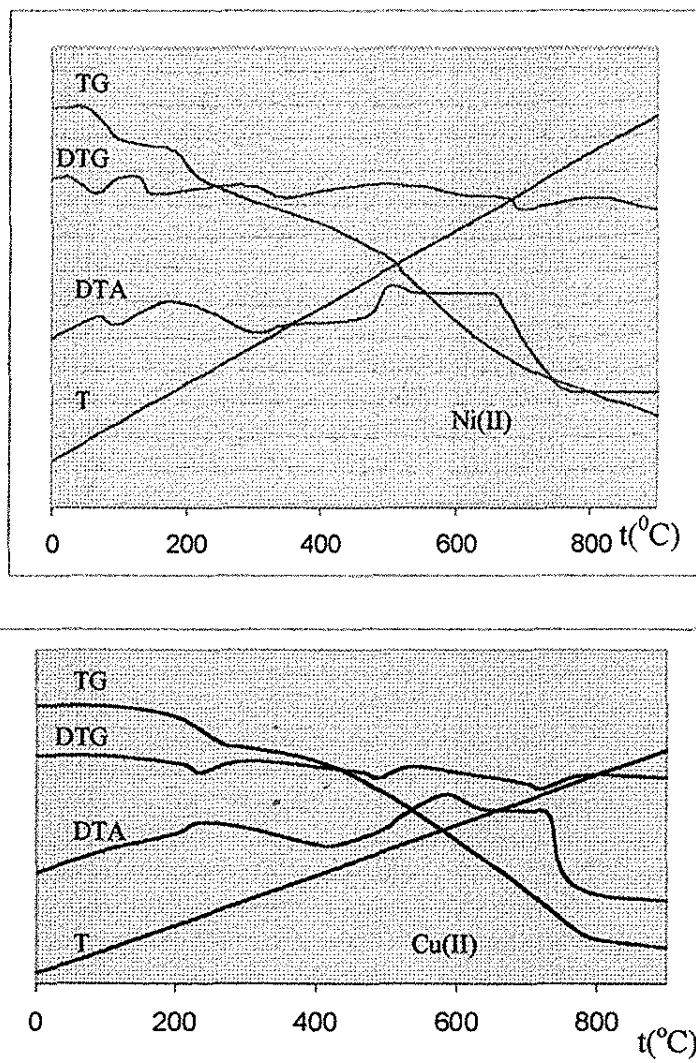


Figure 1. Thermogravimetric curves of the hydrazone complexes

Infrared spectra. IR spectrum of the ligand shows a broad band at 2890 cm^{-1} , due to the OH stretching frequency (Table 2). The metal complexes do not absorb in this region, but show a broad medium band at $3420\text{-}3460\text{ cm}^{-1}$, that may be due to ν_{OH} of coordinated water^{1,2,7,15}. The new bands at $770\text{-}780\text{ cm}^{-1}$ and 900 cm^{-1} appearing in IR spectra of the complexes are attributed to $\rho_{\text{w}}(\text{OH})$ and $\rho_{\text{r}}(\text{OH})$ respectively, of coordinated water¹⁶.

Table 2. Characteristic Bands in the IR Spectra of the Ligand and its Complexes (ν_{\max} , cm^{-1})

Assignments	HL	I	II	III
$\nu_{\text{C=N}}$	1566 s	1590 s (C=N coord.) 1610 s (C=N noncoord.)	1590 s 1620 s	1590 s 1600 s
$\nu_{\text{C=N}^+}\nu_{\text{C=C}}$ conj.	1566 s	1560 s	1550 s	1550 s
$\nu_{\text{C-O}}$ phen.	1280 s	1295 s	1295 s	1290 s
ν_{NN}	965 m	980 m	975 m	980 m
ν_{OH}	2952 m (OH chelated)	3420 ms (H_2O)	3450 s	3460 s
$\rho_{\text{w}}(\text{H}_2\text{O})$	-	780 w	770 w	770 w
$\rho_{\text{r}}(\text{H}_2\text{O})$	-	900 w	910 w	910 w
$\nu_{\text{M-O}}$	-	660 (H_2O) 540 w (O phen.)	590 w 570 w	580 w 565 w
$\nu_{\text{M-N}}$	-	485 w	450 w	460 w

The strong band which occurs at 1566 cm^{-1} is assigned to the stretching vibration of $>\text{C}=\text{N}$ group, $\nu_{\text{C=N}}$ ^{1-4,6-8}. In the IR spectra of the complexes, this band splits in two components, due to the difference in environment of the azomethine groups: one is coordinated and the other non-coordinated. The coordination of one azomethine group (the $>\text{C}=\text{N}$ group in *ortho* to the hydroxy group) is also supported by a upward shift in the position of the band assigned to ν_{NN} (965 cm^{-1} in IR spectrum of the ligand)^{2,3,17}.

The strong band at 1280 cm^{-1} assignable to C-O bonding of phenolic group shifts to higher frequencies, indicating the coordination of the ligand through phenolic oxygen^{4,6,14,17}.

New weak bands appearing in the far-infrared region for all the complexes may be assigned to $\nu_{\text{M-O}}$ and $\nu_{\text{M-N}}$ vibrations, respectively^{1,2,6,7}.

The analysis of the IR spectra of 4-hydroxy-5-methoxy isophthalaldehyde bis-dimethylhydrazone and its Cr(III), Ni(II) and Cu(II) complexes shows that the ligand is coordinated to the phenolic oxygen atom and the nitrogen atom of azomethine group, in the *ortho* position to the phenolic group.

Magnetic and electronic spectral data. The hexacoordination of the metal ions in all the complexes, established by analytical, thermogravimetric and IR spectral data, is confirmed by electronic spectra, characteristic for distorted octahedral complexes.

The μ_{eff} value of the chromium(III) complex is 3,82 MB, according to an octahedral stereochemistry³. The six-coordinated Cr(III) complexes having octahedral symmetry generally show three spin-allowed bands, due to ${}^4\text{A}_{2g} \rightarrow {}^4\text{T}_{2g}$, ${}^4\text{A}_{2g} \rightarrow {}^4\text{T}_{1g}$ and ${}^4\text{A}_{2g} \rightarrow {}^4\text{T}_{1g}(\text{P})$ ¹⁸. For the present complex, the observation of six spin-allowed transitions can be accounted for by a low symmetry ligand field, due to the existence of the chromophore CrO_4N_2 . In such a situation, the UV-VIS absorption bands (Figure 2) can be assigned to the transitions shown in Table 3, assuming an octahedral symmetry with tetragonal distortion, by compression along z axis (direction of azomethine nitrogens, while xOy plane is limited by the oxygen atoms of

water and the phenolic groups of hydrazone). The transitions with low intensity at 14084cm^{-1} and 19723cm^{-1} are spin-forbidden transitions.

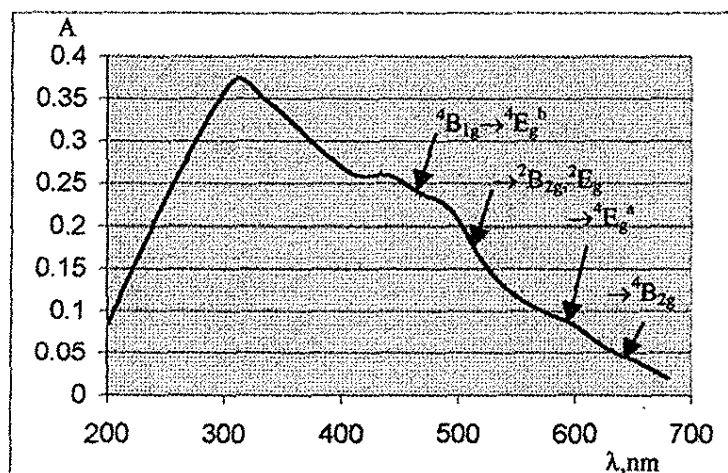


Figure 2. Diffuse-reflection electronic spectrum of the Cr(III) complex

Table 3. Electronic transitions for $[\text{CrL}_2(\text{H}_2\text{O})_2]\text{Cl}$

Observed bands (ν_{max} , cm^{-1})	Assignments
14084	${}^4\text{B}_{1g} \rightarrow {}^2\text{A}_{1g}, {}^2\text{B}_{1g}, {}^2\text{A}_{2g}, {}^2\text{E}_g$
16666	${}^4\text{B}_{1g} \rightarrow {}^4\text{B}_{2g}$
18518	${}^4\text{B}_{1g} \rightarrow {}^4\text{E}_g^a$
19723	${}^4\text{B}_{1g} \rightarrow {}^2\text{B}_{2g}, {}^2\text{E}_g$
20283	${}^4\text{B}_{1g} \rightarrow {}^4\text{E}_g^b$
21459	${}^4\text{B}_{1g} \rightarrow {}^4\text{A}_{2g}^a$
25839	${}^4\text{B}_{1g} \rightarrow {}^4\text{E}_g^c$
26809	${}^4\text{B}_{1g} \rightarrow {}^4\text{A}_{2g}^b$

The splitting of the excited states for this complex permitted the calculation of ligand field parameters.

Using the weak field approach, the positions of the various transitions are expressed in terms of crystal field parameters Dq , D_t and D_s ^{18,19}.

Because the splitting of the first "octahedral" band is equal to $35/4 Dq$, we obtained $D_t = -211\text{cm}^{-1}$, which corresponds to an octahedron compressed along the z axis (the axis of azomethine nitrogens). The splitting of the second "octahedral" band permitted the calculation of $D_s = 152\text{cm}^{-1}$.

Molecular orbital parameters $d\sigma$ and $d\pi$ and AOM parameters are calculated, using the relations proposed by Lever¹⁸. We thus obtained $d\sigma = 167 \text{ cm}^{-1}$ and $d\pi = -755 \text{ cm}^{-1}$, showing that the azomethinic nitrogen is a better σ -donor but a poorer π -donor than oxygen (phenolic and oxygen of water)²⁰.

In the case of this complex, none of the AOM parameters can be written as zero, so we arbitrarily chose $e'_{\sigma} = 7459 \text{ cm}^{-1}$, which represents the value determined by Lever¹⁸ for water, in the complex $[\text{Cren}_2(\text{H}_2\text{O})_2]^{3+}$. Applying the relations¹⁸:

$$Dq_L = 1/10 [e'_{\sigma}(L) - 4e'_{\pi}(L)]$$

$$D_s = 2/7 [e'_{\sigma}(L) + e'_{\pi}(L) - e'_{\sigma}(Z) - e'_{\pi}(Z)]$$

$$D_t = 2/35 [3 e'_{\sigma}(L) - 4e'_{\pi}(L) - 3e'_{\sigma}(Z) + 4 e'_{\pi}(Z)]$$

we obtained the values of AOM parameters given in Table 4 (column 2). If we assume for $e'_{\sigma}(L)$ the value indicated above, we must find $e'_{\pi}(L) = 1370 \text{ cm}^{-1}$. In fact, we found a greater value for $e'_{\sigma}(L)$ which indicates that the phenolic oxygen is a better π -donor than the oxygen of water.

Using the relations:

$\Delta_1 = 3D_s - 5D_t$ and $\Delta_3 = 4D_s + 5D_t$, we have also obtained the values of strong field parameters.

The separation energy between the ground state and the first excited doublet state, equal to $9B_{55} + 3C$, provides the value of B_{55} , assuming $C = 4B_{55}$. The large value obtained, $B_{55} = 670 \text{ cm}^{-1}$ ($\beta = 0,72$), indicates that the ligands form weak π bonds, so that the interelectronic repulsions into the t_{2g} level are strong. The transitions from ${}^4T_{1g}(F)$ to ${}^4T_{1g}$ (equal to $12B_{35}$) is a measure of interelectronic repulsions between the t_{2g} and e_g orbitals, so that we can calculate the value $B_{35} = 400 \text{ cm}^{-1}$ ($\beta = 0,43$). The relation $\beta_{35}^2 = \beta_{33}$. β_{55} gives the value of $\beta_{33} = 0,26$, which is in accordance with strong σ metal-ligand bonds²¹.

Using a strong field approach, expressing the energy of the states in terms of Δ_1 , Δ_2 , Δ_3 and B parameters¹⁸, we obtained the values given in the third column of Table 4.

Table 4. Ligand Field Parameters for $[\text{CrL}_2(\text{H}_2\text{O})_2]\text{Cl}$ (cm^{-1})

Parameter	Weak Field Approach	Strong Field Approach
Dq_L	1666	1666
Dq_z	2037	1797
D_t	-211	-75
D_s	152	-12
$d\sigma$	167	159
$d\pi$	-755	-170
$e'_{\sigma}(L)$	7459	7459
$e'_{\pi}(L)$	1427	1427
$e'_{\sigma}(Z)$	7682	7671
$e'_{\pi}(Z)$	672	1257
Δ_1	1511	341

Δ_3	-447	-425
B_{55}	670	670
B_{35}	400	364
B_{33}	239	195

A comparison between the two sets of data leads to the following conclusions:

- $d\sigma$ is positive, according to a better σ -donor capability of azomethinic nitrogen than oxygen (phenolic and oxygen of water);

- $d\pi$ is negative, signifying that the azomethinic nitrogen is a poorer π -donor than oxygen.

-the agreement between the data obtained by the two approaches is good, except for the values of $e^2\pi(Z)$. This parameter has a greater value in the strong field approach, indicating a more important contribution of the azomethinic nitrogen to the π interactions with metal orbitals. As a consequence of the value of $e^2\pi(Z)$, the values of $d\pi$ and Δ_1 are smaller.

Expressing the distortion from the octahedral symmetry in terms of DS, DT and DQ parameters²², we obtained :

Weak Field Approach

$$DS = -1064 \text{ cm}^{-1}$$

$$DT = -2860 \text{ cm}^{-1}$$

$$DQ = 49191 \text{ cm}^{-1}$$

$$DT/DQ = -0,058$$

Strong Field Approach

$$DS = 84 \text{ cm}^{-1}$$

$$DT = -1016 \text{ cm}^{-1}$$

$$DQ = 47009 \text{ cm}^{-1}$$

$$DT/DQ = -0,022$$

The value of the ratio DT/DQ corresponds to an octahedron compressed along z axis (at the limit, the value for this ratio is -0,45).

The magnetic moment for the *nickel(II)* complex is equal to 3,04 MB, in accordance with an octahedral stereochemistry⁴. This conclusion is supported by the electronic spectrum, characteristic for a tetragonally distorted nickel(II) complex^{18,23-25}.

A comparison with the position of the first octahedral band for the complex compounds of the type ML_6 (10800 cm^{-1} for $[\text{Ni}(\text{NH}_3)_6]^{2+}$ and 8500 cm^{-1} for $[\text{Ni}(\text{H}_2\text{O})_6]^{2+}$), permitted the assignment of the observed bands (Figure 3) to the transitions written in Table 5. The first transition is observed in near-infrared region; the third "octahedral" band is unresolved.

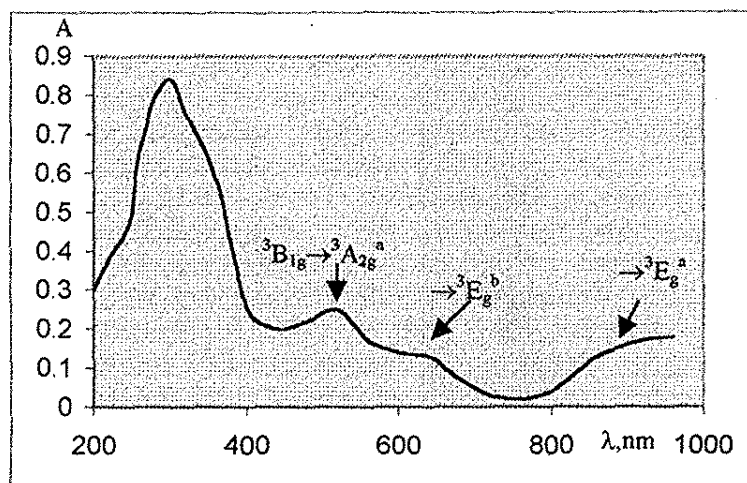


Figure 3. Diffuse-reflection electronic spectrum of the Ni(II) complex

Table 5. Electronic Transitions for $[\text{NiL}_2(\text{H}_2\text{O})_2] \cdot 3\text{H}_2\text{O}$

Observed bands (ν_{max} , cm^{-1})	Assignments
9090	${}^3\text{B}_{1g} \rightarrow {}^3\text{B}_{2g}$
10000	${}^3\text{B}_{1g} \rightarrow {}^3\text{E}_g^a$
17021	${}^3\text{B}_{1g} \rightarrow {}^3\text{E}_g^b$
18760	${}^3\text{B}_{1g} \rightarrow {}^3\text{A}_{2g}^a$
22700	${}^3\text{B}_{1g} \rightarrow {}^3\text{E}_g^c, {}^3\text{A}_{2g}^b$

Using the weak field approach and the strong field approach, as we showed above^{18,19,22,23}, we have obtained the values of the ligand field parameters, reported in Table 6.

Table 6. Ligand Field Parameters for $[\text{NiL}_2(\text{H}_2\text{O})_2] \cdot 3\text{H}_2\text{O}$

Parameters	Weak Field Approach	Strong Field Approach
Dq_L	909	909
Dq_z	1091	1046
D_t	-104	-78
D_s	-311	-267
$d\sigma$	661	547
$d\pi$	206	206
$e'_\sigma(L)$	4118	4271
$e'_\pi(L)$	816	930
$e'_\sigma(Z)$	5000	5000
$e'_\pi(Z)$	1022	1290
Δ_1	-413	-412
Δ_3	-1764	-1459
B	835	927

Because D_t is negative, the sign of the tetragonal distortion is such that the octahedron is compressed along the z-axis. The value of DT/DQ ratio, indicated below, is also in accordance with a weak compression of the octahedral ligand field along the z-axis²².

Weak Field Approach

$$DS = 2177 \text{ cm}^{-1}$$

$$DT = -1410 \text{ cm}^{-1}$$

$$DQ = 26661 \text{ cm}^{-1}$$

$$DT/DQ = -0,052$$

Strong Field Approach

$$DS = 1869 \text{ cm}^{-1}$$

$$DT = -1057 \text{ cm}^{-1}$$

$$DQ = 26244 \text{ cm}^{-1}$$

$$DT/DQ = -0,040$$

The agreement between the values of the ligand field parameters calculated with the two approaches is very good. The negative values of Δ_1 and Δ_3 are in accordance with the following sequence of *d* metal orbitals energy:

$$d_{xy} < d_{xz}, d_{yz} < d_{x^2-y^2} < d_{z^2}$$

It is interesting to observe that the π -donor power of the azomethinic nitrogen of the hydrazone ligand is greater than that of oxygen in the case of Ni(II) complex, contrary to the results obtained for Cr(III) complex.

The magnetic moment for the *copper(II)* complex is equal to 1,76 MB, corresponding to the spin-only value for the unpaired electrons²⁶. The electronic spectrum (Figure 4) shows a broad band in the visible region, with a maximum at 15200 cm^{-1} and another, at 21500 cm^{-1} , characteristic for distorted octahedral stereochemistry^{4,27}.

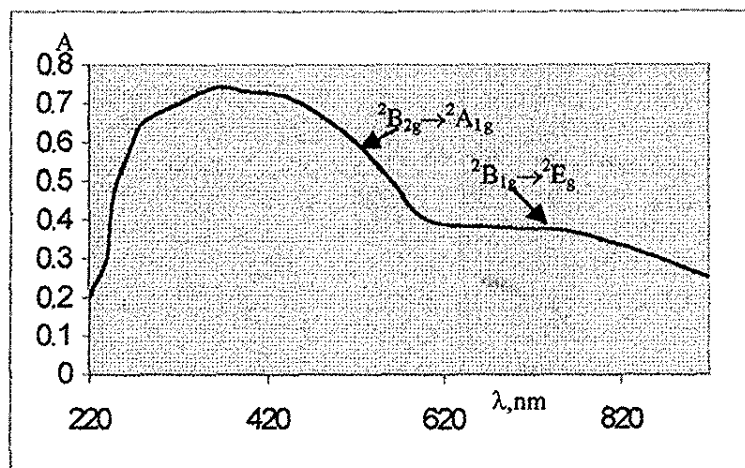


Figure 4. Diffuse-reflection electronic spectrum of the Cu(II) complex

The sign of the octahedron distortion would be established by the Electronic Paramagnetic Resonance (EPR) spectrum, but its anisotropy is not clearly resolved (Figure 5).

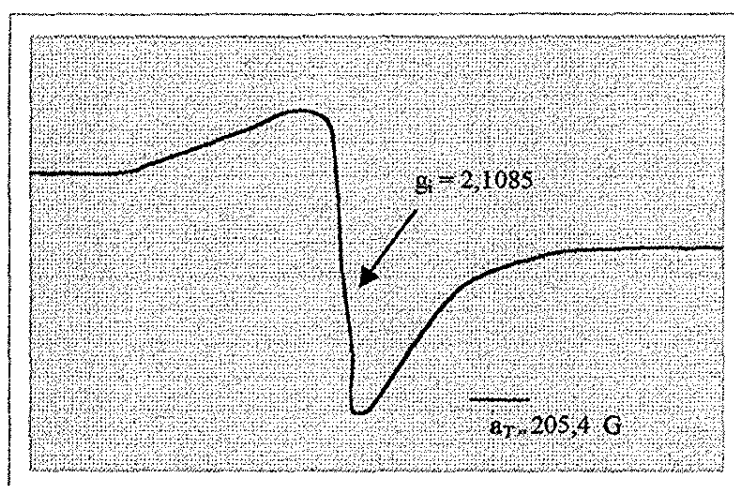


Figure 5. Electronic Paramagnetic Resonance powdered spectrum (X band) of the Cu(II) complex

Based on an analogy with the Cr(III) and Ni(II) complexes, we proposed an octahedral symmetry, distorted by compression along the z-axis. Under this assumption, the

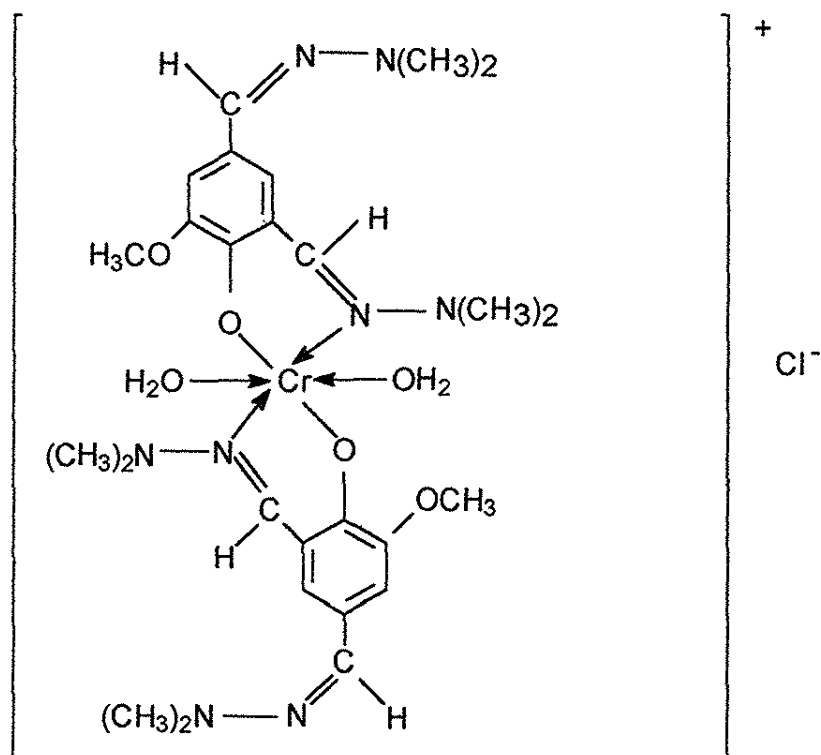
observed bands may be assigned to the following transitions: ${}^2B_{2g} \rightarrow {}^2E_g$ (15200 cm^{-1}); ${}^2B_{2g} \rightarrow {}^2A_{1g}$ (21500 cm^{-1}); CT (23972 cm^{-1}).

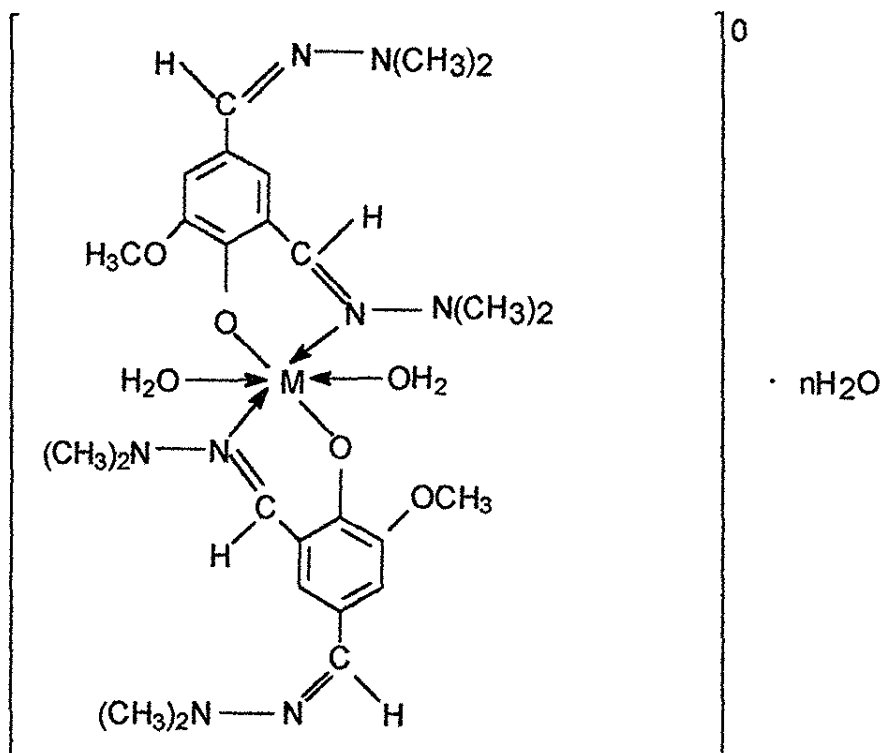
Assuming a compressed octahedral symmetry, $g_{\parallel} = 2,0023$ and g_{\perp} can be calculated with the relation²⁸: $g_i = 1/3 (g_{\parallel} + 2 g_{\perp})$. We thus obtained $g_{\perp} = 2,170$, a value that can be used for the calculation of the spin-orbit coupling constant, λ :

$$g_{\perp} = 2,0023 - 6\lambda/\Delta_2 \qquad \Delta_2 = \Delta E(d_{z^2} - d_{yz,zz})$$

The value obtained for the spin-orbit constant, $\lambda = -410\text{ cm}^{-1}$, gives $\lambda/\lambda_0 = 0,49$ ($\lambda_0 = -830\text{ cm}^{-1}$), indicating an important covalent character of the metal-ligand bond.

On the basis of the results of analytical and physico-chemical analyses, the following structures may be assigned to the complexes:





M = Ni; n=3

M = Cu; n=0

Figure 6. Structures of the complexes studied

REFERENCES

1. R.C. Aggarwal, T.R. Rao, *J. Inorg. Nucl. Chem.*, **40**, 1171-1174(1978)
2. R. C. Aggarwal, B. Singh, *J. Inorg. Nucl. Chem.*, **40**, 1174-1176(1978)
3. R. Chandra, S.K. Sahni, R.N. Kapoor, *Acta Chim. Hung.*, **112(4)**, 385-400(1983)
4. R.L. Dutta, M.Md. Hossain, *J. Sci. Ind. Res.*, **44**, 635-674(1985)
5. M. Mohan, M.P. Gupta, L. Chandra, *Inorg. Chim. Acta*, **151**, 61-68(1988)
6. D.K.Dwivedi, B.V. Agarwala, A.K. Dey, *J. Indian Chem. Soc.*, **65**, 461-463(1988)

7. B.V. Agarwala, P.S.N. Reddy, *Acta Chim. Hung.*, 127(2), 269-275(1990)
8. J.C. Chang, K.L. Mikkelsen, I.M. Simet, *Synth. React. Inorg. Met.-Org. Chem.*, 25(10), 1635-1664(1995)
9. I. Serban, V. Serban, A. Nicolae, *Rev. Chim.*, 44(9), 813-816(1993)
10. I. Serban, V. Serban, A. Nicolae, O. Maior, A. Meghea, *Rev. Chim.*, 44(5), 441-445(1993)
11. I. Serban, V. Serban, A. Nicolae, *Scientific Bulletin of Politechnic Institute of Bucharest*, 52(3-4), 53-56(1990)
12. I. Serban, A. Nicolae, V. Serban, *Scientific Bulletin of Politechnic Institute of Bucharest*, 53(1-2), 57-61(1991)
13. C.G. Macarovici, Ed. "*Quantitative Inorganic Chemical Analysis*", Academia Republicii Socialiste România, Bucharest, 1979, pp. 222, 350, 352
14. S.R. Lukic, D.M. Petrovic, A.F. Petrovic, *J. Therm. Anal.*, 34, 1015-1021(1988)
15. K.H. Shivaprasad, S.A. Patil, B.R. Patil, V.H. Kulkarni, *Acta Chim. Hung.*, 122(2), 169-173(1986)
16. K. Nakamoto, Ed. "*Infrared Spectra of Inorganic and Coordination Compounds*", John Wiley, New York, N.Y., USA, 1963, pp.156
17. K.K. Narang, A. Aggarwal, *Indian J. Chem.*, 13, 1072-1074(1975)
18. A.B.P. Lever, *Coordin. Chem.Rev.*, 3, 119-140(1968)
19. W.A. Baker Jr., M. Phillips, *Inorg. Chem.*, 5(6), 1042-1046(1966)
20. M.A. Hitchman, *Inorg. Chem.*, 11(10), 2387-2392(1972)
21. A.B.P. Lever, Ed. "*Inorganic Electronic Spectroscopy*", Elsevier Publishing Company, Amsterdam, 1968, pp.279
22. J.C. Donini, B.R. Hollebone, G. London, A.B.P. Lever, J.C. Hempel, *Inorg. Chem.*, 14(3), 455-461(1975)
23. R.L. Chiang, R.S. Drago, *Inorg. Chem.*, 10(3), 453-457(1971)
24. D.M.L. Goodgame, M. Goodgame, M.A. Hitchman, M.J. Weeks, *J. Chem. Soc. (A)*, 1769-1772(1966)
25. D.A. Rowley, R.S. Drago, *Inorg. Chem.*, 6(6), 1092-1096(1967)
26. S. Bhardwaj, M.N. Ansari, M.C. Jain, *Indian J. Chem.*, 28A, 81-82(1989)
27. H.R. Singh, B.V. Agarwala, *J. Indian Chem. Soc.*, 65, 591-593(1988)
28. A. Abragam, B. Bleaney, Ed. "*Electron Paramagnetic Resonance of Transition Ions*", Oxford University Press, London, 1970, pp. 448, 449

PHYSICAL CHEMICAL STUDIES OF THE AGGREGATION AND
CATALYTIC PROPERTIES OF THE SURFACTANT
METHYLDODECYLBENZYLTRIMETHYLAMMONIUM CHLORIDE
(MDBTACL)Lavinel G. Ionescu^{a,b} Sílvia Dani^b and Elizabeth Fátima de Souza^c

^a Departamento de Química Pura, Faculdade de Química, Pontifícia Universidade Católica do Rio Grande do Sul - PUCRS, Porto Alegre, RS, Brazil

^b Departamento de Química, Centro de Ciências Naturais e Exatas, Universidade Luterana do Brazil - ULBRA, Canoas, RS, Brazil

^c Instituto de Ciências Biológicas e Química, Pontifícia Universidade Católica de Campinas - PUC-CAMPINAS, Campinas, SP, Brazil

ABSTRACT

The micellization of methyl dodecyl benzyl trimethyl ammonium chloride (MDBTACL) in water was studied by means of surface tensiometry. The critical micellar concentration (CMC) was determined at 25°, 32° and 40 °C and thermodynamic properties such as the free energy of micellization (ΔG°_{mic}), enthalpy (ΔH°_{mic}) and entropy (ΔS°_{mic}) of micellization were measured. The CMC at 25 °C was 1.12×10^{-2} M and the corresponding values of the thermodynamic parameters were: $\Delta G^{\circ}_{mic} = -2.66$ kcal/mol; $\Delta H^{\circ}_{mic} = -0.82$ kcal/mol and $\Delta S^{\circ}_{mic} = +6.17$ e.u. Micelles of the surfactant MDBTACL were good catalysts for the alkaline hydrolysis of p-nitrophenyl diphenyl phosphate (NPDPP) with a maximum catalytic factor of approximately 60, comparable to that of CTAB. Typical activation parameters measured for 0.012 M surfactant and 0.005 M NaOH were: $E_a = 8.5$ kcal/mol; $\Delta H^{\circ\ddagger} = 7.8$ kcal/mol; $\Delta G^{\circ\ddagger} = 19.6$ kcal/mol and $\Delta S^{\circ\ddagger} = -39.3$ e.u. The kinetic results were also analyzed in terms of the pseudo-phase ion exchange models (PPIE) and showed that the model is applicable and gave reasonable fits.

KEYWORDS: methyl dodecyl benzyl trimethyl ammonium chloride; micellization; micellar catalysis; phosphate esters

RESUMO:

A micelização do cloreto de metildodecilbenziltrimetilamônio (MDBTACL) em água foi estudada por métodos de tensiometria superficial. A concentração micelar crítica (CMC) foi determinada a 25°, 32° e 40 °C e propriedades termodinâmicas tais como a energia livre (ΔG°_{mic}) de micelização, a entalpia (ΔH°_{mic}) e a entropia (ΔS°_{mic}) de micelização foram medidas. A CMC a 25 °C foi $1,25 \times 10^{-2}$ M e os valores correspondentes para os parâmetros termodinâmicos foram os seguintes: $\Delta G^{\circ}_{mic} = -2,66$ kcal/mol; $\Delta H^{\circ}_{mic} = -0,82$ kcal/mol e $\Delta S^{\circ}_{mic} = +6,17$ e.u. Micelas do surfactante MDBTACL foram bons catalisadores para a hidrólise alcalina do p-nitrofenil difenil fosfato, com um fator catalítico máximo de aproximadamente 60, comparável ao do CTAB. Parâmetros de ativação representativos medidos experimentalmente para MDBTACL 0,012 M e 0,005 M NaOH foram: $E_a = 8,5$ kcal/mol; $\Delta H^{\circ\ddagger} = 7,8$ kcal/mol; $\Delta G^{\circ\ddagger} = 19,6$ kcal/mol e $\Delta S^{\circ\ddagger} = -39,3$ e.u. Os resultados cinéticos foram analisados em termos do modelo de pseudofase de troca iônica (PPIE) e mostraram que o modelo é aplicável e satisfatório.

INTRODUCTION

This article reports the results obtained for the study of the micellization of methyl dodecyl benzyl trimethyl ammonium chloride [MDBTACL, $(\text{CH}_3)_3\text{N}^+\text{CH}_2(\text{C}_6\text{H}_4)\text{CH}_2(\text{CH}_2)_9\text{CH}(\text{CH}_3)_2 \text{Cl}$] and its application in the micellar catalyzed hydrolysis of *p*-nitrophenyl diphenyl phosphate.

As a part of a systematic study of the micellization process we have studied a variety of surfactants in water, non-aqueous solvents and water solutions containing co-solvents or additives using experimental methods such as surface tensiometry, nuclear magnetic resonance (NMR) and quasi-elastic light scattering (QELS) ¹⁻¹⁴. The study of the surfactant under consideration, MDBTACL, was motivated by its similarity to cetyltrimethylammonium bromide, CTAB, the main difference being the counter-ion chloride, Cl⁻.

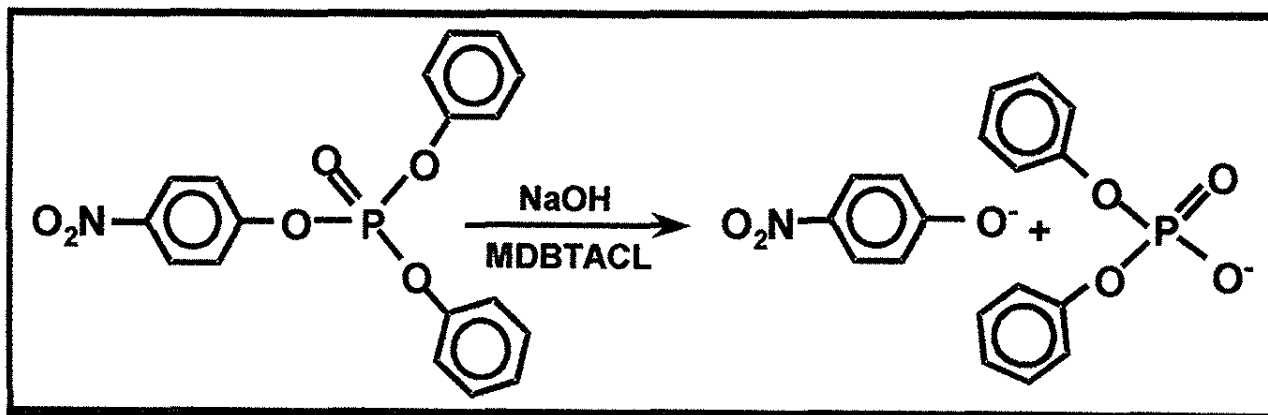
Organic phosphorus compounds, and in particular phosphate esters, are of paramount biological and pharmacological importance and have been widely used as drugs, nerve gases and pesticides ^{15,16}.

In studies described in the literature we have reported the hydrolysis of di- and tri-substituted phosphate esters in the presence of micelles of a variety of surfactants, including some that form functional micelles ¹⁷⁻²⁰.

The micellar catalyzed oxidative cleavage of a carbon-carbon bond in Dicofo^{1(TM)} ²¹ and the micellar catalyzed dehydrochlorination of 1,1,1-trichloro-2,2-bis(*p*-chlorophenyl)ethane (DDT) and some of its derivatives have also been subject of our investigations ^{22,23}.

We have also reported results obtained for the hydrolysis of *p*-nitrophenyl diphenyl phosphate in aqueous solutions in the presence of micelles of diethyl heptadecyl imidazolium ethyl sulfate (DEHIES) and CTAB, sodium hydroxide and dimethylsulfoxide (DMSO) and analyzed the effect of internal pressure of the medium, dielectric constant, donor number and polarity of the solvent and the effect of DMSO on micellization ²⁴⁻²⁸. In a more recent article we have described the physical chemical studies of the aggregation and catalytic properties of the surfactant cetyldimethylethylammonium bromide (CDEAB) ²⁹.

The present article deals with the study of the hydrolysis of *p*-nitrophenyl diphenyl phosphate (NPDPP) in the presence of micelles of methyl dodecyl benzyl trimethyl ammonium chloride (MDBTACL) in aqueous solutions containing NaOH, as illustrated by the following scheme:



EXPERIMENTAL PROCEDURE

Materials. The p-nitrophenyl diphenyl phosphate (NPDP) was prepared using standard methods^{30,31}. A sample was also obtained from Prof. Fred Menger, Emory University, Atlanta, Georgia, USA. The surfactant methyl dodecyl benzyl trimethyl ammonium chloride (MDBTACL) was purchased from Chem. Service, West Chester, Pa., USA. The sodium hydroxide was analytical reagent grade and was purchased from Merck Co.

Surface Tension Measurements. All solutions were prepared volumetrically with deionized double distilled water and contained a series of at least fifteen different concentrations of MDBTACL. The surface tension of the MDBTACL-H₂O solutions was measured at 25°, 32° and 40 °C by means of a Fisher Model 21, Semi-Automatic Tensiometer. Ten milliliters aliquots of the solutions were placed in a Petri dish with a diameter of 6 cm. The temperature of the solutions was brought to the chosen temperature using a water bath and the Petri dish was kept at the desired temperature by placing it in a container through which water was circulated from the constant temperature bath. The tensiometer was set a constant height. The final surface tension of any solution was the average of at least three independent measurements.

The critical micellar concentrations (CMC's) were determined from plots of the surface tension of the solutions versus the concentration or log concentration of MDBTACL. The marked change in the plots was taken as an indication of micelle formation and the inflection point was considered to correspond to the CMC.

The thermodynamic parameters ΔG°_{mic} , ΔH°_{mic} and ΔS°_{mic} were determined using standard equations^{33,34} derived on the basis of the assumption that the process of micellization involves the formation of a distinct micellar phase at the CMC and that the concentration of monomers in solution is constant, once micelles are formed. The experimental accuracy in the values determined for ΔG°_{mic} is about ± 100 cal/mole. On the other hand, ΔH°_{mic} and ΔS°_{mic} are more approximate since they were calculated on the basis of measurements at three temperatures only.

Kinetic Measurements. The hydrolysis of p-nitrophenyl diphenyl phosphate was studied spectrophotometrically by measuring the rate of appearance of the p-nitrophenoxide anion at 4030 Å with a Varian DMS-80 spectrophotometer equipped with a temperature controlled cell compartment. The reaction was studied at 15°, 25° and 35°C at various concentrations of NaOH and MDBTACL. The pseudo-first order rate constant (k_{ψ}), in s⁻¹, was determined from linear plots of logarithm of absorbance versus time and the second order rate constants (k_{2m}) in the micellar phase and (k_2^0) in the aqueous phase, in s⁻¹M⁻¹, were calculated from k_{ψ} and the hydroxide ion concentration. Activation parameters such as the activation energy (E_a), the activation enthalpy ($\Delta H^{o\ddagger}$) and the activation entropy ($\Delta S^{o\ddagger}$) were determined from experimental k_{ψ} values measured at three different temperatures using the following equations.

$$\ln k_{\psi} = \ln A - (E_a/R) (1/T) \quad (1)$$

$$\Delta H^{o\ddagger} = E_a - RT \quad (2)$$

$$\Delta S^{o\ddagger} = 4.576 (\log k_{\psi} - 10.753 - \log T + E_a/4.576T) \quad (3)$$

$$\Delta G^{o\ddagger} = \Delta H^{o\ddagger} + \Delta S^{o\ddagger} \quad (4)$$

where, R corresponds to the gas constant and T to the absolute temperature.

RESULTS AND DISCUSSION

Typical experimental results obtained for the surface tension of MDBTACL in water solutions at 25°, 32° and 40°C are shown in Figure 1.

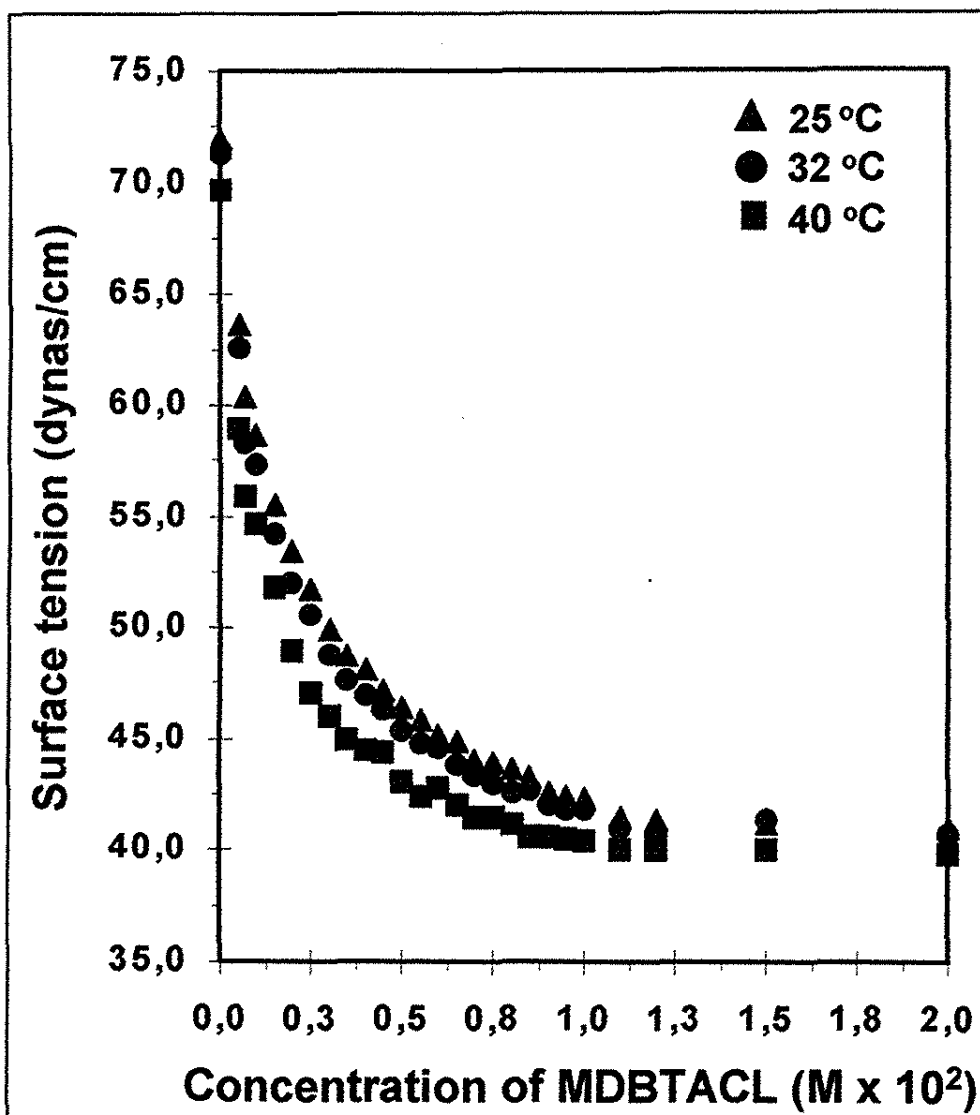


Figure 1. Plot of Surface Tension versus Concentration of Methyldodecylbenzyltrimethylammonium Chloride (MDBTACL) in Water at 25°, 32° and 40°C.

All plots of surface tension versus the concentration of MDBTACL exhibited initial marked drops and subsequent leveled off. The inflection point in the given curve was taken as the CMC. At times, plots of surface tension versus the logarithm of the concentration of surfactant gave a better determination for the CMC. Such results are shown in Figure 2 for the same temperatures.

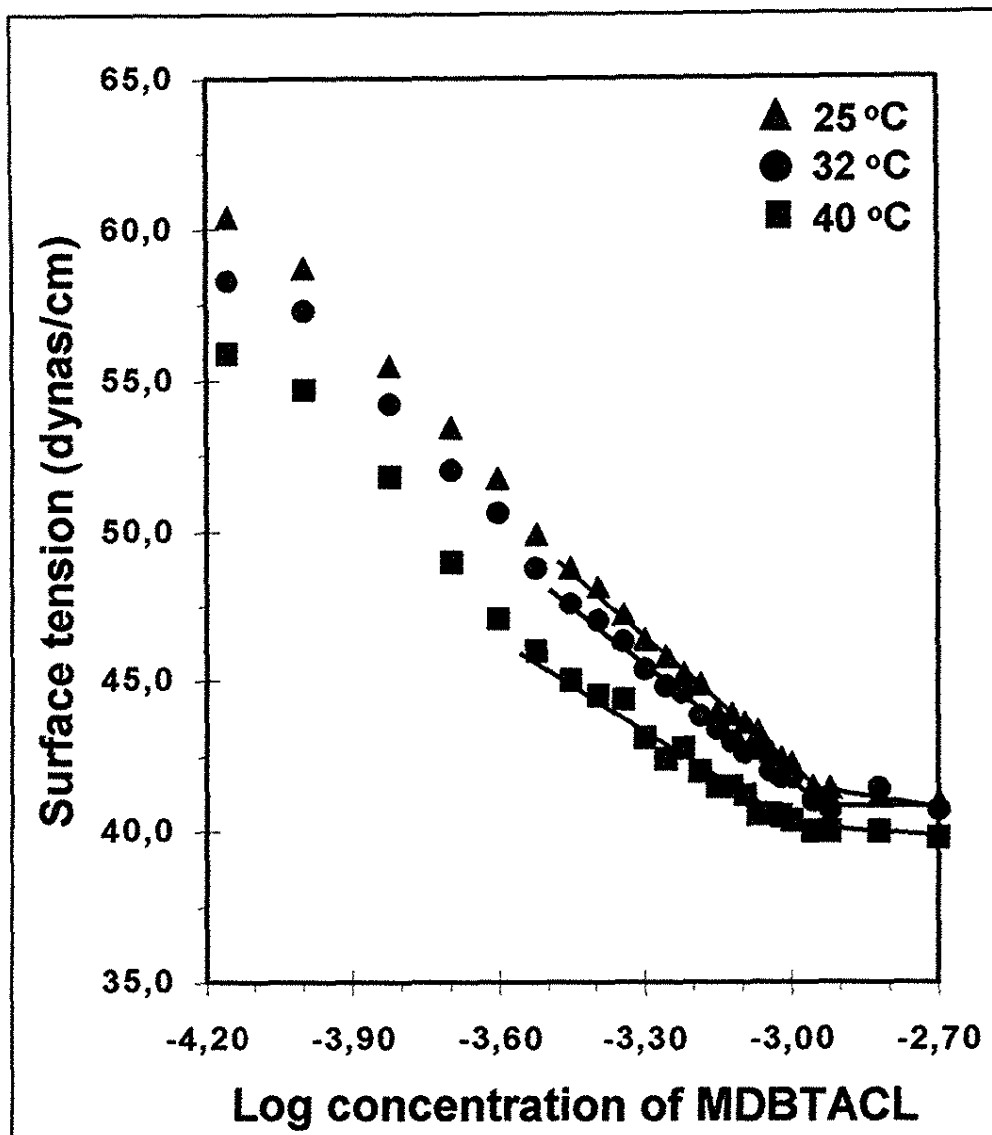


Figure 2. Plot of Surface Tension versus Logarithm of the Concentration of Methyl dodecyl benzyl trimethyl ammonium Chloride (MDBTACL) in Water at 25° and 32° and 40°C.

The experimental results obtained for the critical micellar concentration (CMC) are shown in Table I and compared to cetyltrimethylammonium bromide (CTAB). Table II shows the experimental values obtained for the thermodynamic functions, i.e., the standard free energy of micellization, ΔG°_{mic} , the enthalpy, ΔH°_{mic} , and the standard entropy of micellization ΔS°_{mic} at 25°C, again compared to CTAB^{7,11,14}. As expected, the difference between the experimental values obtained for the CMC and the thermodynamic properties for the two surfactants is very large, the difference being mainly due to the counter-ion that changes from Cl⁻ to Br⁻.

Table I. Critical Micellar Concentration (CMC) of Methyl dodecyl benzyl trimethyl ammonium Chloride (MDBTACL) in Aqueous Solutions Compared to CTAB^{14,29}

Surfactant	Temperature (°C)		
	25	32	40
MDBTACL	1.12×10^{-2} M	1.15×10^{-2} M	1.15×10^{-2} M
CTAB	9.00×10^{-4} M	--	10.0×10^{-4} M

Table II. Some Thermodynamic Properties for the Formation of Micelles of Methyl dodecyl benzyl trimethyl ammonium Chloride (MDBTACL) in Water at 25 °C Compared to CTAB^{14,29}

Surfactant	Free Energy of Micellization at 25 °C ΔG°_{mic} (kcal/mole)	Enthalpy of Micellization ΔH°_{mic} (kcal/mole)	Entropy of Micellization at 25 °C ΔS°_{mic} (e.u.)
MDBTACL	-2.66	-0.82	+6.17
CTAB	-4.14	-1.03	+10.43

Typical profiles for the pseudo-first order rate constant, k_p , as a function of the concentration of MDBTACL for the hydrolysis of p-nitrophenyl diphenyl phosphate (NPDPP) at 25°C in aqueous solutions containing NaOH between 0.003 M to 0.010 M are shown in Figure 3.

The experimental rate profiles obtained are characteristic of micellar catalyzed reaction in aqueous solutions with a maximum at 1.0×10^{-2} M MDBTACL, considerably higher than the concentrations observed for surfactants having Br⁻ as the counter-ion. The addition of MDBTACL to the reaction medium causes an increase in the rate of hydrolysis up to a point (the maximum in rate) where there is total incorporation of the substrate in the micellar phase. Subsequent addition of the surfactant causes a decrease in the reaction rate, probably due to the dilution of the reactive counter-ions in the Stern layer of a higher number of micelles. The catalytic factor measured is approximately 60 compared to 80 for CTAB and CDEAB²⁹.

Table III. Activation Parameters for the Hydrolysis of p-Nitrophenyl Diphenyl Phosphate in Aqueous Solutions of 0.005 M NaOH in the Presence of MDBTACL, CDEAB and CTAB²⁸⁻³⁰ at 25 °C.

Surfactant	Concentration (M)	E_a (kcal/mole)	ΔH^{\ddagger} (kcal/mole)	ΔG^{\ddagger} (kcal/mole)	ΔS^{\ddagger} (e.u.)
--	--	+ 15.2	+14.6	+21.3	-22.2
MDBTACL	12×10^{-1}	+ 8.6	+ 7.9	+19.6	-39.3
CDEAB	18×10^{-4}	+ 9.0	+ 8.4	+19.2	-36.3
CTAB	15×10^{-4}	+ 11.4	+10.8	+18.7	-26.6
CTAB	20×10^{-4}	+ 10.5	+ 9.9	+18.8	-29.9

Representative activation parameters determined for the reaction with MDBTACL are shown in Table III and compared to CTAB and CDEAB²⁹. As can be seen from the analysis of the results the activation parameters for the three surfactants are comparable and similar and to others measured for micellar catalyzed reactions^{29,30}.

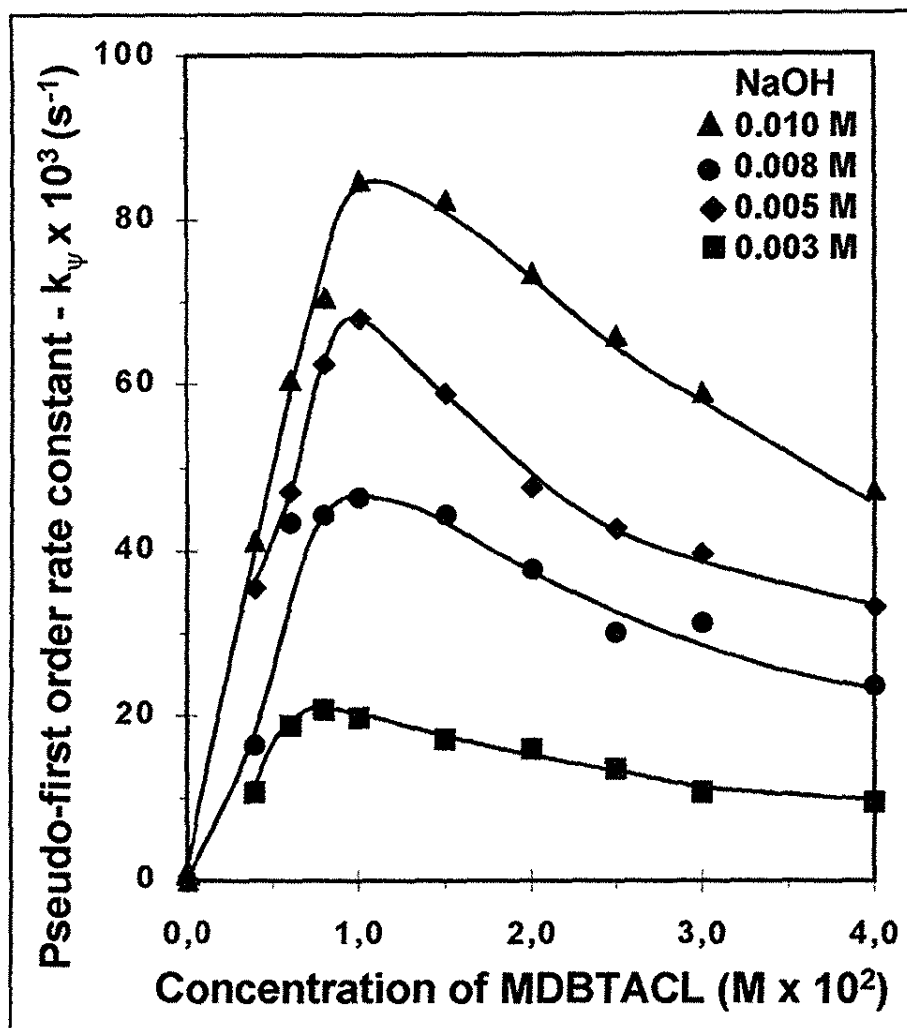


Figure 3. Rate Profiles for the Hydrolysis of p-Nitrophenyl Diphenyl Phosphate in Aqueous Solutions of NaOH and Various Concentrations of MDBTACL at 25°C

Most of the models proposed for micellar catalysis³³⁻³⁹ consider the partition coefficient for the substrate between the micellar and aqueous phase and the distribution of the reagents between the two phases. The hydrolysis of NPDPP with hydroxide ion in the presence of MDBTACL may be considered a bimolecular reaction of OH⁻ ion and the substrate. Since the concentration of OH⁻ in the micellar phase is dependent on the concentration of both chloride ions and surfactant, a quantitative treatment of the reaction rate must consider ion exchange on

or near the micellar surface. For the reaction under consideration, the model proposed by Quina and Chaimovich⁴⁰ reduces to Equation 5, that gives the theoretical dependence of the pseudo-first order constant, k_{ψ} , as a function of the total hydroxide ion concentration

$$k_{\psi} = \frac{\{(k_{2m}/V) K_S K_{OH/Cl} [(Cl)_m/(Cl)_w] + k_2^0\} (OH)_T}{(1 + K_S C_D) [1 + K_{OH/Cl} (Cl)_m (Cl)_w]} \quad (5)$$

where, C_D is the concentration of micellized surfactant, V is the molar volume of the reactive region at the micellar surface, k_{ψ} is the pseudo-first order rate constant, k_{2m} is the second order rate constant in the micellar phase, k_2^0 is the second order constant in the aqueous phase, $K_{OH/Cl}$ is the ion exchange constant, K_S is the binding constant for the substrate, $(Cl)_m$ is the concentration of Cl^- in micellar phase, $(Cl)_w$ is the concentration of Cl^- in aqueous phase, $(OH)_T$ is the total concentration of hydroxide ions and V is the molar volume of surfactant.

With substrates such as p-nitrophenyl diphenyl phosphate that are very insoluble in water and are solubilized by MBDTACL the expression for k_{ψ} can be reduced to a simpler form given by Equation (6):

$$k_{\psi} = \frac{k_{2m}}{C_D V} (OH)_T \frac{K_{OH/Cl} [(Cl)_m/(Cl)_w]}{[1 + K_{OH/Cl} (Cl)_m (Cl)_w]} \quad (6)$$

The concentration of Cl^- in the micellar and aqueous phases can be obtained using the following equations³⁸⁻⁴²:

$$A_1 = C_D + CMC + K_{OH/Cl} (OH)_T + (1 - \alpha) C_D K_{OH/Cl} \quad (7)$$

$$(OH)_m = \frac{(-A_1) + [(A_1)^2 + 4 (1 - K_{OH/Cl}) (OH)_T K_{OH/Cl} (1 - \alpha) C]^{0.5}}{2 (1 - K_{OH/Cl})} \quad (8)$$

$$(Cl)_m = (1 - \alpha) C_D - (OH)_m \quad (9)$$

$$(Cl)_w = \alpha C_D + CMC + (OH)_m \quad (10)$$

where CMC is the critical micellar concentration, α is the degree of ionization of the micelle and $(OH)_m$ is the concentration of OH^- in the micellar phase.

We have calculated the theoretical values of k_{ψ} for the reaction discussed above using $\bar{V} = 0.35$ L/mol⁴³, $K_{OH/Cl} = 0.10$ ⁴⁴, $\alpha = 0.40$ ^{45,46} and various concentrations of MBDTACL and NaOH.

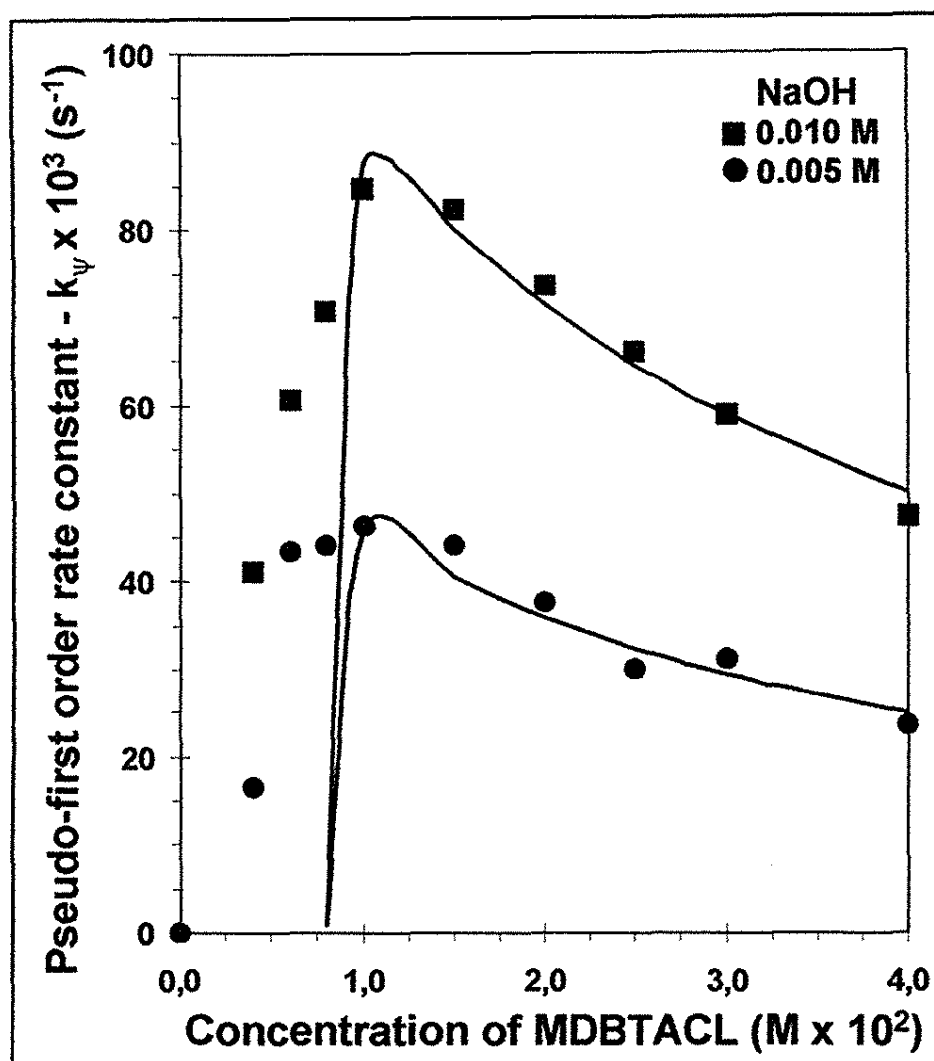


Figure 4. Experimental and Theoretical (—) k_p Values for the Hydrolysis of p-Nitrophenyl Diphenyl Phosphate in Aqueous Solutions of NaOH and Various Concentrations of MDBTACL at 25°C.

The values for k_p were calculated using different values for k_{2m} ranging from $0.60 \text{ M}^{-1}\text{s}^{-1}$ and $1.20 \text{ M}^{-1}\text{s}^{-1}$. The best experimental fits were obtained for $k_{2m} = 0.87 \text{ M}^{-1}\text{s}^{-1}$ and are illustrated in Figure 4. As can be seen, the pseudo-phase ion exchange model gives a reasonable agreement for this micellar catalyzed reaction. At low concentrations of MDBTACL (below the CMC), the presence of the highly hydrophobic solute induces the formation of kinetically active premicelles.

ACKNOWLEDGMENTS

Support received from CNPq - National Research Council of Brazil, FINEP and Sarmisegetusa Research Group, Las Cruces and Santa Fe, New Mexico, USA is gratefully acknowledged.. EFS also acknowledges the financial support from FAPESP, São Paulo, Brazil.

REFERENCES

1. L. G. Ionescu and J. K. Tsang, *Rev. Roum. Biochim.*, *15*, 211 (1978).
2. L. G. Ionescu, T. Tokuhira, B. J. Czerniawski and E. S. Smith, in "*Solution Chemistry of Surfactants*", K. L. Mittal, Ed., Plenum Press, New York, Vol. 1, p. 487, 1979.
3. T. Tokuhira and L. G. Ionescu in "*Solution Chemistry of Surfactants*", K. L. Mittal, Ed., Plenum Press, New York, Vol. 1, p. 507, 1979.
4. L. G. Ionescu, T. Tokuhira and B. J. Czerniawski, *Bull. Chem. Soc. Jpn.*, *52*, 922 (1979).
5. T. Tokuhira, D. S. Fung and L. G. Ionescu, *J. Chem. Soc. Faraday Trans. II*, *75*, 975 (1979).
6. L. G. Ionescu and B. J. Czerniawski, *Rev. Roum. Biochim.*, *18*, 103 (1981).
7. L. G. Ionescu, and V. T. De Fávère in "*Solution Behavior of Surfactants: Theoretical and Applied Aspects*", K. L. Mittal and E. J. Fendler, Eds., Plenum Press, New York, Vol. 1, p. 407, 1982.
8. L. G. Ionescu, *Arch. Biol. Med. Exp.*, *12*(2), 272 (1979).
9. L. G. Ionescu and D. S. Fung, *Bull. Chem. Soc. Jpn.*, *54*, 2503 (1981).
10. L. G. Ionescu, and D. S. Fung, *J. Chem. Soc. Faraday Trans. I*, *77*, 2907 (1981).
11. L. G. Ionescu, L. S. Romanesco and F. Nome in "*Surfactants in Solution*", K. L. Mittal and B. Lindman, Eds., Plenum Press, New York, Vol. 2, p. 789, 1984.
12. L. G. Ionescu and P. E. De Brito Moreira, *Atual. Fis. Quim. Org.*, *2*, 79 (1984).
13. L. G. Ionescu, *Química Nova*, *8*(3), 191 (1985).
14. L. G. Ionescu, S. M. H. Probst, E. F. de Souza, *South. Braz. J. Chem.*, *6*(7), 67-76 (1998).
15. F. A. Gunther, J. D. Gunther, *Chemistry of Pesticides*, Sringer Verlag, New York, 1971.
16. C. Salazar, G. M. Souza, C. P. D. Silva, *Manual de Inseticidas e Acaricidas - Aspectos Toxicológicos*, UFPel, Pelotas, Brazil, 1976.
17. C. A. Bunton, L. G. Ionescu, *J. Am. Chem. Soc.*, *95*, 2912 (1973).
18. L. G. Ionescu, D. A. Martinez, *J. Colo. Wyo. Acad. Sci.*, *7*, 13 (1974).
19. L. G. Ionescu, *Bull. N. Mex. Acad. Sci.*, *14*, 65 (1973).
20. C. A. Bunton, S. Diaz, J.M. Hellyer, I. Ihara, L. G. Ionescu, *J. Org. Chem.*, *40*, 2313 (1975).
21. F. Nome, E. W. Schwingel, L. G. Ionescu, *J. Org. Chem.*, *45*, 705 (1980).
22. F. Nome, A. Rubira, L. G. Ionescu, *J. Phys. Chem.*, *86*, 1181 (1982).
23. L. G. Ionescu, F. Nome, In *Surfactants in Solution*, K. L. Mittal, B. Lindman, Eds.; Plenum Press: New York, Vol. 2, p. 1107, 1984.
24. L. G. Ionescu, E. F. Souza, *South. Braz. J. Chem.*, *1*, 75 (1993).
25. L. G. Ionescu, E. F. Souza, In *Surfactants in Solution*, A. K. Chattopadhyay, K. L. Mittal, Eds.; Marcel Dekker: New York, Vol. 64, p. 123, 1996.
26. L. G. Ionescu, E. F. Souza, *South. Braz. J. Chem.*, *3*, 63 (1995).
27. L. G. Ionescu, D. A. R. Rubio, E. F. Souza, *South. Braz. J. Chem.*, *4*, 59 (1996).
28. E. F. Souza, L. G. Ionescu, *Coll. and Surfaces A*, *149*, 609 (1999).
29. L.G. Ionescu, S. Dani and E.F. Souza, *South. Braz. J. Chem.*, *7*(8), 105 (1999).
30. L.G. Ionescu, V.L. Trindade and E.F. Souza, *Langmuir*, *16*(3), 988 (2000).
31. A. M. Ross, J. Toet, *Tev. Trav. Chim.*, *77*, 1946 (1958).
32. A. S. Kirby, J. Jounas, *J. Chem. Soc. B*, 1165 (1970).
33. N. Muller in "*Reaction Kynetics in Micelles*", E. H. Cordes, Ed., Plenum Press, New York, p.1-23, 1973.
34. D. G. Hall, *Trans. Faraday Soc.*, *66*, 1351, 1359 (1970).
35. S. Dani, Master's Thesis, Universidade Federal do Rio Grande do Sul, Porto Alegre, RS, Brazil, 1991, 169 pp.

36. J. H. Fendler, E. J. Fendler, *Catalysis in Micellar and Macromolecular Systems*, Academic Press: New York, 1975.
37. I. V. Berezin, K. Martinek, A. K. Yatsimirskii, *Russ. Chem. Rev.*, 42, 787 (1973).
38. K. Martinek, A. K. Yatsimirskii, A. V. Levasov, I. V. Berezin, In *Solubilization and Microemulsions*; K. L. Mittal, Plenum Press: New York, Vol. 2, p. 489, 1977.
39. L. S. Romsted, In *Solubilization and Microemulsions*; K. L. Mittal, Ed., Plenum Press: New York, Vol. 2, p. 509, 1977.
40. F. Quina, H. Chaimovich, *J. Phys. Chem.*, 83, 1844 (1979).
41. N. Funasaki, *J. Phys. Chem.*, 83, 1998 (1979).
42. C. Otero, E. Rodenas, *Can. J. Chem.*, 63, 2892 (1984).
43. R.F. Bakeeva, L.A. Kudryavtseva, V.E. Bel'skii, S.B. Fedorov, B.E. Inanov, *Russ. Chem. Bull*, 45(8), 1900 (1996).
44. L.Ya. Zakharova, L.A. Kudryavtseva, A. I. Konovalov, *Russ. Chem. Bull*, 47(10), 1868 (1998).
45. O. El Seoud, A. Blasko, C.A. Bunton, *Langmuir*, 10, 653 (1994).

**CHEMILUMINESCENCE, AN OUTSTANDING
PHYSICOCHEMICAL METHOD**

MARIA GREABU, D. O. CROCNAN, R. OLINESCU

Department of Biochemistry, University of Medicine and Pharmacy 'C Davila',
Eroilor Sanitari Blvd., 76241 Bucharest, Romania.

ABSTRACT

Luminescence has been known from ancient times. However, consistent theories about the mechanisms involved in this process have been proposed only during the last few decades. The luminescence phenomenon is the result of the absorption of energy by atoms or molecules followed by their de-excitation, with photon emission in the visible part of the spectrum. The source of energy that leads to the excited species in bioluminescence and chemiluminescence is a chemical reaction that may or may not involve enzymes. This paper presents a short review of the present state of knowledge about chemiluminescence and discusses some of their applications in biology and medicine.

RESUMO

A luminescência é um processo conhecido desde a antiguidade. Teorias consistentes para explicar este fenômeno foram propostas porém somente durante as últimas décadas. A luminescência é o resultado da excitação de átomos ou moléculas seguida por emissão de energia em forma de fótons na região visível do espectro. Na bioluminescência e quimiluminescência a fonte de energia que leva às espécies excitadas é uma reação química que pode ser catalizada ou não por enzimas. O presente trabalho apresenta uma resenha do conhecimento atual sobre quimiluminescência e discute algumas aplicações deste processo na biologia e na medicina.

KEYWORDS: chemiluminescence, bioluminescence, phagocytosis, HPLC-detection, microbiology

1. A SHORT HISTORY

The luminescence phenomenon of cold light has been known from ancient times and its appearance was often thought to be due to supernatural power. Many old stories refer to strange lights or flames such as glowing hands and luminous corpses, glowing trees or shining animals¹⁻³.

Many of these stories originate from the observations of natural luminescent phenomena like those enumerated in Table 1.

Table 1- Exhibiting bioluminescence organisms

<i>Noctiluca miliaris</i>	a marine dinoflagellate
<i>Renilla reniformis</i>	sea pensy
<i>Diplocardia longa</i> <i>Octachaetus multiporus</i>	earth worms
<i>Latia neretoides</i>	a fresh water limpet
<i>Arachnocampa luminosa</i>	the New Zealand glow-worm
<i>Chaetopterus variopedatus</i>	a marine polichete annelide
<i>Watasenia scintilans</i>	a luminous squid
<i>Photobacterium phosphoreum</i>	a luminous fungus
<i>Photinus Pyralis</i>	the American firefly
<i>Pholas Dactilus</i>	a bivalve

Some of the first references about this phenomenon appeared in the works of Aristotle (384-322 BC) in Ancient Greece, who described the bioluminescence of dead fish and fungi in *De Anima*⁴, or three centuries letter when Pliny the Elder during the Roman Empire described some luminescent species known nowadays as *Lucerna piscis* and *Pelagia noctiluca*.

After centuries of apparent silence in this field only in 1669 Robert Boyle (1627-91)^{1,2} established some of the properties of bacterial and fungal luminescence and demonstrated the importance of air whose reduction in surrounding medium of 'shining flesh' or 'shining wood' determined a large decrease of the light intensity. In the same year an alchemist of Hamburg, Henning Brand gave the first example of artificial chemiluminescence, by isolating a substance, he called "phosphorus" in distilled urine, and reduction of the remaining material. The product he obtained had a blue light³ glow and this was thought to be the cause of all cold light phenomena. Only in 1821 this idea was disproved by J. Macaire⁵ who concluded that luminous material was composed mainly of 'albumin', and required oxygen. Later, in 1887 Rafael Dubois isolated two extracts from the luminous organ of the click beetle, *Pyrophorus*, extracts he named luciferin and luciferase, a hot-water, respectively a cold-water extract. Separately these two substances did not emit light, though the mixing of the two restored the emission. His conclusion showed clearly that the luminescence was the result of a chemical reaction between the two substances⁶.

But it was only the last few decades that the development of some consistent theories about the mechanisms involved in these processes were determined. The

luminescence phenomenon or cold light is the result of the absorption of energy by some atoms or molecules followed by their de-excitation with a photon emission in the visible region of spectrum. The absorption of energy can be the result of different phenomena like: heat (candoluminescence and piroluminescence), irradiation (photoluminescence, radioluminescence), electrical excitation (electro- and piezoluminescence), structural rearrangements in solids (bio- and cristaloluminescence) or chemical reaction (chemi- and bioluminescence).

2. ELECTRONIC EXCITATION

Chemiluminescence (CL) is a complex phenomenon in which a product of an exo-energetic reaction is endowed with the energy released in one crucial step. This excited product follows the universal laws of photophysics and returns to its ground state with photon emission to give direct chemiluminescence or transfers its excitation energy to another fluorescer giving rise to sensitised chemiluminescence. The basic differences between chemiluminescence and the better known fluorescence and phosphorescence involves the excitation mechanisms and the final structure of atom/molecule processed.

i) in fluorescence and phosphorescence the excitation mechanism is the absorption of a photon that forms the excited state of the molecule in chemiluminescence the excited state is formed as a result of a chemical reaction,

ii) in fluorescence and phosphorescence the de-excitation with photon emission will result in the return of the atom or molecule to the ground state. In chemiluminescence the chemical reaction will lead to a new product formation, in an excited state and this will return to the ground state with the emission of light in the visible region of the spectrum. In fluorescence and phosphorescence the absorption-emission processes may be repeated over and over while in chemiluminescence it occurs only once time for each molecule.

No matter how the luminescence arise, the main step involved is the electronic excitation.

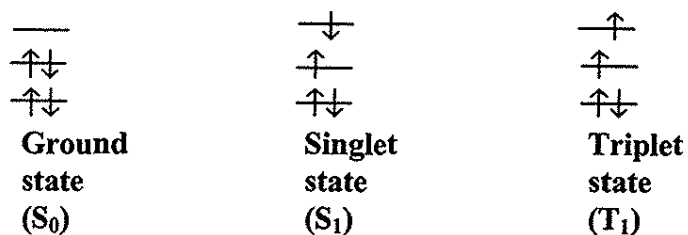


Fig. 1 - Electronic configuration of a ground state (S₀) and electronically excited singlet (S₁) and triplet (T₁) state

This is illustrated in Fig.1. where the electronic configuration of a molecule in the ground state is depicted by S₀, the first excited singlet state by S₁, which represents the fluorescent state, and the first triplet state T₁ defines the phosphorescent state. The crucial orbitals that show the electron population are the highest occupied and lowest

unoccupied molecular orbitals. In the S_0 and S_1 states, the electrons possess antiparallel spin configurations (hence, singlet states) and in T_1 , a parallel arrangement (hence, triplet state)

While in the ground state S_0 the electrons to be excited are accommodated in the same molecular orbital, i.e., the highest occupied molecular orbitals, in the excited states S_1 and T_1 the highest occupied and lowest unoccupied molecular orbitals are singly occupied.

While singlet excited states with lifetimes shorter than 10^{-8} seconds are less important in most bimolecular processes of biological systems the triplet states with longer lifetimes are prone to participate in bimolecular events such as chemical reactions or physical processes (energy transfer) with biomolecules, even when the latter ones are present only in low concentrations. The energy transfer processes may lead to sensitized emission like in sensitised chemiluminescence .

3. THE EMISSION EFFICIENCY

As was already mentioned chemiluminescence is observed when light is emitted from a chemical reaction. If the reaction occurs in a living system or is derived from one, the process is called bioluminescence (BL). The intensity of light is generally observed to increase initially and later decrease with time as the reactants are consumed. This fact can be described by the chemiluminescence quantum yield or efficiency which is photon emitted per mole of added or reacted chemiluminescence species and is expressed in Einstein mol^{-1} (1 Einstein = 6.023×10^{23} photons). An empirical equation relates the chemiluminescence quantum yield Q_{CL} with the yield of the chemical reaction Y_R , the fluorescence quantum yield of the primary excited product, Q_F and the chemiexcitation efficiency, Q_{CE}

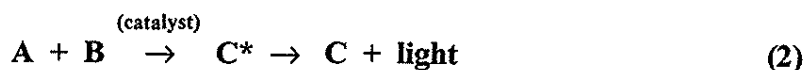
$$Q_{CL} = Y_R \times Q_F \times Q_{CE} \quad (1)$$

Q_{CE} is the percentage of molecules crossing from the transition state of the reactant to an electronically excited state of the product. This process is not well understood, Q_{CE} can only be calculated from E_q (1) and is the measure of the chemiexcitation step of the entire process.

The quantum yields found in nature are surprisingly high and often approach unity, in contrast to those of nonbiological origin, which with few exceptions (like oxalate chemiluminescence) are the best of the order of 10^{-2} Einstein mol^{-1} .

4. METHODOLOGY IN CHEMI AND BIOLUMINESCENCE (CL and BL)

For the generalised chemiluminescence reaction, E_q (2) any of the components, including the catalyst if one is used, can be measured as the analyte.



An efficient chemiluminescence reaction may be dependent on five factors:

1. - The chemiluminescence substrate whose reaction determines the formation of the molecule in excited state, molecule that is responsible for luminescent emission (direct chemiluminescence) or acts as a ground state for the de-excitation by photon emission (sensitized chemiluminescence).

2. - An electron acceptor, like oxygen in the case of a oxidising reaction - all chemiluminescence reactions

3. - A catalyst - could be an enzyme or a metal ion. It can have one of three functions:

- reduce the activation energy by accelerating the reaction
- provide a high efficiency medium for the chemiluminescence reaction
- develop an oxidant.

4. - Cofactors - usually convert one or more substrates in a form able to react or interact with the catalyst.

5. - An energy acceptor, if the chemiluminescence process is of the sensitising type.

Not always all these components are necessary. The simplest case is that in which only components 1 and 2 are involved. The reaction conditions are adjusted so that the light measured is a function of the level of analyse to be determined.

Because the signal is transient, measurement of the emission intensity is time dependent. The signal is often recorded at a specific time after mixing or by integration of light during the entire time or during a specific fraction of time when light is emitted. The instrumentation usually involves some means of mixing the reactants and a detector to measure light. The reactants can be mixed directly in front of the detector, or an optical fiber can be used to transmit the emitted light. Sometimes other sources of light are removed from the chemiluminescence signal with a filter that is placed in front of the detector.

The measurements reported for the applications described in this paper are performed in one of three ways. Static measurements in solution, involve mixing reagents in front of the detector. Often, mixing is achieved by the forced injection of a final reagent into a tube containing the other reagents. The last reagent has to be chosen so that it triggers the chemical reaction. Flow systems can be used to mix the reagents when the analyte is injected into one, or more streams of chemiluminescence reagents. Analyte on solid surfaces such as filter papers can be measured by saturating the surface with chemiluminescence reagents and recording the light emitted with a microtiter plate reader or by contact printing with photographic detection.

Investigation of chemiluminescence systems has proved difficult due to the often complex, multistep chemical reactions involved, and the variety of parameters which influence light emission. Early reaction steps and competing luminescent reaction may obscure the identity of the reaction step which produces the emitting species.

Reactants and solvents require careful purification to remove trace amounts of contaminants. This involves repeated treatment until constant light output is achieved. Even low amounts of impurities may markedly affect the intensity-time decay curve or result in as much as a tenfold variation of light intensity.

Mechanistic studies follow three approaches: (1) the reaction pathway for the chemical process must be established in terms of the intermediates (stable and transitory) and reaction products, (2) the key reaction step involving conversion of chemical energy into electronic excitation energy is identified, and (3) the mechanism whereby excitation energy appears as the excited state of the emitter is characterised. Kinetic studies may indicate the portion of the overall reaction directly related to the light emission process. The light produced in these reactions must be characterised in terms of spectral distribution and total quanta of emitted light. A conventional spectrograph may be used to determine the spectral distribution. Some other techniques for the same purpose involve the use of a rapid scan monochromators using photographic films or a phototube-recorder to display intensity⁶⁻⁷.

The central unit of the detecting system is the photomultiplier tube. Recent developments afford routine measurement of light intensities of less 1000 photons/sec incident to the photocathode. Thus systems with extremely low light output (quantum yield less than 10^{-12}) can be studied. A number of factors affect photomultiplier accuracy in making absolute or even relative measurements of light intensity. These effects may be minimised by using calibrations methods using standard radioactive sources or simple chemical light sources.

The development of "image intensifiers" offered photon gains of up to 10^6 . This kind of device is similar to a photomultiplier in its mode of operation. Incident photons are converted to electrons as they strike a photoactive cathode and are then accelerated to the first of several plates at which point several secondary electrons are released. These secondary electrons are in their turn accelerated to another plate when the releasing electron process is repeated. But the essential difference is that the photomultiplier tube provides an output electrical signal which is independent of the point at which the photons strike the cathode surface while the image intensifier tube converts the amplified electrons back into photons at a phosphor anode exit screen and with focusing methods provides an exit image identical with that formed by the original photons, image that is recorded photographically.

5. BIOLUMINESCENCE ASSAYS

The luminescence associated with biological systems that achieve such high quantum yields as mentioned before is known as bioluminescence. Some other differences between chemi- and bioluminescence are summarised in Table 2.

Table 2. Differences between bioluminescence and chemiluminescence

Bioluminescence	Chemiluminescence
enzymatic process	usually non-enzymatic process
biological function in: protection reproduction nurturing	apparently non-biological function
developed organs and special structures for guiding amplifying and changing the colour of the emitted light.	is usually spontaneous and does not develop special organs.

The components involved in the light generating reaction in bioluminescence include a luciferin in reduced form as substrate, together with a luciferase as specific enzyme. An energy-supplying substrate or cofactor is present, often in the form of NAD(P)H or ATP.

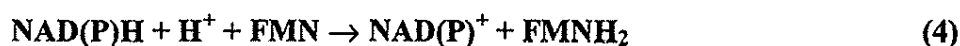
Firefly luciferase for example in the presence of luciferin (LH₂), ATP, Mg²⁺ and molecular oxygen catalyses the production of light according to the net following reaction (Eq. 3).



where $h\nu$ will have a λ_{max} of 560 nm.

Under appropriate conditions the intensity of the light produced is proportional to the ATP concentration.

In the luminescent marine bacteria systems used for analytical purposes, the light is produced by two consecutive enzymatic reactions. In the first one, catalysed by NAD(P)H: FMN oxidoreductase, FMNH₂ is produced (reaction 4) and there utilised in the second reaction catalysed by a luciferase to produce the luminescent signal (reaction 5) in the presence of molecular oxygen and an aldehyde (R-CHO)



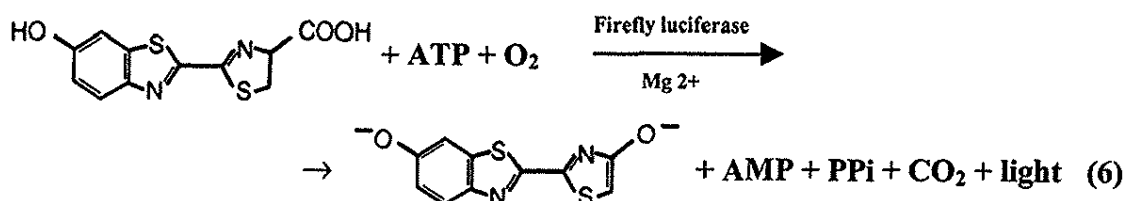
where $h\nu$ has a λ_{max} of about 490 nm.

When NAD(P)H is the limiting substrate of this bi-enzymatic system, the light intensity is proportional to the NAD(P)H concentration. The two most useful light - emitting enzyme systems were isolated from *Beneckea harvey* and *Photobacterium fischeri*.

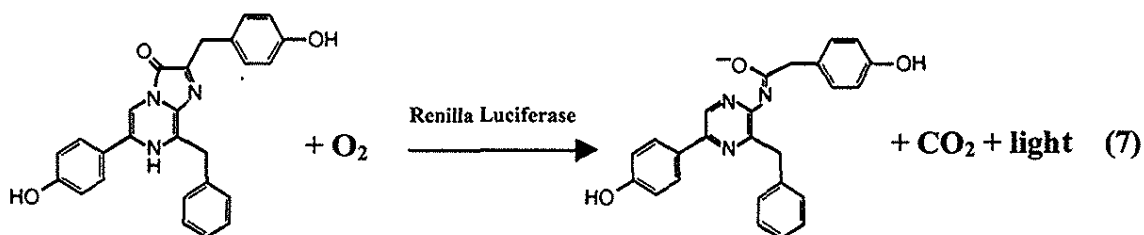
In addition of the direct measurement of either NAD(P)H or ATP by the bioluminescence reactions described above, the analysis of some NAD(P)H or ATP dependent enzymes and their substrates can be performed via the bacterial or the firefly luminescent system.

A new development of the bioluminescence technique is referred as dual luciferase reporter assay used in the quantification of gene expression. Changes in the activity of one reports correlate to the effects of the specific experimental conditions of gene expression, while the constitutive activity of the second reporter provides an internal control by which experimental values can be normalised.

The system can use both firefly and Renilla luciferases in a doubly emitting light system produced by the reactions 6 and 7.



Beetle luciferin



Coelenterazine

Some other bioluminescence assays involve dehydrogenase and kinase and components of reactions catalysed by these enzymes. Bioluminescence can be measured using NAD(P)H - dependent BL marine bacterial reaction and ATP - dependent firefly luciferase reaction.

This type of reaction is very sensitive and offers possibilities to be used it in analysis of microsamples of ATP and phosphocreatinine in simple muscle fibres⁷, pyrophosphate in mucosal biopsies as a marker of malignancy in the large intestine⁸, intracellular inorganic pyrophosphate in lymphocytes and nucleotide triphosphate pyrophosphatydialase in fibroblast⁹. Bioluminescence assays, unlike spectrophotometric assays, are less effected by turbidity and this can be exploited in coupled enzyme assays for bile acids in hyperlipemic sera¹⁰.

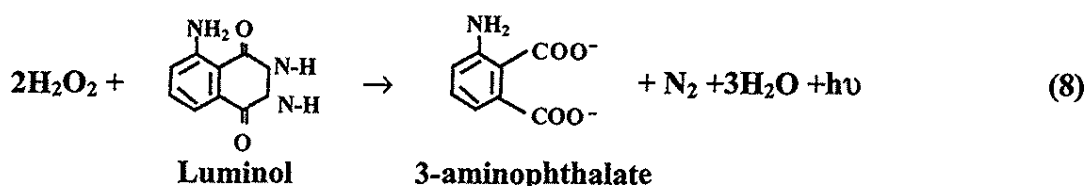
Recombinant auxotrophic microorganisms containing the bacteria luciferase gene provide novel means of assaying vitamins and aminoacids; e.g., in the presence of thiamine and a long chain aldehyde, the microorganism produces bacterial luciferase, which oxidises the aldehyde in a bioluminescence reaction¹¹.

Photoproteins, such as aequorin, form the basis of very sensitive assays for ionised calcium^{12,13}. Aequorin can also be used in an immobilised form (covalent or physical adsorption)^{14,15}.

6. CHEMILUMINESCENT ASSAYS

Any component of a reaction that involves hydrogen peroxide is amenable to chemiluminescence analysis. Usually peroxide production is detected using the luminol or a peroxyoxalate reaction. New assays based on this principle continue to appear e.g., platelet - activating factors¹⁶ oxalate^{17,18} phosphatidylcholine hydroperoxides in blood plasma¹⁹, choline containing phospholipids²⁰ and acetylcholine²¹, cephalosporine antibiotics intensify and prolong the light emission from Co¹¹ - luminol-peroxide reaction and form the basis of a simple assay for compounds such as cephalothin²².

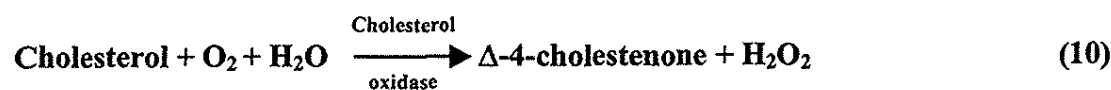
The best known chemiluminescent synthetic molecule is luminol (5 - amino - 2,3 - dihydro - 1,4 - phthalasinedione), which can produce light in the presence of H₂O₂ and a catalyst (reaction 8).



where $h\nu$ has a max of 430 nm.

Diaryl oxalates such as TCPO (bis [2, 4, 6 - trichlorophenyl] oxalate) also undergoes a chemiluminescence oxidation reaction with hydrogen peroxide. The diaryl oxalate reaction, sensitized with fluorophore can be then used for H_2O_2 determination.

Enzyme - catalysed system producing hydrogen peroxide can be coupled to chemiluminescence detection. Some examples, are given below:



Working with a luminol H_2O_2 system under standard conditions the antioxidant or pro-oxidant capacity of a third molecule can be tested. In this way the antioxidant capacities of some vitamins like ascorbic acid (vitamin C)^{23,30}, vitamins K_3 ²⁴ B_2 and A ²⁵ the pineal gland hormone, melatonin^{26,27} or some purinic and pirimidinic bases²⁸ were tested. It was also possible the testing of the influence of some iron containing ions²⁹.

7. MICROBIOLOGY AND COMPETITIVE BINDING ASSAYS

ATP is present in all living cells and thus cells can be detected and enumerated via assay for ATP using bioluminescence firefly luciferase-luciferin reaction³¹⁻³³. This bioluminescence assay has brand applications e.g. antimicrobial susceptibility testing³⁴⁻³⁶ determination of bactericidal activity³⁷ evaluation of microbial growth³⁸, studying cell chemotaxis³⁹, sperm viability⁴⁰ and antitumor chemosensitivity testing⁴¹. This type of assay has been automated using a microtiter plate luminometer⁴² where both somatic and microbial cell ATP can be determined in a sample using a sequential analytical process involving a detergent, lipid to protect the bioluminescence reagents, a hydrolytic enzyme, and a bactericide⁴³. Cell counts can also be determined with a chemiluminescence method using a menadione-Fe-EDTA-luminol reagent (detection limit for yeast cells 8.8×10^4 ⁴⁴).

Since the development of radioimmunoassays, many assays that rely on the specificity of the antigen-antibody binding reaction, have been based on this principle. Scheme (12) represent a typical competitive binding assay for the determination of an antigen (Ag) where unlabelled and labelled antigen (Ag) compete for the sites on the antibody (Ab)



After equilibration, the amount of bound and free labelled antigen can be measured, and a calibration curve can be used to determine the analyte.

The earliest immunoassays used radioactive labels. Difficulties with these labels, including waste disposal and unstable reagents, have prompted the development of nonradioactive tags, including fluorescent derivatives. However, even methods using fluorescent labels have not provided the low levels of detectability required for most immunoassay. For this reason chemiluminescence tags are attractive alternatives because chemiluminescence are among the few with the required sensitivity and detectability.

The chemiluminescence immunoassay is carried out similarly to radioimmunoassays using an immunogen labelled with a chemiluminescence reagent, and the final measurement is made by adding the required reagents and recording the light emitted. Unfortunately, unlike radioactive and even many fluorescent labels, which are relatively unaffected by binding to another species, the chemical binding of a chemiluminescence reagent often significantly affects its ability to chemiluminescence efficiently. A series of chemiluminescence immunoassays are presented in Table 3.

Table 3. Examples of Chemiluminescence Immunoassays

Analyte	Label	Chemiluminescence system	Detection limit
Methotrexate	Firefly luciferase	luciferin/ATP	2.5 pmol
Dinitrophenol	Bacterial luciferase	luciferin/ATP	15 pmol
Estriol	Bacterial luciferase	FMNH/oxidoreductase/ NADH/decanol	50 pg
Dinitrophenol	ATP	luciferin/luciferase	10 mM
Dihydroepian- drosterone	HRP	luminol/hydrogen peroxide	25 pg
Albumin	Fe (III) complex	luminol/hydrogen peroxide	2 µg
Estriol-16α- glu-curonide	Aminobutyl-ethyl isoluminol	hydrogen peroxide/microperoxidase	10 pg
Thyroxine	Fluorescamine	trichlorophenylxalate/hy- drogen peroxide	2ng/ml

8. PHAGOCYtic CHEMILUMINESCENCE

The production of reactive oxygen species by phagocytic cells of the immune system, such as polymorphonuclear leukocytes and macrophages is recognised to be a key event in the function of these cells during infections and inflammations^{47, 48, 49}.

The release of reactive oxygen species by activated polymorphonuclear leukocytes and macrophages is also associated with an emission of chemiluminescence of low intensity. Depending on the particular requirements of an assay systems whole⁵⁰ purified polymorphonuclear leukocytes^{45-47, 51-53} or alveolar macrophages⁵³ natural kills cells⁵⁰ when are used as a source of chemiluminescence The in vitro activation of the phagocytic cells was triggered by various stimuli such as: opsonized zymosan^{45-47, 51-52}

or bacteria⁵⁴ and phorbol myrimethionyl-lucyl-phenilalanine⁵⁵. In several studies^{45, 46} was reported that chemiluminescence emission of human activated polymorphonuclear leukocytes in healthy individuals depends on age and the presence of physical or psychical stress, but also on different chemicals and is induced by the ingestion vitamins and certain drugs. In this way ascorbic acid and natural antioxidants like, superoxide dismutase and melatonine were tested, but also antiinflammatory drugs like; indomethacyn, diclofenac, phenylbutazone, sodium salicylate and acetyl salicylate. The results evidenced an inhibitory effect of the chemiluminescence emission of polymorphonuclear leukocytes of the ascorbic acid and natural antioxidants while some cytostatics were reported to enhance leukocyte phagocytosis⁵⁶.

9. HIGH PERFORMANCE LIQUID CHROMATOGRAPHY DETECTION

One area of great interest to researchers is the development of detectors for high performance liquid chromatography and the use of postcolumn reactions to active selectivity and sensitivity. Chemiluminescence is particularly attractive in this mode, especially when sensitivity is needed. A variety of reactors an presented in Table 4.

Table 4. Examples of chemiluminescence detection with high performance liquid chromatography

ANALYTE	LABEL	CHEMILUMINESCENCE SYSTEM	DETECTION LIMIT
Creatinine kinase isoenzymms		Firefly luciferin/luciferase	350 u/l
Bile acids		Bacterio-luminescence	
Aminoacids	Dansyl chloride	Trichlorophenyl oxalate/hydrogen peroxide	low fmol
Polycyclic aromatic amines		Trichlorophenyl oxalate/hydrogen peroxide	sub pg
Co(II), Cu(II)		Luminol/hydrogen peroxide	sub pg
Aliphatic alcohols aldehydes ethers sacharides		Luminol/Co(II)	low µg
Cholic acid	Aminobuthyl ethyl isoluminol	Hydrogen peroxide/Fe(III)	20 fmol

The luminol reaction was the first chemiluminescence reaction demonstrated in a postcolumn reactor. Luminol and hydrogen peroxide were added postcolumn, but researchers had to ensure the compatibility of separation conditions with postcolumn reaction conditions. Metals are usually separated under acidic conditions using hydrogen

chloride, but as previously mentioned, the luminol reaction is most efficient in basic conditions. Therefore lithium chloride was used in the mobile phase.

Coupling a photochemical reaction that produces hydrogen peroxide to be detected with luminol, chemiluminescence has been used to determine aliphatic alcohols, aldehydes, ethers, and saccharides.

The isoluminol label used in immunoassay applications has been adapted as the high performance liquid chromatography derivatizing agent for amines and carboxylic acids. Addition of hydrogen peroxide and metal catalyst postcolumn allows the detection of femtomole amounts of these compounds. Metamphetamine and its metabolite amphetamine can be detected in urine at 5 and 10 pmol, respectively by derivatizing the molecules with N-(4-aminobutyl)-N/ethylisoluminol, followed by reversed-phase chromatography (C₁₈ column) and postcolumn detection with a mixture of ferricyanide - NaOH - peroxide - β - cyclodextrin⁵⁷.

Alternatively, dansyl derivatives can be prepared and detected postcolumn by means of the chemiluminescence of the bis (2,4,6 - trichlorophenyl) oxalate - peroxide reaction⁵⁸. If the drug is fluorescent (e.g., the coronary vasodilator, dipyridamole), than it can be detected directly using hydrogen peroxide and a peroxioxalate reagent⁵⁹.

Some chemiluminescence assays have combined and immobilised enzyme reactors for various analytes in serum including glucose, urate (10 pmol/20 μ l injection) and lactate (10 pmol/20 μ l)⁶⁰⁻⁶².

10. SENSORS AND IMAGING

A. chemiluminescence or bioluminescence sensor can be constructed by immobilising reagents onto a nylon membrane attached at the end of a fiber optic bundle linked to a photomultiplier tube⁶³⁻⁶⁵ e.g. alcohol can be measured using bacterial luciferase, NAD(P)H: FMN oxidoreductase, and alcohol dehydrogenase coimmobilized at the end of the fiber optic probe⁶⁶.

Photon counting video-imaging using charged coupled device cameras permitted simultaneous analysis of multiple samples^{67,68} and spatial resolutions of chemiluminescence and bioluminescence emission from reactions occurring in tissue samples e.g. imaging of ATP and lactate distribution in human melanoma tissue⁶⁹. Another application was a combination of firefly luciferase reporter gene and firefly luciferin esters that readily enter cells, to study HIV-1 virus that transactivator protein expression in cells⁷⁰. Imaging was also successfully used to determine metabolite distribution in tissue samples⁷¹ using a viscous solution of reagents applied as a frozen layer to the tissue section in order to minimise loss of resolution due to diffusion of products.

11. DETERMINATION OF NITRIC OXIDE

Endothelial cells, smooth muscle cells, macrophages, neutrophils, Kupffer cells and other cell types generate superoxide (O_2^-)⁷² and nitric oxide (NO)⁷³. The simultaneous mediators like interferon γ ⁷⁴, calcium ionophores⁷⁵, lipopolysaccharide⁷⁶

and phorbol ester⁷⁷. Thus concomitant NO and O_2^- generation may be enhanced in a variety of pathophysiological situations such as ischemia - reperfusion, acute inflammatory processes, atherosclerosis, bacterial infections and sepsis.

Both NO and O_2^- are free radical species that rapidly react with each other in aqueous solution at pH = 7.4 , yielding peroxyxynitrite anion (ONOO⁻)⁷⁸. Peroxyxynitrite is an unstable species at physiological pH, protonating to peroxyxynitrous acid (ONOOH) which spontaneously decompose to NO₂ and ·OH in 20-30% yield.



The remaining ONOOH will directly isomerize to nitrate (NO₃)⁷⁹.

Luminol chemiluminescence has been widely used to detect the production of reactive oxygen species (O_2^- , H₂O₂, ·OH) from enzyme, cell and organ systems⁸⁰⁻⁸² and has been useful for examining the kinetics and reaction mechanisms of the oxygen radical process.

In order to yield light, luminol has to undergo a two-electron oxidation and form an unstable endoperoxide. This luminol endoperoxide decomposes to an excited state, 3 aminophthalic acid, which relaxes to the ground state by emitting photons^{81, 83}. In most cases of luminol chemiexcitation in biological systems O_2^- is a key intermediate⁸⁴, but alternative pathways of chemiexcitation not requiring O_2^- have been described⁸⁵⁻⁸⁷.

REFERENCES

1. R. Boyle, *Phil. Trans. Roy. Soc. Lond.* 2, 605-612, (1667)
2. R. Boyle, *Phil. Trans. Roy. Soc. Lond* 7, 5108-5116, (1672)
3. E. N. Harvey, *A History of Luminescence from the Earliest Times until 1900*, American Philosophical Society, Philadelphia, (1957).
4. Aristotle, (384-322 B.C.).*De Anima*, *De Sensu*, *Historia Animalium* *Meteorologia*, Oxford, England (1923).
5. J. Macaire, *Memoire sur la Phosporescence des Lampyres*, *Ann. de Chimie*, 17, 151,
6. R. Dubois, *Compt. Rend.*, 105, 690, (1887).
7. R. Wilborn, K. Soederlund, A. Lundin, E. Hultman, *J. Biolum. Chemilum*, 6, 123-129, (1991).
8. M. H. Vatn, B. Tuhus, A. Northelm, *Cancer J.*, 3, 366-369, (1990).
9. B. A. Barshop, D.T. Adamson, D. C. Vellom, F. Rosen, B. L. Epstein, J. E. Seegmiller., *Anal. Biochim.*, 197, 266-272. (1991).
10. S. Lekhakula, S. Boonpisit, B. Amomkitticharoen, *J. Biolum. Chemilum*, 6, 259-269, (1991).
11. T. Yamamoto, Japanese Patent 02 179697, 1990; *Chem. Abstr.*, 114, 58481 W, (1991).
12. Y. Yashimoto, Y. Hiromoto, *Int. Rev. Cytol.*, 129, 45-73, (1991).
13. O. Shimonaura, *Cell Calcium.*, 12, 635-643, (1991).
14. A. Erisumi, S. Yoshino, S. Inone, Japanese Patent 03 153099, 1991; *Chem. Abstr.* 116, 55139 W. (1992).

15. A. Erisumi, S. Yoshino, S. Inone, Japanese Patent 03 153700, 1991. *Chem. Abstr.*, 116, 55138 W, (1992).
16. Y. Hasegawa, E. Kunow, J. Shinodon, H. Yuki, *Lipids*, 26, 1117-1121, (1991).
17. S. Albrecht, H. Broudl, W. D. Boehn, R. Beckert, H. Kroschwith, V. Newmeister, *Anal. Chim. Acta*, 255, 413-416 (1991).
18. S. Albrecht, W.D. Boehn, R. Beckert, H. Kroschwith, V. Newmeister, W. Nanoss, In "*Bioluminescence and Chemiluminescence: Current Status*", P.E. Stanley, L. J. Kricka, Wiley, Chichester, U. K., pp.463-466, (1991).
19. T. Miyazawa, *Free Radical Biol. Med.*, 7, 209-217, (1989).
20. E. Bisse, J. Gissler, H. Wieland, In "*Bioluminescence and Chemiluminescence. Current Status*"; Wiley, Chichester, U. K., , pp.467-470, (1991).
21. S. Schulman, J. Perrin, G.F. Yan, S. Chen, *Anal. Chim. Acta* , 255, 383-385, (1991).
22. G. H. G. Thorpe, T. P. Whitehend, British Patent Appl. 2. 245 062, 1991. *Chem. Abstr*, 116, 16;96392, (1992).
23. D. O. Crocnan, R. Olinescu, Gr. Turcu, *Rom. J. Biophys*, 6, (3-4), 169-179, (1996).
24. D. O. Crocnan, R. Olinescu, Nita Stela. *Rom. J. Biophys*, 6, (3-4), 180-191, (1996).
25. D. O. Crocnan, R. Olinescu, Olga Ianas, Irina Badescu Stela Nita. *Rom. J. Biophys*, 6, (1-2), 61-69, (1996).
26. R. Olinescu, Stela Nita, D. O. Crocnan, Olga Ianas, *Rom. J. Biophys*, 5, (2-3), 97-104, (1995).
27. R. Olinescu, D. O. Crocnan, Stela Nita, Olga Ianas, Irina Badescu, *Rev. Roum. Biochim.*, 32, (1-2), 57-66, (1995).
28. R. Olinescu, D. O. Crocnan, Gr. Turcu, *Rom. J. Biophys*, 6 (2-3), 27-34, (1997).
29. R. Olinescu, D. O. Crocnan, Gr. Turcu, *Rom. J. Biophys*, 6 (2-3), 35-44, (1997).
30. R. Olinescu, Maria Greabu, "*Chemiluminescence and Bioluminescence*", Ed. Tehnică, Bucharest, Romania (1987).
31. P.E. Stanley, B. J. McCarthy, *Soc. Appl. Bacteriol. Tech. Ser.*, , 26, 73-80. (1989).
32. G. B. Salo-Newby, C. Goodfield, I. R. Johnson, P. Massay, D. A. Stafford, A. Hampton A. K. Campbell, *Soc. Appl. Bacterial Tech. Ser.*, 26, 261-269, (1989).
33. J. G. .M. Hastings, P. F. Wheat, K. M. Osley, *Soc. Appl. Bacterial Tech. Ser.*, 26, 229-233, (1989).
34. D. I. Limb, P. F. Wheat, J. G..M. Hastings, R. Spencer, *J. Med. Microbiol.* 35, 89-92. (1991).
35. L. E. Nilsson, S. Aansehn, , S. E. Haffner, *Soc. Appl. Bacterial Tech. Ser.*, 26, 207-213, (1989).
36. Y. De Routlin de la Roy, N. Messedi, G. Grollier, B. Grignon, J. *Biolum. Chemilum.*, 6, 193-210, (1991).
37. Y. Miyahira, T. Takenachi, *Comp. Biochem. Physiol. A. Comp. Physiol.*, 100 A, 1031-1034, (1991).
38. G. Partsch, C. Schwarzer, *J. Biolum. Chemilum.*, 6, 159-167, (1991).
39. C. Gottlieb, K. Svanborg, M. Bygdanon, *Andrologia*, 23, 421-425, (1991).
40. H. V. Nguyen, B. V. Sevin, H. E. Averette, J. Perras, D. Donato, M. Penalver, *Gynecol. Oncol.*, 45, 185-191, (1992).
41. E. Schram, Swiss Patent 678065, 1991 *Chem. Abstr.*, 115, 227798h, (1991).

42. S. Yanashaji, S. Onishi, Japanese Patent 03266998, 1991, *Chem. Abstr.*, 116, 102236 W, (1992).
43. Y. Hasegawa, E. Kunow, J. Shindow, H. Yuki, *Lipids* 26, 1117-1121, (1991).
44. S. Albrecht, H. Brandl, W. D. Boehn, R. Beckert, H. Kroschwity, V. Neumeister, *Anal. Chem. Acta*, 255, 413-416, (1991).
45. D. O. Crocnan, R. Olinescu, Gr. Turcu, *Rom J. Biophys.* 7, (1-2), 169-179, (1997).
46. R. Olinescu, Maria Greabu, D. O. Crocnan, F. A. Kummerow, Valy Constantinescu, *Rom. J. Biophys.*, 7, (1-2), 180-189, (1997).
47. R. C. Allen, R. S. Strjenholm, *Biochem. Biophys. Res. Comm.*, 47, 680-687, (1972).
48. E. P. Brestel, *Biochem. Biophys. Res. Comm*, 126, 482-488, (1985).
49. P. De Sale, *J. Bioch. Chemilum.*, 4, 251-262, (1989).
50. S. L. Nelfand, F. Werkmeister, S. C. Roder, *J. Exp. Med*, 43, 744-752, (1982).
51. B. R. Anderson, A. M. Brendzel, F. Blintt, *Infect. Immunol.*, 17, 62-68. (1977).
52. F. A. Bonoba, A. Gargani, *Pathol. Biol.*, 44, 705-711, (1996).
53. M. J. Parnham, C. Bittner, J. Winkelman, *Agent and Action*, 21, 617-621, (1991).
54. P. Robinson, D. Wakefield, R. Penny, *Infection Immunity*, 43, 744-752, (1982).
55. C. Dohlgreen, *J. Biochem. Chemilum.*, 6, 29-35, (1991).
56. M. Giordano, M. S. Palermo, M. A. Isturis, *Int. J. Immunopharmacol*, 7, 19-23, (1985).
57. K. Nakashima, K. Suetsugu, K. Yoshido, K. Imai, S. Akiyama, *Anal. Sci*, 7, 815-816, (1991).
58. N. Takoyama, K. Hayakama, H. Koboyashi, *Chem. Abstr.*, 115, 2636, (1991).
59. A. Nishitoni, Y. Tsukamoto, S. Kanda, K. Imai, *Anal. Chim. Acta*, 251, 247-253, (1991).
60. K. Kakashimo, N. Hayasido, S. Kawaguchi, *Anal. Sci*, 7, 715-718, (1991).
61. M. Tabato, H. Totani, F. Murochi, *Anal. Biochem.*, 193, 112-117, (1991).
62. M. Tabato, M. Totani, J. Endo, T. Murochi, *G. B. F. Monogr.*, 14, 113-122, (1991).
63. N. Morel, M. Israel, *Neurocytochem. Methods*, 58, 169-182, (1991).
64. L. J. Blum, P. R. Coulet, *Fibr. Opt. Chem. Sens Biosensors*, 2, 301-313, (1991).
65. L. J. Blum, S. M. Gautier, P. R. Coulet, *J. Mater. Sci. Mater. Med.*, 2, 202-204, (1991).
66. P. R. Coulet, L. J. Blum, S. M. Gautier, *Biosens. Fundam. Technol. Appl.*, 17, 419-424, (1992).
67. D. Champlat, *Spectra*, 2000, 157, 25-29, (1991).
68. D. H. Leaback, C. E. Hosper, K. Pirzod, *Soc. Apl. Bacterial Tech. Ser.*, 26, 277-287, (1989).
69. W. Mueller-Klieser, M. Kroeger, S. Walenta, E. D. Rofstad, *Int. J. Radiat. Biol.*, 60, 147-159. (1991).
70. F. F. Craig, A. C. Simmonds, D. Watemore, F. McCapua, *Biochem. J.*, 276, 637-641, (1991).
71. W. Mueller-Klieser, W. Walenta, German Patent 3935974, 1991, *Chem. Abstr.*, 115, 68001 z. (1991).
72. G. M. Rosen, B. A. Freeman, *Proc. Natl. Acad. Sci.*, 81, 7268-7273, (1984).
73. M. A. Marletto, *Trends Biochem.*, 14, 488-492, (1989).
74. A. H. Ding, C. F. Nathan, D. J. Striehr, *J. Immunol.*, 141, 2407-2412, (1988).

75. T. Matsubara, M. Ziff, *J. Cell Physiol*, 127, 207-210, (1986).
76. D. Striehr, M. T. Marletto, *Proc. Natl. Acad. Sci. USA*, 82, 7738-7742, (1985).
77. J. F. Wang, P. Komarov, H. Sier, M. Great, *Biochem. J.*, 279, 311-314. (1991).
78. M. Saran, C. Michel, W. Boro, *Free Rad. Res. Commun.*, 10, 221-226, (1990).
79. J. S. Beckman, T. W. Beckman, J. Chen, P. A. Marshall, B. A. Freeman, *Proc. Natl. Acad. Sci, USA*, 87, 1620-1624, (1990).
80. R. Rodi, H. Rubbo, E. Prodanov, *Biochim. Biophys. Acta*, 994, 89-93, (1989).
81. R. C. Allen, *Methods Enzymol.*, 133, 449-493, (1986).
82. S. L. Archer, D. P. Nelson, K. E. Wein, *J. Appl. Pysiol*, 133, 449-493, (1989).
83. R. Rodi, H. Rubbo, L. Thompson, E. J. Prodanov, *J. Free Rad. Biol. Med.*, 8, 121-126, (1990).
84. E.K. Miller, I. J. Fridovich, *Free Rad. Biol. Med.* 2, 107/110 (1986).
85. G. Merenyi J. Lind, T. E. Eriksen, *Photochem. Photobiol.*, 41, 203-208 (1985).
86. A.K. Campbell "Chemiluminescence: Principles and Applications in Biology and Medicine", Ellis Horwood Ltd., Chichester, England, (1988).
87. J.W. Hastings I. Kricka and P.E. Stanley, Eds., "Bioluminescence and Chemiluminescence": Molecular Reporting with Photons", John Wiley and Sons, Chichester, England, (1997).

PRE-CONCENTRATION OF Cd, Cu, Ni, Pb and Zn FROM FUEL
ETHANOL AND NATURAL WATER SAMPLES BY SORPTION
ON P-AMINOBENZOIC MODIFIED CELLULOSE AND
SUBSEQUENT FLAME AAS DETERMINATION

*Pedro de Magalhães Padilha^a, Ariovaldo de Oliveira Florentino^a, Fabrício Vieira de Moraes^a, Fábio Arlindo Silva^a, Cilene C. F. Padilha^b, Julio C. Rocha^c

^aInstituto de Biociências, Departamento de Química e Bioquímica, UNESP,
CP 510, 18618-000, Botucatu - SP, BRAZIL, E-mail: padilha@ibb.unesp.br

^bInstituto de Biociências, Departamento de Física e Biofísica, UNESP, CP 510,
18610-000, Botucatu - SP, BRAZIL

^cInstituto de Química, Departamento de Química Analítica, UNESP, CP 355,
14800-900, Araraquara - SP, BRAZIL

ABSTRACT

This work describes the synthesis of p-aminobenzoic modified cellulose (Cell-PAB), and the results of a study on the sorption and pre-concentration (using batch and in flow-through column methods) of Cd(II), Cu(II), Ni(II) Pb(II) and Zn(II) in ethanol and aqueous medium. The sorption capacities for each metal ion were (in mmol.g⁻¹): Ethanol medium: Cd(II) = 1.45, Cu(II) = 1.85, Ni(II) = 1.65, Pb(II) = 1.40 and Zn(II) = 1.50; Aqueous medium: Cd(II) = 1.30, Cu(II) = 1.80, Ni(II) = 1.50, Pb(II) = 1.20 and Zn(II) = 1.40. A recovery of almost 100% of the metal ions was obtained from ethanol as well as aqueous medium, the ions being sorbed in column packed with 1 g of Cell-PAB, using 5 mL of 2.0 mol L⁻¹ HCl solution as eluent. An enrichment factor of 45 (250 mL sample, 5 mL concentrate) was obtained by this preconcentration procedure. The sorption-desorption procedure applied allowed the development of a preconcentration method for metal ions at trace level in fuel ethanol and natural water samples. After elution the metal ions were determined by flame atomic absorption spectrometry.

RESUMO

Este trabalho descreve a síntese da celulose modificada com grupos p-aminobenzóico (Cell-PAB), e os resultados de um estudo de sorção e pré-concentração (em batelada, e em fluxo utilizando-se a técnica de coluna) de Cd(II), Cu(II), Ni(II), Pb(II) e Zn(II) em meio etanólico e aquoso. A capacidade máxima de sorção da Cell-PAB determinada para os íons metálicos estudados foram (mmol g⁻¹): Meio Etanólico: Cd(II) = 1.45, Cu(II) = 1.85, Ni(II) = 1.65, Pb(II) = 1.40 e Zn(II) = 1.50; Meio Aquoso: Cd(II) = 1.30, Cu(II) = 1.80, Ni(II) = 1.50, Pb(II) = 1.20 e Zn(II) = 1.40. Os resultados obtidos nos experimentos em fluxo, mostraram uma recuperação de praticamente 100% dos cátions metálicos sorvidos na coluna empacota com 1g de Cell-PAB, utilizando-se 5 mL de HCl 2,0 molL⁻¹ como eluente. A sorção-dessorção dos íons Cd(II), Cu(II), Ni(II), Pb(II) e Zn(II), serviu como base para o desenvolvimento de um método de pré-concentração e subsequente determinação por espectrometria de absorção atômica de chama do teor desses cátions em amostras de etanol combustível e amostras de água natural.

Keywords: Fuel ethanol, water samples analysis, pre-concentration, p-aminobenzoic modified cellulose.

* Author to whom correspondence should be addressed

INTRODUCTION

The direct determination of trace metals in fuel ethanol and natural water samples by conventional analytical methods can be performed after a time-consuming liquid evaporation procedure prior to any measurements. However methods using on line flow preconcentration system, liquid-liquid extraction, sorption and ion exchange, as separation procedures for metal ions have been successfully applied¹⁻⁶.

In recent years, the use of chemically modified silica gel/cellulose with various chelating organofunctional groups aiming to adsorb and preconcentrate metal ions from solutions, have been described⁷⁻¹⁰. Particularly, a column packed with the material on line with a flow analysis system has been suggested as an effective and reliable process for preconcentration of the metal ions from water and fuel ethanol samples before the determination by atomic absorption spectrometry¹¹⁻¹³. In such a combined system the enrichment of the analyte and removal of some interferents, which may be present in the solution, can considerably improve the analytical methodology extending the limit of detection to lower concentrations. In the last decade the sorption of metal ions on cellulose collector has been thoroughly studied for the preconcentration of metal ions from both aqueous and non-aqueous media^{8,9}. According to these studies, cellulose collector for on line separations provide high distribution coefficients (K_d) for trace of analyte even in salt solution, multi-element capability and fast separation kinetics^{6,11}.

This paper describes the preparation of chemically modified cellulose with p-aminobenzoic groups aiming to find an efficient collector for preconcentration and subsequent determination by flame atomic absorption spectrometry (FAAS) of the metal ions present in ethanol, used as fuel for car engines, and natural water samples (Rio Tietê-São Paulo State, Brazil). First the material was tested with a synthetic ethanol or aqueous solutions containing some metal ions and later it was used in a real samples.

EXPERIMENTAL**Synthesis of p-aminobenzoic modified cellulose****Chlorination of cellulose**

The chlorination of cellulose was performed according to the method of Smiths and van Grieken¹⁴.

Preparation of Cell-PAB

A sample of 16 g of Cell-Cl, was treated at 110°C under mechanical agitation for 5 h with sodium *p*-aminobenzoate saturated solution of in 300 mL of purified dimethylformamide (DMF) e 250 mL of high-purity water (Milli-Q system Millipore). In this reaction, the sodium *p*-aminobenzoate group replaced the chlorine group attached to cellulose as shown in equation (I):



The resulting modified cellulose (Cell-PABNa) was filtered off, washed with 100 mL of DMF, repeatedly with ethanol and dried in desiccator over silica gel. The dry Cell-PABNa was treated with an ethanol/distilled-deionized water mixture (80:20 (v/v)), and subsequently with 2.0 mol L⁻¹ hydrochloric acid solution, in order to obtain the *p*-aminobenzoic cellulose (Cell-PAB). The quantity of *p*-aminobenzoic groups attached to on cellulose surface were determined by nitrogen analysis using the Kjeldhal method¹⁵.

Sorption of the metal ions by Cell-PAB

Sorption of MX_n by Cell-PAB from a solution can be described by the equilibrium given by equation (II):



The time required to reach the sorption equilibrium was determined by placing 50 mL of a 5.10⁻³ mol L⁻¹ aqueous or ethanol solutions of the metal ions (Cd(II), Cu(II), Ni(II) Pb(II) and Zn(II)) in various flasks and by shaking them with 100 mg of Cell-PAB. At different time intervals, an aliquot of the supernatant solution from each flask was separated and its metal ion concentration determined by complexometric titration using EDTA as the titrant¹⁶.

The amount of the metal ion sorbed by the solid phase, was calculated using the equation (III):

$$N_f = \frac{N_i - N_s}{m} \quad (\text{III})$$

where N_i represents the initial quantity of the metal ions in the solution, N_s the final quantity of metal ion in the solution equilibrated with the solid phase, m is the Cell-PAB mass used and N_f is the quantity of metal ions collected by Cell-PAB.

Loading capacity

The loading capacity of Cell-PAB was determined at 25° C using the batch sorption method⁷. Different aliquots of ethanol or aqueous standard solutions of each metal chloride, containing $5.00 \cdot 10^{-3}$ mol L⁻¹ of the studied metal ions, were diluted to 50 mL samples, and kept at 25° C. To every sample solution 100 mg of Cell-PAB was added and stirred for 60 min under mechanical agitation. After the period of time chosen, Cell-PAB was separated by centrifugation and the metal ions concentrations remaining in the solution were determined by complexometric titration with Na₂EDTA¹⁶. The quantity of metal ions collected on Cell-PAB was calculated according to equation (III).

Anion influence

The influence of dissolved salts on the sorption of metal ions by Cell-PAB was evaluated by adding aliquots of 0.10 mol L⁻¹ NaCl, NaNO₃, NaClO₄ to solution of Cu(II) ions, under the same conditions as described before.

Pre-concentration and recovery of the metal ions

This study was carried out using a 15 cm length and 0.6 cm inner diameter glass column packed with 1 g of Cell-PAB. Initially, the column was washed with ethanol or Milli Q-water and then 250 mL of 25 µg L⁻¹ Cd(II), Zn(II) and 50 µg L⁻¹ of Cu(II), Ni(II), Pb(II) ethanol or aqueous solutions were percolated through the column with a flow rate of 2.0 mL min⁻¹. The column was washed with 50 mL of ethanol or Milli Q-water then the metal ions were eluted with 2.0 mol L⁻¹ HCl solution. All fractions obtained during the elution stage were gathered separately and analysed by flame atomic absorption spectrometry (FAAS).

Determination of metal ions in ethanol fuel

About 250 mL of ethanol fuel samples were percolated through the column packed with 1 g of Cell-PAB. The adsorbed metal ions were eluted with 5 mL of 2.0 mol.L⁻¹ HCl solution and the metal ions analysed by FAAS. The concentrations of the metal ions were also determined by a conventional pre-concentration method, in which the first step was been the evaporation of the ethanol solution to dryness¹⁷, and determination of the metal ions by ICP-AES (Inductively Couple Plasma Atomic Emission Spectrometry).

Determination of metal ions in natural water samples

Samples collected from natural water were immediately filtered through 0.45 μm membrane . After acidification ($\text{pH} < 2.0$) with $6.0 \text{ mol L}^{-1} \text{ HNO}_3$ solution they were stored in highly purified PE containers. Water samples from organic-rich sources (250 mL) were digested in digestion tubes (in triplicate) using 10 mL of HNO_3 concentrate and 1 mL of H_2O_2 30% (v/v), after evaporation to 50 mL. The resulting solutions were transferred to 250 mL volumetric flasks after adjustment the pH at 5.0 using acetate buffer. The water samples (digested or without digestion with pH maintained at 5.0 with acetate buffer) were percolated through the column packed with 1 g of Cell-PAB. The adsorbed metal ions were eluted with 5 mL of $2.0 \text{ mol L}^{-1} \text{ HCl}$ solution and the metal ions analysed by F AAS.

Determination by Flame Atomic Absorption Spectrometry (FAAS)

The metal ions collected from the Cell-PAB column were determined by Flame AAS according to the standard guidelines of the manufacturers (Spectrometer: SHIMADZU AA-6800), choosing resonance lines of sensitivity of metals and deuterium-arc lamp background correction. For the calibration, synthetic standard solutions containing $1.0 \text{ mol L}^{-1} \text{ HCl}$ comparable to the samples, were used.

RESULTS AND DISCUSSION

Characteristics of the modified cellulose

The chemical analysis of Cell-PAB yielded a $1.90 \pm 0.05 \text{ mmol.g}^{-1}$ of the organofunctional molecules attached on cellulose surface and $1.10 \pm 0.06 \text{ m}^2.\text{g}^{-1}$ as the specific surface area¹⁸. The attached functional groups were very stable under the various cycles of adsorption-elution of the metal ions by the adsorbent in the column.

Sorption isotherms

An important aspect of this modified cellulose is the time necessary for the sorption process to achieve the equilibrium condition. Figure 1 shows the plot of N_t in function of time for Cu(II) from ethanol and aqueous solutions as example. The system attains the equilibrium condition very rapidly, about 10 min for both solutions.

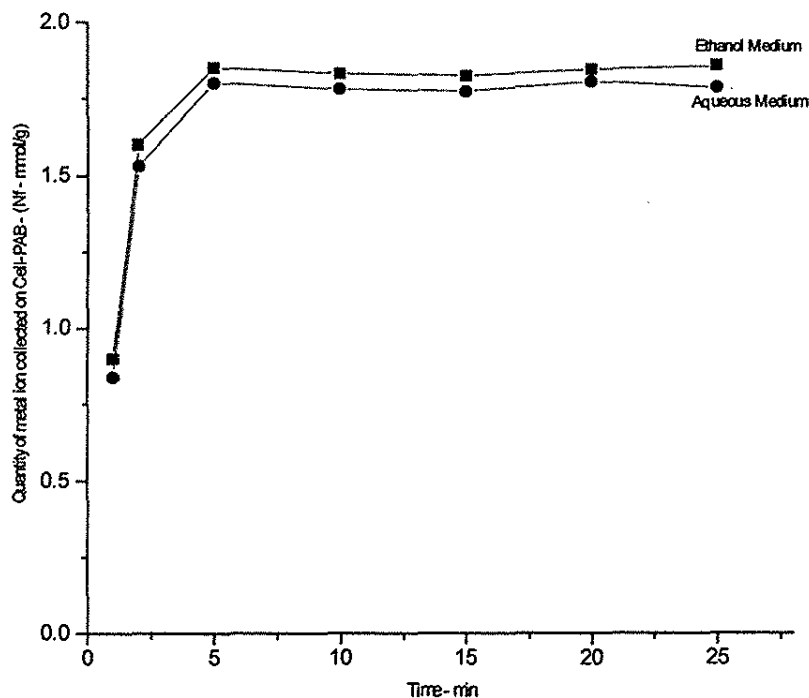


Fig. 1. Plots of N_f (Quantity of metal ion collected) versus time for Cu(II) from ethanol and aqueous solutions at 25°C.

The sorption capacities for each metal ion in ethanol and aqueous medium, determined from saturation condition (N_f^{\max}) of the isotherms are shown in Figures 2 and 3, were (in mmol g^{-1}): Ethanol medium: Cd(II) = 1.45, Cu(II) = 1.85, Ni(II) = 1.65, Pb(II) = 1.40 and Zn(II) = 1.50; Aqueous medium: Cd(II) = 1.30, Cu(II) = 1.80, Ni(II) = 1.50, Pb(II) = 1.20 and Zn(II) = 1.40. Comparing the values of N_f^{\max} obtained with the number of organofunctional molecules (p-aminobenzoate in this case) determined for Cell-PAB, the maximum quantity of metal ions sorbed is comparable to the number of organofunctional molecules contained in Cell-PAB (1.90 mmol g^{-1}).

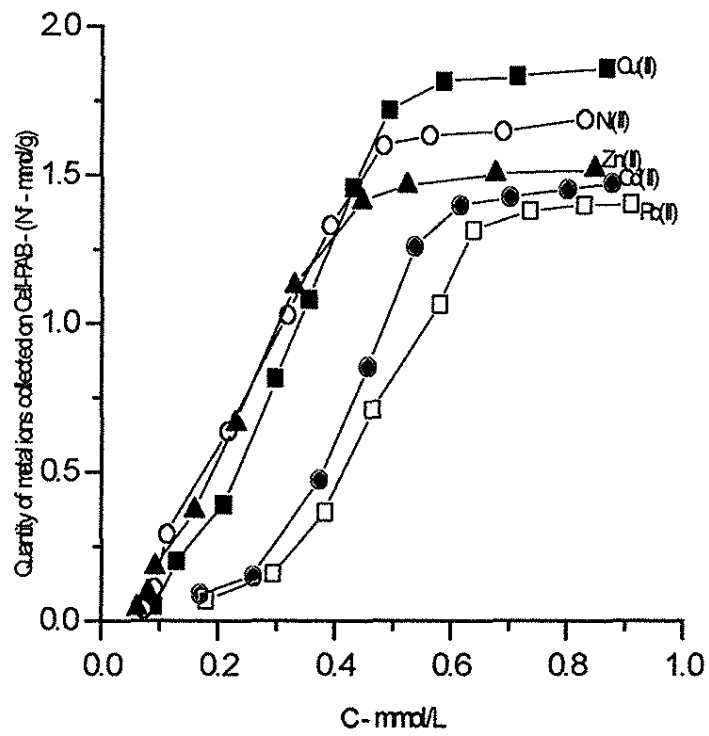


Fig. 2. Sorption of metal ions from ethanol solution at 25°C

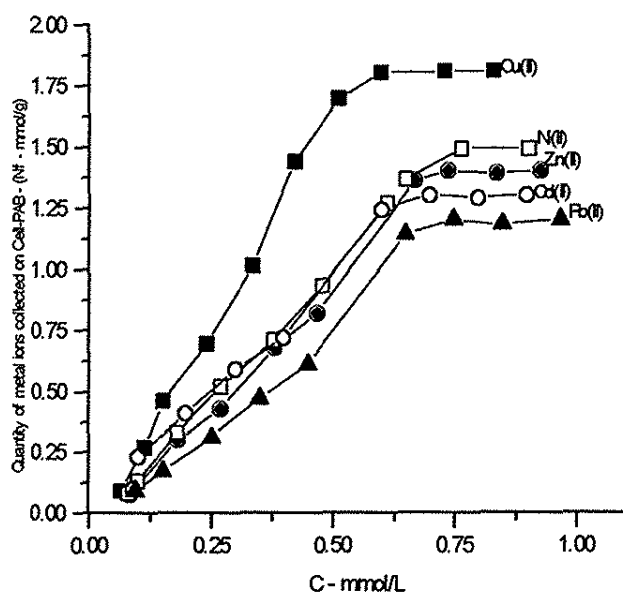


Fig. 3. Sorption of metal ions from aqueous solution at 25°C.

According to this finding, the metal ions are bound to the carboxylate groups by ion exchange or by coordination with the nitrogen of the p-aminobenzoic molecule attached on the cellulose surface.

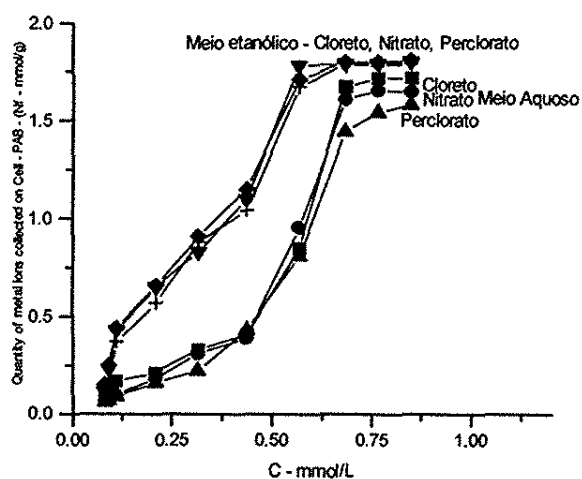


Fig. 4. Influence of anions in the sorption of Cu(II) on p-aminobenzoic modified cellulose (Cell-PAB) from ethanol and aqueous solutions at 25°C.

The influence of electrolytes on the pre-concentration process is related to their tendency to form complexes with the metal ion to be sorbed or exchanged. This is shown in Fig.4, where the influence of competing anions at the concentration level studied (0.10 mol L^{-1} of NaCl, NaNO_3 , NaClO_4) is relatively weak. Thus, the cation-anion interaction in solution potentially decreasing the transfer of the metal ion from the solution to the solid phase, seems to be of little significance¹⁹.

Pre-concentration of the metal ions

Table 1 shows the recovery values, from column packed with 1 g of Cell-PAB, using HCl as eluent. According to these data, 5 mL of 2.0 mol L^{-1} HCl solution is enough to elute almost 100% of the metal ions as much ethanol or aqueous solutions. A 48-fold enrichment was obtained during the pre-concentration procedure (250 mL, 5 mL concentrate) to which the metal ions were subjected. The time to carry out the proposed analytical procedure was 130 min).

Table 1. Recoveries of metal ions using the column method at 25°C , and 2.0 mol L^{-1} HCl solution as eluent ($n = 3$, 250 mL of $25 \mu \text{L}^{-1}$ Cd(II), Zn(II) and $50 \mu \text{g L}^{-1}$ of Cu(II), Ni(II), Pb(II) ethanol or aqueous solutions, volume of eluent = 5 mL)

Ion	Percent Recovery	
	Ethanol Solutions	Aqueous Solutions
Cd(II)	98 ± 2	99 ± 3
Cu(II)	99 ± 1	97 ± 1
Ni(II)	99 ± 2	98 ± 1
Pb(II)	97 ± 3	98 ± 3
Zn(II)	98 ± 3	97 ± 3

Determination of metal ions in fuel ethanol

The recovery experiment for each metal ion from a synthetic solution served as basis for a fast method for pre-concentration and determination of metal ions in a fuel ethanol.

Table 2 shows the concentrations of the metal ions in fuel ethanol samples produced in three different industries. In general, Cd(II) does not occur in fuel ethanol or its content is lower than the contents of the other metals by a factor of 10-100. The metals, Ni(II), Pb(II) were not found in detectable amount. The concentrations of Cu(II) are the highest in the analysed samples, and correspond to the contents of this metal normally found in fuel ethanol²⁰. These

results are in accordance with results obtained using the conventional pre-concentration method¹⁷.

Table 2. Determination of metal ions in ethanol fuel after pre-concentration by the proposed method (PM) (n = 3, 250 mL of sample, volume of eluente= 5 mL) and by the conventional pre-concentration method(CM)¹⁹.

Samples	Concentration found ($\mu\text{g L}^{-1}$)							
	Cu		Ni		Pb		Zn	
	PM	CM	PM	CM	PM	CM	PM	CM
1	56 ± 6	52 ± 3	22 ± 5	19 ± 4	Nd	nd	21 ± 2	19 ± 3
2	63 ± 9	55 ± 4	24 ± 4	21 ± 3	Nd	nd	19 ± 2	17 ± 4
3	76 ± 9	73 ± 5	19 ± 3	22 ± 2	Nd	nd	21 ± 2	20 ± 2

1. From Usina da Barra, 2. From Usina Barra Grande, 3. From Usina São Manuel; nd - not detected

Determination of metal ions in water samples

The proposed pre-concentration method was successfully applied to determination of Cd(II), Cu(II), Ni(II), Pb(II) and Zn(II) in water samples of Rio Tietê-São Paulo State, Brazil with and without previous digestion. The results are shown in Table 3.

Table 3. Determinations of metal ions in water samples of Rio Tietê (with and without digestion, 250 mL sample, n = 3)

Metal Ions	Concentration - (μL^{-1})			
	PMD	PMWD	ICP-AES/D	ICP-AESWD
Cd	19 ± 2	15 ± 1.5	17 ± 3	13 ± 1
Cu	103 ± 5	55 ± 4	97 ± 5	61 ± 4
Ni	76 ± 6	62 ± 5	70 ± 4	59 ± 6
Pb	36 ± 4	29 ± 5	34 ± 4	27 ± 3
Zn	424 ± 16	220 ± 18	433 ± 13	16 ± 11

PMD - Pre-concentration method with digestion; PMWD - Pre-concentration method without digestion; ICP-AES/D - Determinations by ICP-AES with digestion; ICP-AES/WD - Determinations by ICP-AES without digestion.

It can be observed from Table 3 that the FASS determinations to exhibit a difference in the metal ions concentrations of 15-60% lower as compared to the digested samples. This difference has been attributed to interfering of

environmental ligands (e.g aquatic humic substances) present in the samples which may form inert or labile complexes^{21,22}, metal ions being less accessible for the p-aminobenzoic groups of Cell-PAB. After digestion of the water samples, the metal ions bound to aquatic humic substances as inert complexes can quantitatively react with the functional groups of Cell-PAB. These results are in accordance with results obtained by direct determination with ICP-AES, also shown in Table 3, using the conventional pre-concentration method that consist of the evaporation of water sample close to dryness followed by acid digestion²³.

CONCLUSIONS

p-Aminobenzoic groups attached to a cellulose surface can readily be used to adsorb metal ions from ethanol and aqueous solutions. Its relatively high chemical stability in ethanol or aqueous medium, and the fast sorption kinetics of the metal ions, turn this sorbent potentially useful for pre-concentration of traces of heavy metal ions in fuel ethanol or natural water samples. Thus, Cell-PAB can be proposed as a reliable trace collector in flow systems. However, the preconcentration of metal ions by Cell-PAB from organic-rich natural waters, require a previous digestion of the sample in order to mineralize aquatic humic substances which form inert complexes with metal ions.

ACKNOWLEDGEMENTS

The authors wish to thank FUNDAÇÃO DE AMPARO À PESQUISA DO ESTADO DE SÃO PAULO (FAPESP) for the financial support (Process 95/052331-0 and 99/12916-0) and the Usinas Barra, Barra Grande and São Manuel, that supplied the ethanol for this work.

REFERENCES

- 1.I.M.R.A. Bruning and E.B Malm, *Bol. Tec. Research and Development Center of Petrobras Company*, Rio de Janeiro,15 (1980)..
- 2.I.M.R.A. Bruning and E.B. Malm, *Bol. Tec. Petrobras*, 217 (1982).
- 3.V. Carbonel, A. Salvador, and M. de la Gardia, *Fresenius J. Anal. Chem.*, **355**, 529 (1992).
- 4.D. Rodrigues, P. Fernandez, C. Perez-Conde, A. Gutierrez, C. Cámara, *Fresenius J. Anal. Chem.*, **355**, 529 (1992).
- 5.M. Renli, M. Willy Van and A. Freddy, *Anal. Chim. Acta*, **293**, 251(1994).
- 6.P. Burba,J. C. Rocha and A. Shulte, *Fresenius Z. Anal. Chem.*, **346**, 414 (1993).

7. P. M. Padilha, J.T.S. Campos, J. C. Moreira and C. C. Federici, *Química Nova*, **18**, 529.(1995).
8. P. Lessi, N. L. D. Filho, J. C. Moreira and J. T. S. Campos, *Anal. Chim. Acta*, **327**, 183 (1996).
9. N. L. D. Filho, Y. Gushikem and W. L. Polito, *Anal. Chim. Acta*, **306**, 167 (1995).
10. P. M. Padilha, J. C. Rocha, J. T. S. Campos, J. C. Moreira and C. C. Federici, *J. Braz. Chem. Soc.*, **8(4)**, 333 (1997).
11. P. M. Padilha, J. C. Rocha, J. C. Moreira, J. T. S. Campos and Federici, C. C., *Talanta*, **45**, 317 (1997).
12. L. A. M. Gomes, P. M. Padilha, J. C. Moreira, N. L. D. Filho and Y. Gushikem, *J. Braz. Chem. Soc.*, **9(5)**, 494 (1998).
13. P. M. Padilha, C. C. F. Padilha and J. C. Rocha, *Química Analítica*, **18**, 117 (1999).
14. J. Smits, R. Van Grieken , *Makromol Chem.*, **72**, 105 (1978).
15. A. I. Vogel, A. I., *Textbook of Quantitative Chemical Analysis*, Copyright, Longman Group UK Limited (1989), pp. 249.
16. L. T. Kubota, M. Ionashiro and J. C. Moreira, *Ecl. Quim.*, **13**, 19 (1988).
17. N. L. D. K. Tanaka, S. Woly nec, S. Fairbanks and F. B. P. Pinto, *VIIIth National Seminar on Corrosion*, Rio de Janeiro, Brazil, 59 (1981).
18. S. Brunaur, P. Emmet and E. Teller, *J. Am. Chem. Soc.*, **60**, 309 (1938).
19. L. T. Kubota, J. C. Moreira, and Y. Gushikem, *Analyst*, **114**, 1385 (1989).
20. D. K. Tanaka, Woly nec, S.; *Proc. of IXth National Seminar on Corrosion*, Rio de Janeiro, Brazil, 166 (1982).
21. I. A. S. Toscano, J. C. Rocha and P. Burba, *Talanta*, **44**, 69 (1997).
22. P. M. Padilha, L. A. M. Gomes, C. C. F. Padilha, J. C. Moreira and N. L. D. Filho, *Analytical Letters*, **32**, 1807 (1999).
23. M. J. S. Yabe, E. Oliveira, *Química Nova*, **21(5)**, 551(1998).

SOUTHERN BRAZILIAN JOURNAL OF CHEMISTRY

ISSN 0104-5431

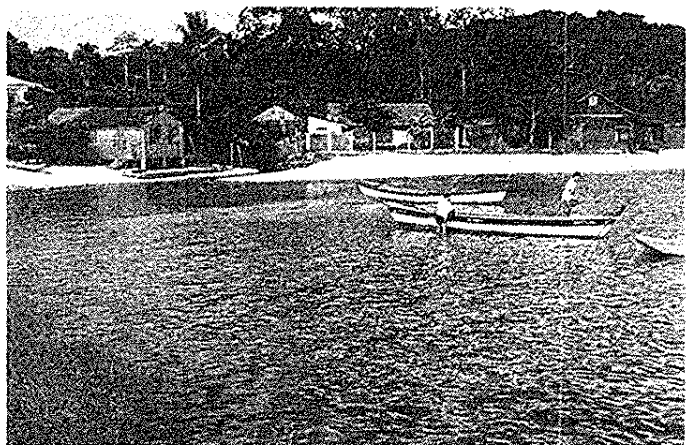
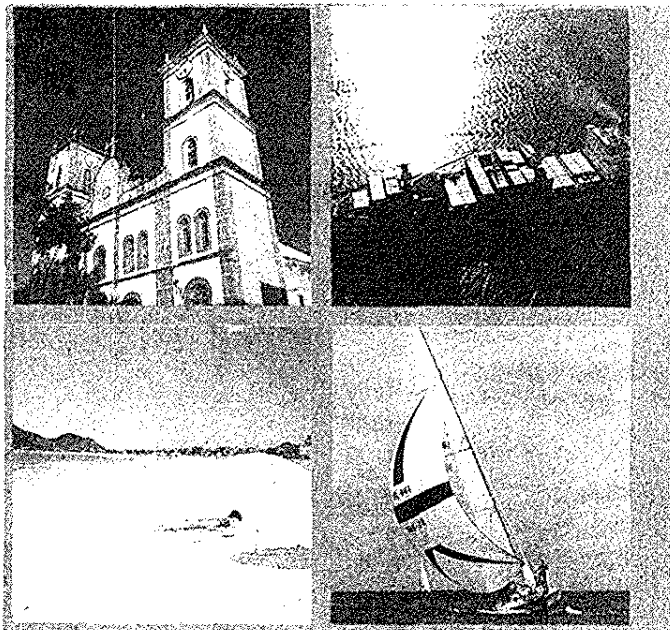
VOLUME EIGHT, NUMBER NINE DECEMBER 2000

AUTHOR INDEX / ÍNDICE DE AUTORES

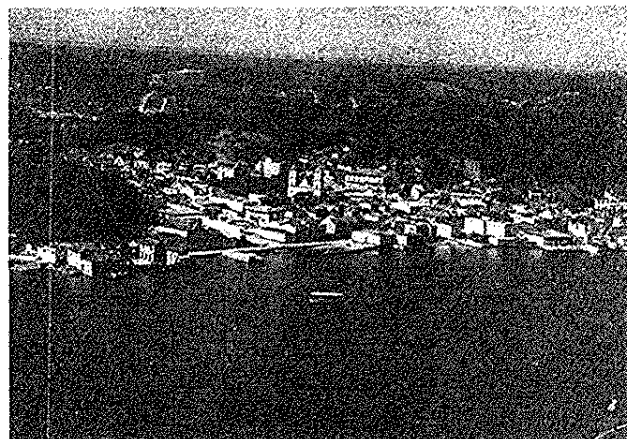
125

Calinescu, Mirela	57,71
Carneiro, Paulo Irajara Borba	53
Crocnan, D. O.	37,97
Dani, Silvia	85
Emandi, Ana	57,71
Endres, Luciano	25
Florentino, Ariovaldo de Oliveira	113
Ganescu, Ion	45
Göktürk, S.	1
Gropeanu, Radu	13
Greabu, Maria	37,97
Ionescu, Lavinel G.	85
Mahramanlioglu, M.	1
Moraes, Fabrício Vieira de	113
Mureseanu, Mihaela	45
Negoiu, Dumitru	57
Nicolae, Anca	71
Olinescu, R.	37,97
Padilha, Cilene C. F.	113
Padilha, Pedro de Magalhães	113
Panea, Ioan	13
Panea, Teodora	13
Paruta, Lidia	71
Pleniceanu, Maria	45
Rittner, Roberto	53
Rocha, Julio C.	113
Rosu, Tudor	53
Rusu, Olimpia	45
Silva, Fábio Arlindo	113
Souza, Elizabeth Fátima de	85
Tunçay, M.	1
Wolf, Carlos R.	25

SOUTHERN BRAZILIAN JOURNAL OF CHEMISTRY



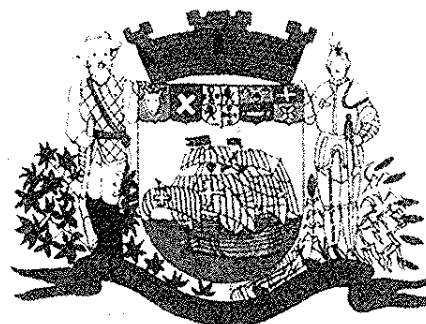
PAULAS



VISTA AÉREA CENTRO



CENTRO



PREFEITURA MUNICIPAL
SÃO FRANCISCO DO SUL

15 de Abril de 1504

SÃO FRANCISCO DO SUL, SANTA CATARINA, BRAZIL'S THIRD OLDEST CITY.
(FOUNDED APRIL 15, 1504)

SÃO FRANCISCO DO SUL, SANTA CATARINA, A TERCEIRA CIDADE MAIS ANTIGA
DO BRASIL. (FUNDADA EM 15 DE ABRIL DE 1504)

SOUTHERN BRAZILIAN JOURNAL OF CHEMISTRY

ISSN 0104-5431

The *SOUTHERN BRAZILIAN JOURNAL OF CHEMISTRY* is an international forum for the rapid publication of original scientific articles dealing with chemistry and related areas. At the present there are no page charges and the authors will receive twenty five free reprints of their papers.

SPECIAL COMBINATION OFFER FOR NEW SUBSCRIBERS!

SUBSCRIPTION INFORMATION

PRICE: Brazil and Latin America: US\$ 35.00 per issue.

Other Countries: US\$ 50.00 per issue, including
air mail delivery.

Persons or institutions outside Brazil should send
subscription fee payable to Dr. L. G. Ionescu, c/o SBJC
8532 Howard Circle, Huntington Beach, California, USA
92647

ORDER FORM

- Please enter my subscription for _____ issues of
Southern Brazilian Journal of Chemistry.
- Please send me _____ copies of the Southern Brazilian
Journal of Chemistry Vol. 1,2,3,4,5, ...9 (1993-2000)
(Circle desired copies.)
- I enclose a check or money order in the amount of \$ _____
- Please send me a Pro Forma Invoice for the above
order.

SOUTHERN BRAZILIAN JOURNAL OF CHEMISTRY

Lavinel G. Ionescu, B.S., M.S., Ph.D., Editor
Caixa Postal 15032, Agronomia
Porto Alegre, RS BRASIL 91501-970

TEL. 55 51 485-1820 FAX 55 51 320-3612 or 55 51 477-1313

Email: LGIPUCRS a MUSIC.PUCRS.BR
LAVINEL a MOZART.ULBRA.TCHE.BR

INFORMATION FOR AUTHORS

The Southern Brazilian Journal of Chemistry - SBJC will publish review articles, original research papers and short communications dealing with chemistry and interdisciplinary areas such as materials science, biotechnology, bioengineering and other multidisciplinary fields.

Articles report the results of a complete study. They should include an Abstract, Introduction describing the known art in the field Experimental or Materials and Methods, Results and Discussion, Acknowledgments (when appropriate) and References.

Short Communications should be limited to 1500 words, including the equivalent space for figures and/or tables and should include an Abstract and concise Experimental.

Manuscripts may be submitted on-line or in triplicate (original and two copies by registered mail) and are received with the understanding that the original has not been submitted for publication elsewhere. It is implicit that all the persons listed as authors have given their approval for the submission of the paper and that permission has also been granted by the employer, when necessary.

Manuscripts must be written in American or British English, single spaced, on A4 sheets (21 cm x 29.5 cm) and one side only and should be numbered beginning with the title page. Type must be 12 Arial or Times New Roman.

Margins of at least 3 cm should be left at the top and bottom and both sides of each page. The first page of the paper should contain only the title of the paper, the name(s) and addressees of the author(s), an abstract of not more than 250 words and 4-8 keywords. We reserve the right to translate the abstract in Portuguese. Abstracts are required of all papers including reviews and short communications.

Figures and Tables with short explanatory titles, each on a separate sheet, should be adequate for direct reproduction and identified in pencil on the back of each page by Arabic numerals, corresponding to the order they appear in the manuscript. Tables and Figures (BMP or JPG format) may also be included directly in the text when convenient and the article may submitted in a quasi-final form in order to facilitate editorial work.

References should be numbered in the sequence they appear in the text, cited by superior numbers and listed at the end of the paper in the reference section in the numerical order they appear in the text. The style for references is shown below:

1. L. G. Ionescu and D. S. Fung, *J. Chem. Soc. Faraday Trans. I*, 77, 2907-2912 (1981).
2. K. L. Mittal, Ed., "*Solution Chemistry of Surfactants*", Plenum Press, New York (1984), Vols. 1-3, pp. 1-2173.

IUPAC Rules should be used for the name of chemical compounds and preference should be given to 51 units.

Authors are invited to send manuscripts by registered air mail to the EDITOR - SBJC, C.P. 15032, Agronomia, Porto Alegre, RS BRASIL 91501, or by e-mail to lavinel@ibest.com.br or lavinel@pop.com.br.

VISIT OUR SITE: <http://www.sbjchem.he.com.br>

SCIENCO
**SOUTHERN BRAZILIAN JOURNAL
OF CHEMISTRY**

ISSN 0104-5431

The *SOUTHERN BRAZILIAN JOURNAL OF CHEMISTRY - SCIENCO* publishes original research articles in chemistry and related interdisciplinary areas and is intended to fill a gap in terms of scientific information for Southern Brazil.

Occasionally the journal will include review papers and articles dealing with chemical education and philosophy and history of science. It will be published mainly in English, with abstracts in Portuguese and only occasional papers in other languages. At the present there are no page charges and the authors will receive twenty five reprints of their papers free of charge.

We have set high standards for the articles to be published by ensuring strong but fair refereeing by at least two reviewers. We hope that this journal will provide a forum for dissemination of high quality research in chemistry and related areas and are open to any questions and suggestions.

The Editor

SUBSCRIPTION INFORMATION

Brazil and Latin America:
US\$ 35.00 per issue.

Other Countries: US\$ 50.00 per issue,
including air mail delivery. Persons or
institutions outside Brazil should send
subscription fee payable to Dr. L. G. Ionescu,
c/o SBJC, 8532 Howard Circle, Huntington Beach,
California, USA 92647

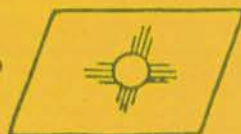
MAILING ADDRESS

SOUTHERN BRAZILIAN JOURNAL OF CHEMISTRY - SBJC
Lavinel G. Ionescu, B.S., M.S., Ph.D., Editor
C.P. 15032, Agronomia
Porto Alegre, RS BRASIL 91501-000
Tel. (051) 485-1820 FAX (051) 339-1564

FINANCIAL SUPPORT

SARMISEGETUSA RESEARCH GROUP

SANTA FE, NEW MEXICO, U.S.A.



Endless Column, 1937, cast iron
CONSTANTIN BRANCUȘI